AD NUMBER

AD875993

NEW LIMITATION CHANGE

TO

Approved for public release, distribution unlimited

FROM

Distribution authorized to U.S. Gov't. agencies and their contractors; Administrative/Operational Use; Aug 1970. Other requests shall be referred to Air Force Flight Dynamics Lab., Attn: FDF, Wright-Patterson AFB, OH 45433.

AUTHORITY

AFFDL ltr, 1 Feb 1973

AFFDL-TR-70-53

FLEXIBILITY AS PARAMETER OF MODEL PARACHUTE PERFORMANCE CHARACTERISTICS

HELMUT G. HEINRICH
THOMAS R. HEKTNER
UNIVERSITY OF MINNESOTA

TECHNICAL REPORT AFFDL-TR-70-53

AUGUST 1970

AIR FORCE FLIGHT DYNAMICS LABORATORY
AIR FORCE SYSTEMS COMMAND
WRIGHT-PATTERSON AIR FORCE BASE, OHIO

NOTICES

When Government drawings, specifications, or other data are used for any purpose other than in connection with a definitely related Government procurement operation, the United States Government thereby incurs no responsibility nor any obligation whatsoever; and the fact that the Government may have formulated, furnished, or in any way supplied the said drawings, specifications, or other data, is not to be regarded by implication or otherwise as in any manner licensing the holder or any other person or corporation, or conveying any rights or permission to manufacture, use, or sell any patented invention that may in any way be related thereto.

This document is subject to special export controls and each transmittal to foreign governments or foreign nationals may be made only with prior approval of the Vehicle Equipment Division (FDF), Air Force Flight Dynamics Laboratory, Wright-Patterson AFB, Ohio, 45433.

The distribution of this report is limited because it contains technology identifiable with items on the strategic embargo lists excluded from export or re-export under U.S. Export Control Act of 1949 (63 STAT. 7), as amended (50 U.S.C. App. 2020.2031), as implemented by AFR 400-10.

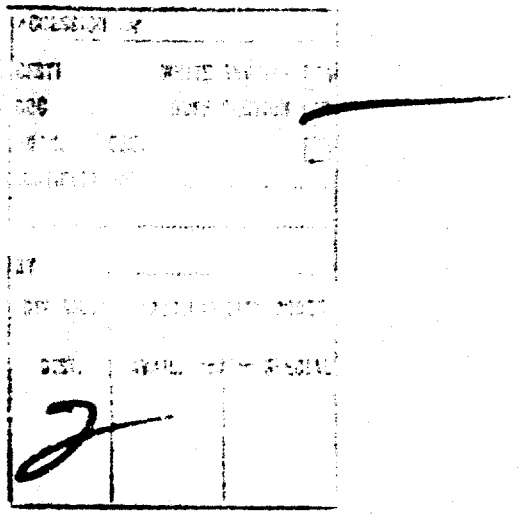

Copies of this report should not be returned unless return is required by security considerations, contractual obligations, or notice on a specific document.

FLEXIBILITY AS PARAMETER OF MODEL PARACHUTE PERFORMANCE CHARACTERISTICS

HELMUT G. HEINRICH
THOMAS R. HEKTNER
UNIVERSITY OF MINNESOTA

FOREWORD

This report was prepared by the Department of Aerospace Engineering and Mechanics of the University of Minnesota in compliance with U. S. Air Force Contract No. F33615-68-C-1227, "Theoretical Deployable Aerodynamic Decelerator Investigations," Task 606503, "Parachute Aerodynamics and Structures, " Project 6065, "Performance and Design of Deployable Aerodynamic Decelerators." The work on this report was performed between December 16, 1967, and October 15, 1969.

The work accomplished under this contract was sponsored jointly by U. S. Army Natick Laboratories, Department of the Army; Bureau of Aeronautics and Bureau of Ordnance, Department of the Navy; and Air Force Systems Command, Department of the Air Force, and was directed by a Tri-Service Steering Committee concerned with Aerodynamic Retardation. The work was administered under the direction of the Recovery and Crew Station Branch, Air Force Flight Dynamics Laboratory, Wright-Patterson AFB, Ohio. Mr. James H. DeWeese (FDFR) was the project engineer.

The study was conducted in cooperation with Mr. Robert A. Noreen and several students of Aerospace Engineering of the University of Minnesota. The authors wish to express their gratitude to all who rendered their services to the accomplishment of this work, especially to Mr. J. H. DeWeese for his numerous constructive suggestions.

This report was submitted by the authors in December, 1969.

This technical report has been reviewed and is approved.

GEORGE A. SOLT, JR.
Chief, Recovery and Crew Station Branch
Air Force Flight Dynamics Laboratory

ABSTRACT

Parachute model tests offer the possibilities of efficiently conducting parametric performance studies. Meaningful model experiments must, however, consider besides the effects of Reynolds and Mach Numbers, those of porosity as well as structural characteristics particularly when non-steady processes shall be investigated. In the following the model stiffness index is defined and its effect upon static and dynamic performance characteristics investigated. Quantitative data and stiffness indexes of cloth samples and parachute models are determined. A new technique of construction is described which provides parachute models with a lower stiffness index than previously available. Results of wind tunnel and catapult experiments with parachute models of different stiffness indexes are shown and, when possible, compared with results of full size tests.

TABLE OF CONTENTS

ILLUSTRATIONS

ILLUSTRATIONS (CONT.)

ILLUSTRATIONS (CONT.)

ILLUSTRATIONS (CONT.)

LIST OF TABLES

SYMBOLS

C	effective porosity
C_D	drag coefficient
C_T	tangent force coefficient
d	diameter of lower strip curvature
D	diameter
D_{max}	maximum width of the suspended strip specimens or model canopies
D_{max}/L	strip stiffness index
$D_{p_{max}}$	maximum projected diameter of the inflated parachute
E_p	canopy skirt elongation
F	force
g	gravity
L	length of strip specimens
m	mass
S	area
T	dimensionless filling time, t/t_f
t	time
v	velocity
W	weight; width of strip specimens
w_{cl}	weight of cloth per ft^2
α	angle of attack
ρ	density
η	canopy stiffness index, $\frac{D_{max}}{L} \cdot \frac{W_c}{S_o w_{cl}}$

γ	angle of suspension line cone or angle of ribbon handles of strips
σ	standard deviation

Subscripts:

a	apparent
c	canopy
cl	cloth
eff	effective
f	filling
i	included, inlet
o	nominal, total
p	parachute, projected
s	suspended, snatch when used with velocity
st	stable or trim when used with α
W	wind tunnel

I. INTRODUCTION

Classical and contemporary experiments have shown that the aerodynamic and dynamic performance characteristics of ballistic and lifting bodies can satisfactorily be predicted from results of model experiments provided that the conventional model similarity laws are obeyed. Considering as a classical example model studies of conventional airplane wings, one notices that such wings are investigated in view of their steady state aerodynamic characteristics as well as in respect to aero-elasticity phenomena in which aerodynamic and strucural forces are coupled through elastic deformations. Following this convention, terms concerning steady state and non-steady performance characteristics shall be used in the following to express characteristics in which a) the elasticity is neglected, and b) in which interaction between aerodynamic, structural forces, and elastic deformations occur. As well known, influential similarity conditions for steady state aerodynamic measurements are the Mach- and Reynolds-Numbers and for low density considerations eventually the Knudson-Number. The more complicated relationships which occur when aerodynamic and elastic forces interact are explained in Ref 1.

Under consideration of these and other similarity conditions, the results of model experiments are transferable to the performance data of prototype objects over a surprisingly wide range of environmental conditions. For example, in Ref 2 it is shown that aerodynamic data of the Apollo capsule obtained in wind tunnel studies and experiments in a firing tube with models having a diameter of merely 0.95 cm agree perfectly with those obtained from full size Apollo missions. Significant for these tests, however, is that all models as well as the prototype space capsule are for all practical purposes rigid bodies for which the steady state as well as the non-steady aerodynamic phenomena, belonging to the field of dynamic stability, are well understood (Ref 3).

Contrary to these very satisfactory results of model technique is the fact that the performance characteristics of parachutes obtained in wind tunnel tests differ in many cases considerably from those observed in full size drop tests. This discrepancy has been recorded in view of the steady state performance, steady descent, as well as in the non-steady phase, usually called the parachute inflation. Considering first the recorded discrepancies related to the steady state performance and assuming that parachute models and prototypes have been tested under suitable Mach and Reynolds Number conditions and also that the test results have been properly evaluated, the question arises as to the

accuracy of the recordings obtained during the testing of the full size parachute. These recordings are obviously somewhat difficult to make because unknown wind currents as well as possible glide angles and dynamic stability phenomena may have influenced the performance characteristics. In support of the practical parachute experiments and in view of the characteristic trim angle of the various parachute types, the term, effective drag coefficient, $C_{D_{eff}} = C_T/\cos^2\alpha$ has been introduced (Ref 4) many years ago. However, in spite of careful consideration of the possible glide and other environmental conditions it has so far been impossible to establish for parachutes the same satisfactory agreement between actual prototype performance characteristics and those predicted on the basis of model tests as customarily obtained for other more conventional aerodynamic objects.

The efforts to predict the non-steady parachute inflation characteristics on the basis of model tests date at least back to the year 1941 (Ref 5). However, in general, a satisfactory agreement between results of model tests and observations of full size tests has so far not always been established.

The question arises then, why do parachutes behave in these respects so differently from other more conventional objects. In the search for possible reasons, one notices quickly that parachutes have at least two additional features not commonly found in aerodynamics and dynamics of conventional airborne vehicles, namely, porosity and flexibility. These two parameters enter certainly into performance characteristics of model as well as full size parachutes, and the question is merely under which condition and how their influence is felt.

One may assume that in the steady state condition a possibly existing, varying deformation of the parachute canopy is relatively small, and that this phase is primarily governed by the steady state aerodynamic coefficients and the parachute size. The coefficients are strongly influenced by the porosity of the parachute material (Ref 6), and the relationship between coefficients and porosity as well as the dependency of porosity from Mach and Reynolds Number effects is fairly well understood (Ref 7). However, even under careful consideration of all these facts, the results of parachute model tests and full size tests under steady state conditions still disagree, and it appears to be justified to investigate a possible relationship between the model flexibility and average inflated size of the model and to compare the characteristic flexibility of model and

prototype parachutes. Therefore, it is one objective of the following discussion to investigate this relationship and at least find an indication whether or not the flexibility of model parachutes does influence their steady aerodynamic coefficients.

The non-steady performance phases encompass the dynamic stability and the inflation process of the parachute. The dynamic stability is strongly influenced by the steady state coefficients as well as by the shape and deformation of the canopy profile under moderate or strong oscillatory motion. In this view the instantaneous shape is, of course, influenced by the canopy deformation or flexibility. The problems of dynamic stability are fairly well understood, and ways and means are known to achieve satisfactory dynamic stability of parachutes (Ref 8).

In the other non-steady phase, during the inflation, a parachute canopy evolves from the form of an elongated, somewhat cylindrical sack to a thin shell having an approximate form of a semi-ellipsoid or a hemisphere. The inflation process is governed by the balance of the mass in- and outfluxes which in turn depend on the effective canopy porosity. The relationship between porosity and Mach and Reynolds Numbers is known (Ref 7) and can be introduced in the respective equations which simulate the parachute opening process. However, there is a possibility that parachute models as well as full size parachutes may have a random tendency to open faster or slower depending on their inherent stiffness of, if one may use the term loosely, elasticity. Stiffness, elasticity, or degree of flexibility have so far not been established quantitatively and can therefore not be introduced in the respective equations. If now model tests show that the model stiffness characteristics influence significantly the opening process, then the prediction of opening characteristics of full size parachutes based on results extracted from model tests will be a very difficult if not unsolvable problem as long as the stiffness characteristic of model and full size parachutes cannot be related to each other.

In order to gain some knowledge in this area, the opening characteristics of models with different stiffness or flexibility will be established and, when possible, compared with those reported from full size tests. In order to pursue this on a quantitative basis, a stiffness index will first be derived and the comparison of the models and the full size parachutes will be accomplished on the basis of these stiffness indexes.

II. STIFFNESS INDEX

There are indications that canopy stiffness features influence the opening characteristics of full size as well as model parachutes. In view of the questions concerning the validity of model tests, it is first of all necessary that the stiffness or flexibility characteristics of parachutes be suitably defined. Unfortunately no previous publication on this subject has been found; therefore, an original attempt was made to express the degree of canopy stiffness or flexibility in terms of characteristic dimensions. In view of this necessity, Fig 1 shows an attempt to characterize the contour of parachutes when freely suspended. Using initially the ratio of maximum diameter, D_{max}, and the nominal diameter, D_o, as characteristic, one finds for a 28 ft prototype parachute and a conventionally built 5 ft parachute model, the ratios of D_{max}/D_o of 0.09 and 0.29 respectively. This indicates that the prototype parachute is much more flexible than the geometrically similar model built out of the same parachute cloth. Several other measurements were made, and in all cases the models proved to be much stiffer than the prototype parachute.

Conceptually it was postulated that model flexibility or stiffness would influence the opening characteristic of parachutes and one possibility of checking this assumption is to perform parachute opening experiments with models of a different degree of flexibility. Since conventionally built models on hand were relatively much stiffer than a related full size parachute, it was the first objective of this study to build much more flexible parachute models.

The basic parachute cloth cannot be altered because the porosity features of the material must be preserved, and it is probably beyond the state of the art to weave "model cloth". However, it appeared to be possible to build more flexible models by using different types of seams, more flexible suspension lines, and other modes of suspension line fastening. Therefore, the first attention was directed toward the elements which composed the parachute canopy, and this leads to the study of stiffness of model strips.

Figure 2 shows a characteristic model strip while Fig 3 indicates an experiment in which the model strips display certain stiffness characteristics. The ratios of maximum diameter versus length or width of the strip reflect again the stiffness or flexibility of the strip and for the time being shall be called stiffness indexes.

A large number of sample strips with different seams and various suspension lines attached to the strips were investigated in this manner and the results as well as the scheme of the seam arrangement are shown in Fig 4. One notices that the strips without finished seams have the lowest stiffness index, and furthermore that the strip which was cut with a heated sharp edge is at least as flexible as the strip cut with a scissor. Cutting with a heated edge* provides seared edges of the strip which prevents the material from fraying. Since the lightest nylon cloth with a 1.1 oz weight per square yard is for model building the most important material, additional experiments were made with longer strips of this type. The results of these tests are shown in Fig 5. In both figures it can be seen that the strips without finished seams and stitched down suspension lines or bands have the lowest stiffness indexes. It should be mentioned that in these strip tests care must be exercised to exclude or diminish deformation effects due to static electricity charges, which in these tests were removed by humidifying the surrounding air.

Reviewing the results of the strip and canopy measurements, one notices that the larger canopies and the longest strips are more flexible than smaller canopies and shorter strips. Also it appears reasonable to assume that model canopies built on the principle of the most flexible strips will provide parachutes with a relatively low stiffness index. Parachute models have been built in many different ways. Most of them were built somewhat similar to full size parachutes which then result in relatively stiff models with stiffness indexes at least four times as high as the one of the related prototype parachute. Therefore, it was decided to employ the hot-knife-cut technique in the fabrication of model canopies. Also, new fabrication methods had to be developed particularly for the fastening of thin and very flexible suspension lines. After several attempts to develop suitable construction methods, the particular design details shown in Fig 6 produced the most satisfactory one. It will be noticed that in this fabrication method, the suspension lines can slide over the canopy cloth in a somewhat similar fashion as the suspension lines of full size parachutes. The model suspension lines are merely anchored at the canopy vent and skirt. The parachute canopy itself has instead of a skirt seam or band merely a seared edge. This technique has also been expanded to fabricate ringslot canopies as shown in Fig 7.

Parachute models made in this fashion had the appearance of much higher flexibility, and they were also considerably lighter than conventionally built models. In view of the fact that in inflation tests primarily the enclosed air has to accelerate the material of the canopy,

* see appendix

the specific weight of the canopy surface is probably also very important. Therefore, a weight term was introduced into the parachute canopy stiffness index in the form of the ratio of the weight per unit area of the ready made canopy divided by the unit weight of the canopy cloth. The stiffness index of the parachute canopy assumes then the form

$$\eta = \frac{D_{max}}{D_o} \cdot \frac{W_c}{S_o \cdot w_{cl}}$$

One notices that this is basically a stiffness-weight characteristic which for convenience shall be defined as stiffness index. These so derived values together with other related terms are shown in Table I, and Fig 8 shows graphically the stiffness indexes of flexible and conventional models of the prototype parachute together with the ranges covered by the data obtained from the strip tests. From Table I and Fig 8 one notices that the stiffness index of the most flexible model parachute is approximately 1.65 as high as the one of the prototype, whereas the conventionally built canopy had a stiffness index approximately three times as high. The weight savings on the ringslot parachute is even higher which results in a considerable reduction of the ringslot canopy stiffness index.

Since for dynamic testing a certain canopy strength is required and no further weight savings and/or better fabrication methods were conceived, the most flexible parachute models are considered to be the end result of these efforts at this time.

III. THE EFFECT OF MODEL STIFFNESS

After parachute models with lower stiffness indexes became available, studies were made in which the performance characteristics of conventional and new, more flexible models were established, compared with each other, and when possible also compared with recordings obtained from full size tests. These comparative studies were made in view of drag, inflation, opening force characteristics, and parachute squidding. In the following these groups of experiments will be described and analyzed.

A. Shape and Drag Studies

The possible effect of model stiffness upon the canopy profile and projected area is, of course, the feature most easily detected. Comparative profile and frontal views of solid flat circular, conventional, and flexible models are shown in Fig 9. As can be seen, the depth to diameter ratio of the two models varies noticeably and in other tests with different size models and different numbers of suspension lines, the more flexible model of the circular flat as well as the ringslot type parachutes were always more flat as illustrated in Fig 9.

The average value of the depth to projected diameter ratio of the flexible model is about 7% lower than the one of the identical but conventionally built models. An evaluation of the projected areas at zero angle of attack showed that the frontal area of the parachute model with the lower stiffness index was in the average 8% larger than the one of the stiffer model.

Following these geometric studies, comparative tentative force measurements on conventional and flexible models were made. The measurements indicated that the tangential force at the approximate trim angle of 20° of the two models was for the flexible model on the average 8% higher than the one of the conventional or stiffer model. The figure of 8% and the approximate trim angle of 20° need verification through more exact three-component measurements.

The U. S. Army Natick Laboratories conducted drop tests with a 100 ft flat circular, solid cloth parachute (Ref 9). These tests were carefully observed and the engineering staff of the U. S. Army Natick Laboratories reported an average value of effective drag coefficients of $C_{D_{eff}} = 0.90$

with minimum and maximum values of 0.86 and 0.93. These results shall now be compared with older wind tunnel results in view of the findings concerning the effect of model parachute stiffness.

In Ref 6 the coefficients of flat circular parachutes as function of effective porosity have been established by means of conventionally built or relatively stiff parachute models. Figures 10 and 11 represent the essential results concerning the stability and drag characteristics.

The 100 ft parachutes were made from standard parachute cloth, MIL-C-7020 Type II, which specifications require a nominal porosity of 130 + 30 cubic ft per square ft and per minute. The nominal porosity is related to a differential pressure of $\frac{1}{2}$ inch of water column (= 2.60 lb/ft^2). The actual parachute descends with less differential pressure. Consequently the effective porosity during the parachute descent is less than the one which corresponds to the nominal porosity. Assuming that this difference amounts to 10%, one finds for the adjusted porosity from Figs 10 and 11 the trim angles and the related tangent force coefficients. For the three effective porosities, corresponding to the nominal porosities of 100, 130, and 160 cubic ft per square foot and per minute, one obtains, after correcting the values by 8% in view of the described area increase, the coefficients of effective drag $C_{D_{eff}}$ = 0.86, 0.905 and 0.94 respectively. These wind tunnel results compare now very favorably with those measured from full size field tests. It may be mentioned that in these tests the Reynolds Numbers of the model experiments and the full size tests amounted to 4.2×10^5 and 1.7×10^7, respectively.

B. Area- and Velocity-Time Histories During Model Parachute Inflation

The governing terms in the equation of motion, representing the process of parachute inflation, are the instantaneous values of projected and inlet areas, canopy volume and velocity, as well as their time derivatives. The influence of canopy stiffness upon the inflation process, if it exists, must be noticeable in these quantities. Therefore, wind tunnel experiments under finite mass conditions were made with conventionally built and highly flexible models with the objective to establish possibly existing differences.

Wind tunnel inflation tests of parachutes with a finite suspended mass are described in Refs. 5, 10, and 11.

Figure 12 shows the experimental arrangement used in Ref 11 which, while still available, was also used for the performance of the inflation studies concerned with the effect of model stiffness.

For the wind tunnel tests schematically shown in Fig 12, the equation of motion of the suspended finite mass (Ref 11) amounts

$$m_s \frac{dv}{dt} = \tfrac{1}{2}\rho C_D S\,(v_W - v)^2 - W_s + (v_W - v)\left(\frac{dm_i}{dt} + \frac{dm_a}{dt}\right) - (m_p + m_i + m_a)\,\frac{dv}{dt}\,.$$

or in terms of force upon suspended weight

$$F = m_s \frac{dv}{dt} + W_s = \tfrac{1}{2}\rho\, C_D S(v_W - v)^2 + (v_W - v)\left(\frac{dm_i}{dt} + \frac{dm_a}{dt}\right) - (m_p + m_i + m_a)\,\frac{dv}{dt}\,.$$

These equations show the characteristic values of area, velocity, volume, and instantaneous force itself. The contributions of the various terms to the resultant force are shown in Ref 11, and it may be stated that the effect of each one is significant and has to be considered.

Reviewing then the results of the respective tests, Figs 13, 14, and 15 show the individual area-time recordings of experiments with conventionally built model parachutes (Ref 11). Similarly Figs 16, 17, and 18 present individual area-time recordings obtained from experiments with highly flexible models under the same environmental conditions.

In the following figures, Figs 19, 20, and 21, the average area-time curves of the conventional and more flexible models are compared. One notices that in all cases the rate of growth of the projected area of the more flexible models was in the early phase of inflation smaller than the one of conventional models. In the final phase, the so-called overinflation of the more flexible model was considerably higher than the one of the conventional or more stiffer models. The projected area of the parachute models, related to the instant T=1, was measured in the wind tunnel at a wind velocity of approximately 50 fps. They amounted to 3.0 ft^2 and 3.25 ft^2 for the conventional and flexible models respectively.

For further comparison, the average area-time history, reported by Berndt (Ref 12) and Berndt and DeWeese (Ref 13), of full size parachutes are marked in Figs 19, 20, and 21. As shown, the stiffness index of the full size parachute is considerably smaller than the one of the most flexible model parachute. Therefore, the slower rate of area growth of the prototype parachute compared with the one of the two models fits the concept that parachutes with lower stiffness indexes have a slower area increase. At the lowest velocity the model characteristic fits the full size parachute best. It is also seen that the velocity influences the rate of area growth of the models. This effect, however, cannot be explained at this time.

In summary from these measurements one can conclude that the stiffness index of a parachute influences significantly the slope of the area-time relationship.

Further characteristic terms in the equation of motion are the velocity-time functions. For the conventional parachute model, Figs 22, 23, and 24 show the relative velocity versus time at three different snatch velocities (Ref 11) while Figs 25, 26, and 27 show the velocity-time histories recorded with the more flexible model. For easier comparison, these velocity characteristics are combined in Figs 28, 29, and 30.

These velocity curves show characteristics as one can expect from the area-time relationships. Corresponding to the rate of projected area growth, the system velocity of the stiffer model increased initially faster and then slower than the one of the more flexible model.

Figures 31 and 32 are sequence pictures taken from a high speed motion film showing in profile and projection the stiffer and the more flexible models during the period of inflation. These figures demonstrate clearly the characteristics which one gets from analyzing the area- and velocity-time histories.

C. Force-Time Histories

Force-time or acceleration-time histories were influenced by the effects of the model or prototype parachute stiffness. By means of the test arrangement shown in Fig 12, numerous force-time recordings were made, and Figs 33, 34, and 35 show individual data points and curves representing averages of experimental data obtained with the more flexible model, $\eta = 0.60$. Similar measurements were made with the conventional model, $\eta = 1.04$, and in Figs 36, 37, and 38 the results of both series of tests are compared. The similarity of the force-time histories was evident, and the maximum parachute force of the flexible model was 30 to 40 per cent lower than the one of the stiffer model.

It will be noted that in the force-time diagrams the conventionally built models showed in the initial phase an extremely strong force oscillation. This should not be considered realistic, because this phenomenum was probably caused by mechanical vibrations and electric noise. In subsequent tests the test apparatus was improved and the recordings assumed a more steady form.

All curves showing the characteristics of the inflation process are related to the dimensionless filling time, $T = t/t_f$. The filling time, t_f, is defined in accordance with Ref 12 as that instant at which the parachute canopy initially reaches the same projected area as it will assume at the steady state descent. Figure 39 shows the average filling times obtained with the conventional and the flexible parachute models. This characteristic time differs considerably for the two parachutes, which can be assumed to be caused by the difference of model stiffness. It should be mentioned, however, that the definition of filling time in this manner refers to a geometric condition and, as shown in Figs 25 through 30, is, in general, not the instant at which equilibrium is reached.

IV. PARACHUTE SQUIDDING STUDIES

Another, but so far insufficiently explained parachute performance, is the so-called squidding. In full size experiments this phenomenon has been observed in numerous cases. Usually squidding occurs if the surface loading of the parachute is too high, the nominal or effective porosity exceeds certain limits, and in cases of relatively high release velocities. Some indications also have been obtained that the stiffness of the parachute skirt influences the squidding characteristic or the so-called critical speed. In view of these known facts, free flight model tests were made in which the two parachute models were injected into calm air by means of a parachute catapult. Between the parachute canopy and suspended weight, strain gage force sensors were arranged and force-time recordings during deployment, inflation, and descent were obtained. The descending parachute models were also photographed with a high speed motion picture camera.

The objective of these tests was to find possibly existing inflation characteristics related to model stiffness indexes to see if the often observed squidding phenomenon could be reproduced in model tests, and under which conditions this squidding would occur.

Figures 40 and 41 show the previously mentioned force recordings. Referring to Fig 40, it was physically observed that under the test conditions as identified, the conventional model, $\eta = 1.04$, inflated regularly and in a relatively short time. Under the same test conditions, the flexible model, $\eta = 0.60$, failed several times to inflate fully prior to ground impact. Related to these observations, one notices in the three diagrams reproduced in Fig 40 significant differences. One sees that in the case where the flexible parachute did inflate, the force onset and the peak forces were lower and the time to reach equilibrium force conditions longer than the respective values of stiffer models. In summary, the flexible parachute, when it inflated, had a lower but longer force-time history. In cases where the parachute model with the lower stiffness index failed to inflate, the sensor indicated at ground impact an abrupt force reduction to zero from a level much higher than that corresponding to steady state condition. From the indicated time scale, it can also be concluded that the average speed of the squidding parachute during the filling distance was much higher than in the cases when the same parachute did inflate.

IV. PARACHUTE SQUIDDING STUDIES

Another, but so far insufficiently explained parachute performance, is the so-called squidding. In full size experiments this phenomenon has been observed in numerous cases. Usually squidding occurs if the surface loading of the parachute is too high, the nominal or effective porosity exceeds certain limits, and in cases of relatively high release velocities. Some indications also have been obtained that the stiffness of the parachute skirt influences the squidding characteristic or the so-called critical speed. In view of these known facts, free flight model tests were made in which the two parachute models were injected into calm air by means of a parachute catapult. Between the parachute canopy and suspended weight, strain gage force sensors were arranged and force-time recordings during deployment, inflation, and descent were obtained. The descending parachute models were also photographed with a high speed motion picture camera.

The objective of these tests was to find possibly existing inflation characteristics related to model stiffness indexes to see if the often observed squidding phenomenon could be reproduced in model tests, and under which conditions this squidding would occur.

Figures 40 and 41 show the previously mentioned force recordings. Referring to Fig 40, it was physically observed that under the test conditions as identified, the conventional model, $\eta = 1.04$, inflated regularly and in a relatively short time. Under the same test conditions, the flexible model, $\eta = 0.60$, failed several times to inflate fully prior to ground impact. Related to these observations, one notices in the three diagrams reproduced in Fig 40 significant differences. One sees that in the case where the flexible parachute did inflate, the force onset and the peak forces were lower and the time to reach equilibrium force conditions longer than the respective values of stiffer models. In summary, the flexible parachute, when it inflated, had a lower but longer force-time history. In cases where the parachute model with the lower stiffness index failed to inflate, the sensor indicated at ground impact an abrupt force reduction to zero from a level much higher than that corresponding to steady state condition. From the indicated time scale, it can also be concluded that the average speed of the squidding parachute during the filling distance was much higher than in the cases when the same parachute did inflate.

V. SUMMARY AND CONCLUSION

The preceding results indicate a moderate influence of the model stiffness index upon the coefficient of effective drag and a relatively strong influence upon the significant time functions, the measured forces or related acceleration, and the parachute squidding characteristics.

The coefficient of effective drag, $C_{D_{eff}}$, increased by approximately 8% when the stiffness index of otherwise identical parachute models decreased from $\eta = 1.04$ to 0.60. Introducing this drag increase as a correction factor to earlier measurements performed on models with at least $\eta = 1.04$ provided wind tunnel coefficients which were practically the same as the coefficients obtained in field tests with 100 ft parachutes. All tests were made in the incompressible flow regime at Reynolds Numbers of 4.2×10^5 and 1.7×10^7.

The profiles of the model with the lower stiffness index were wider and lower than the ones of the stiffer model. The projected area of the more flexible model was approximately 8% larger than the one of the stiffer model. The force measurements were made at the approximate trim angle of 20°. However, these tests were of an exploratory nature and more complete measurements are desirable.

During the inflation the time histories of area, velocity, and force showed a strong dependence upon the model stiffness index. The area-time history of the flexible model at low wind tunnel speed approximated surprisingly close the characteristics of the full size curve. In finite mass wind tunnel tests the peak forces of the stiffer model were 30 to 40% higher than those of the more flexible model.

In free flight tests where the models were ejected by means of a catapult, the model with the lower stiffness index went into a squidding condition whereas the stiffer model inflated regularly. The maximum inflation forces of the stiffer model were also in these tests higher than those of the more flexible models.

As a consequence of these findings, one must conclude that without careful consideration of the stiffness index, the inflation characteristics of model parachutes are not necessarily valid information on which basis the opening performance of full size parachutes can be predicted.

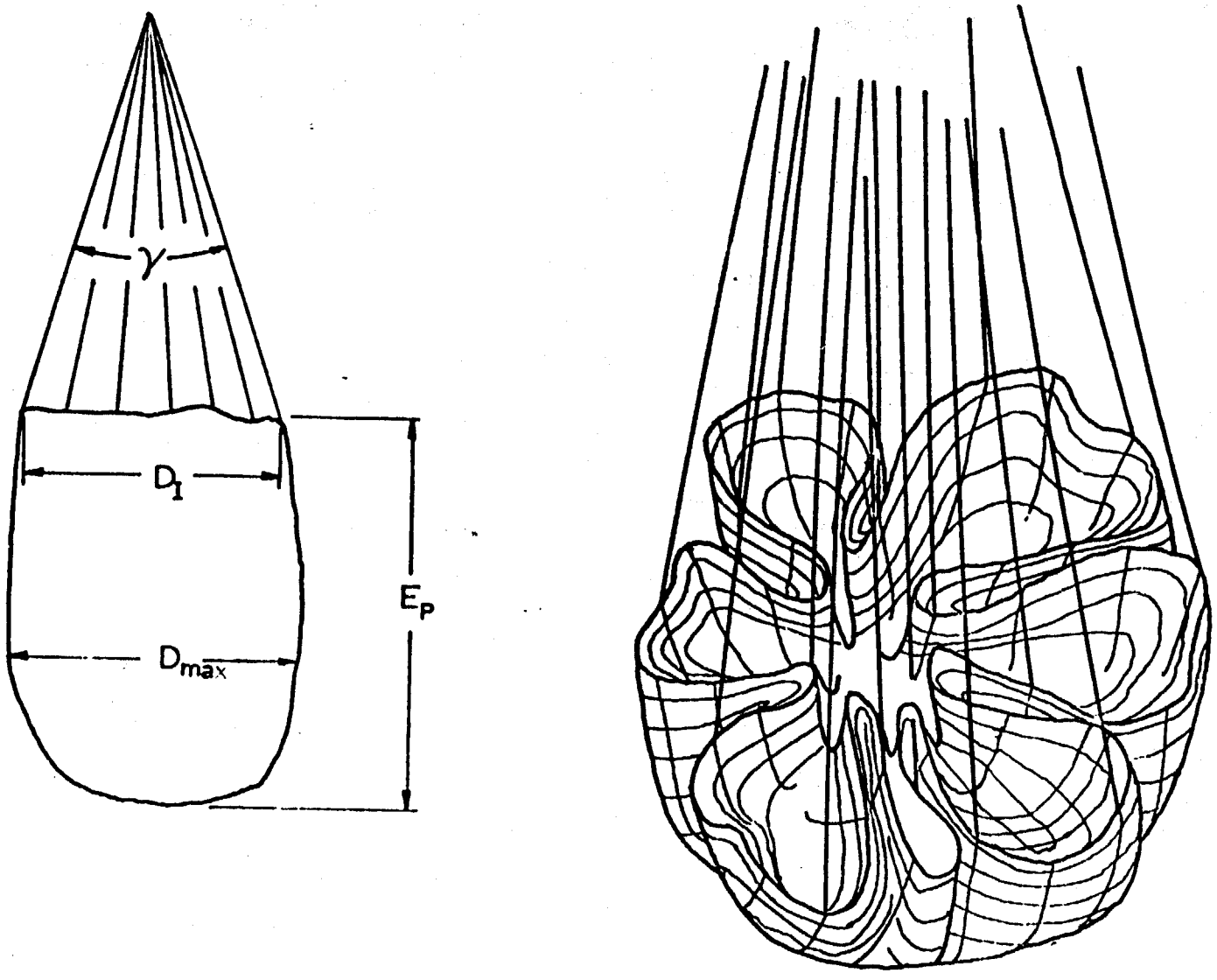

Fig 1 Parachute Canopy Suspension Test Characteristics

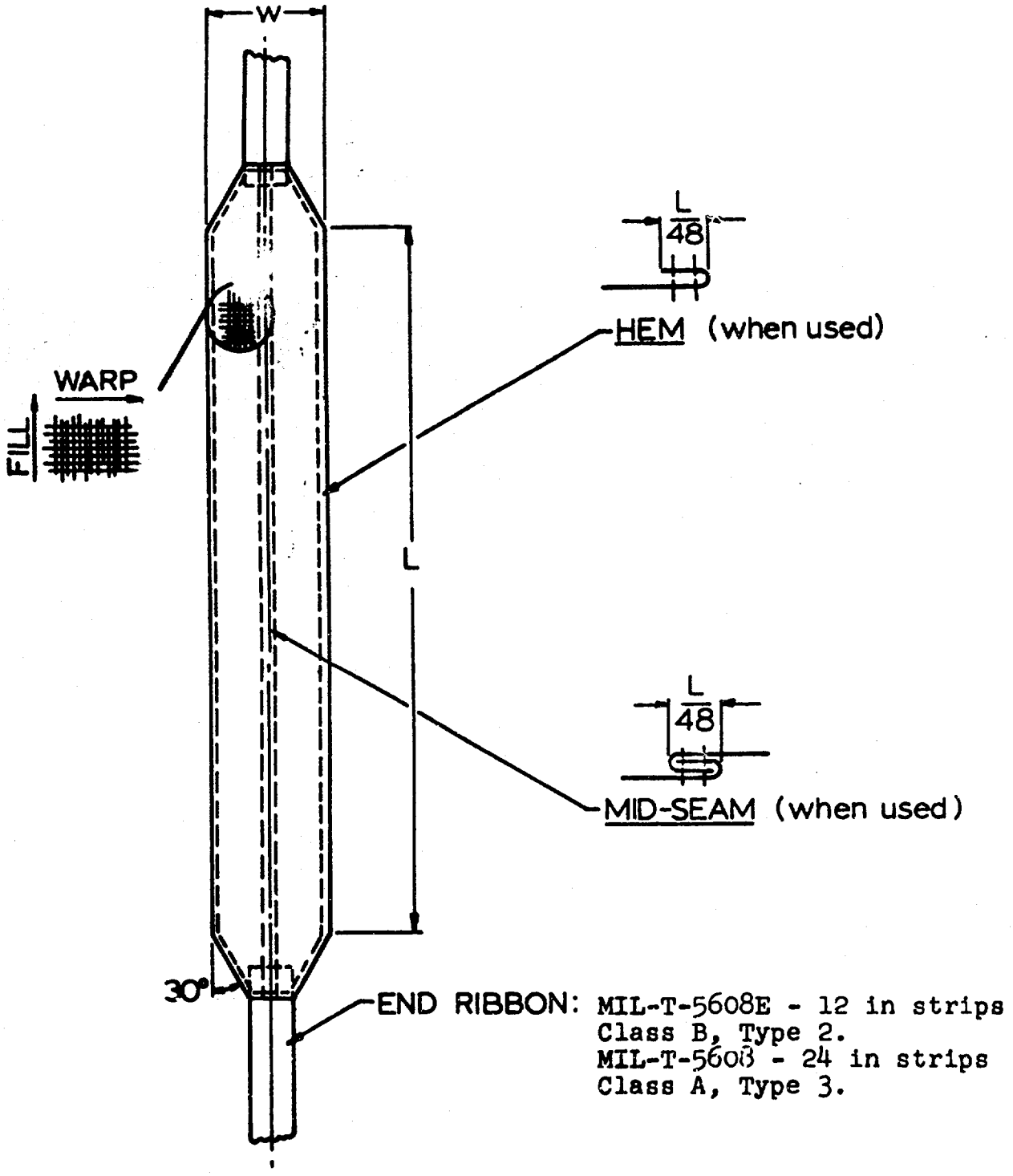

Fig 2 Strip Fabrication Details

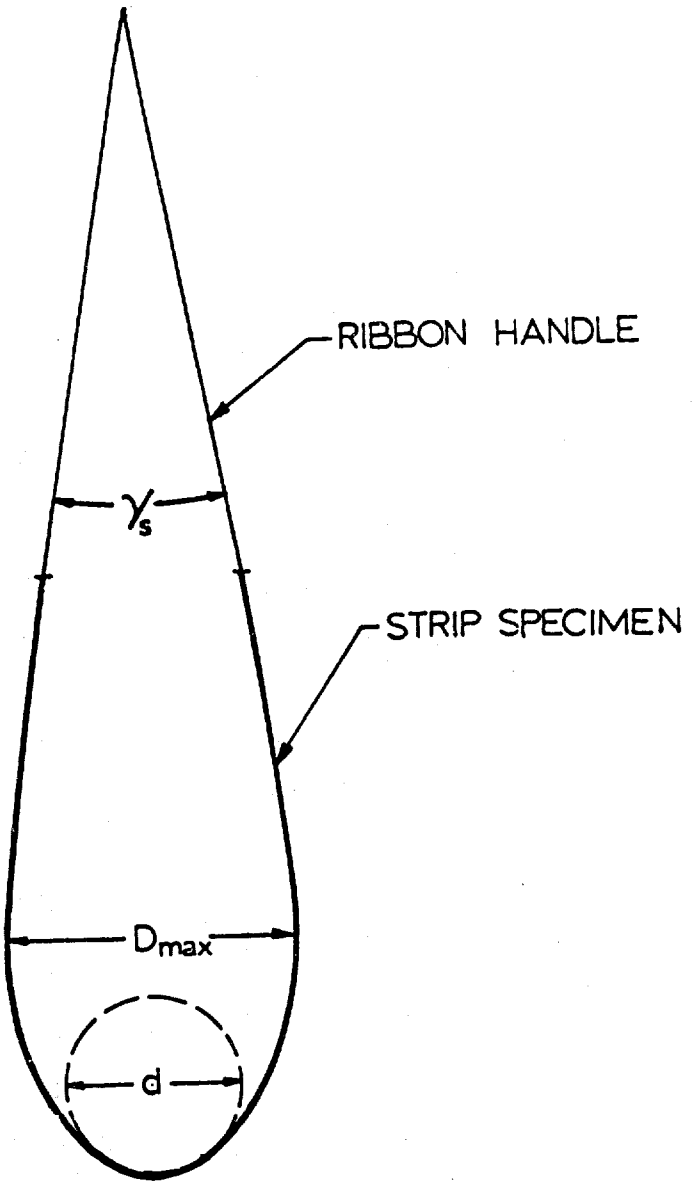

Fig 3 Stiffness Parameters Obtainable from Strip Test

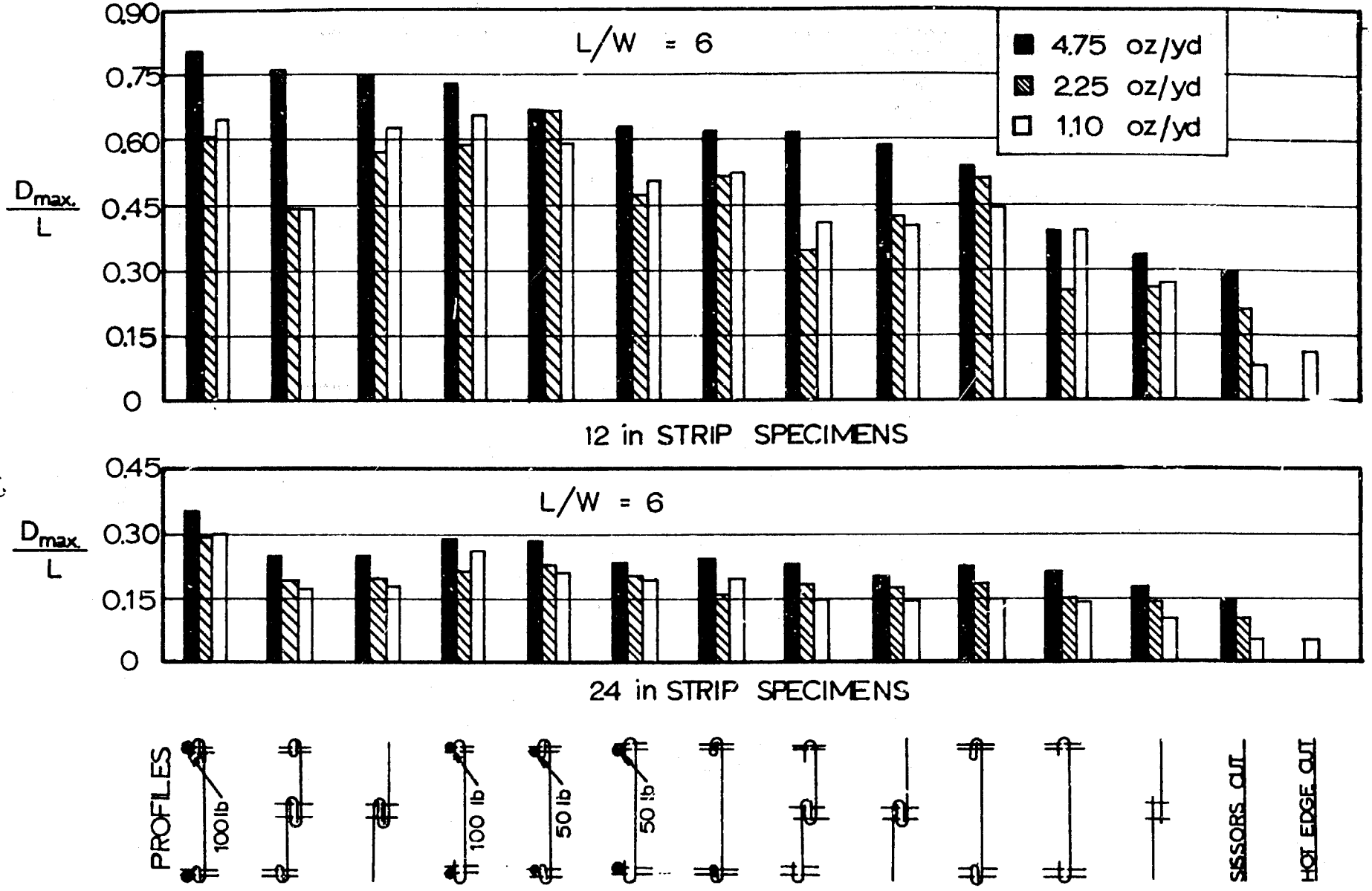

Fig 4 Stiffness Indexes of Geometrically Similar 12 in and 24 in Strips of Different Nylon Materials

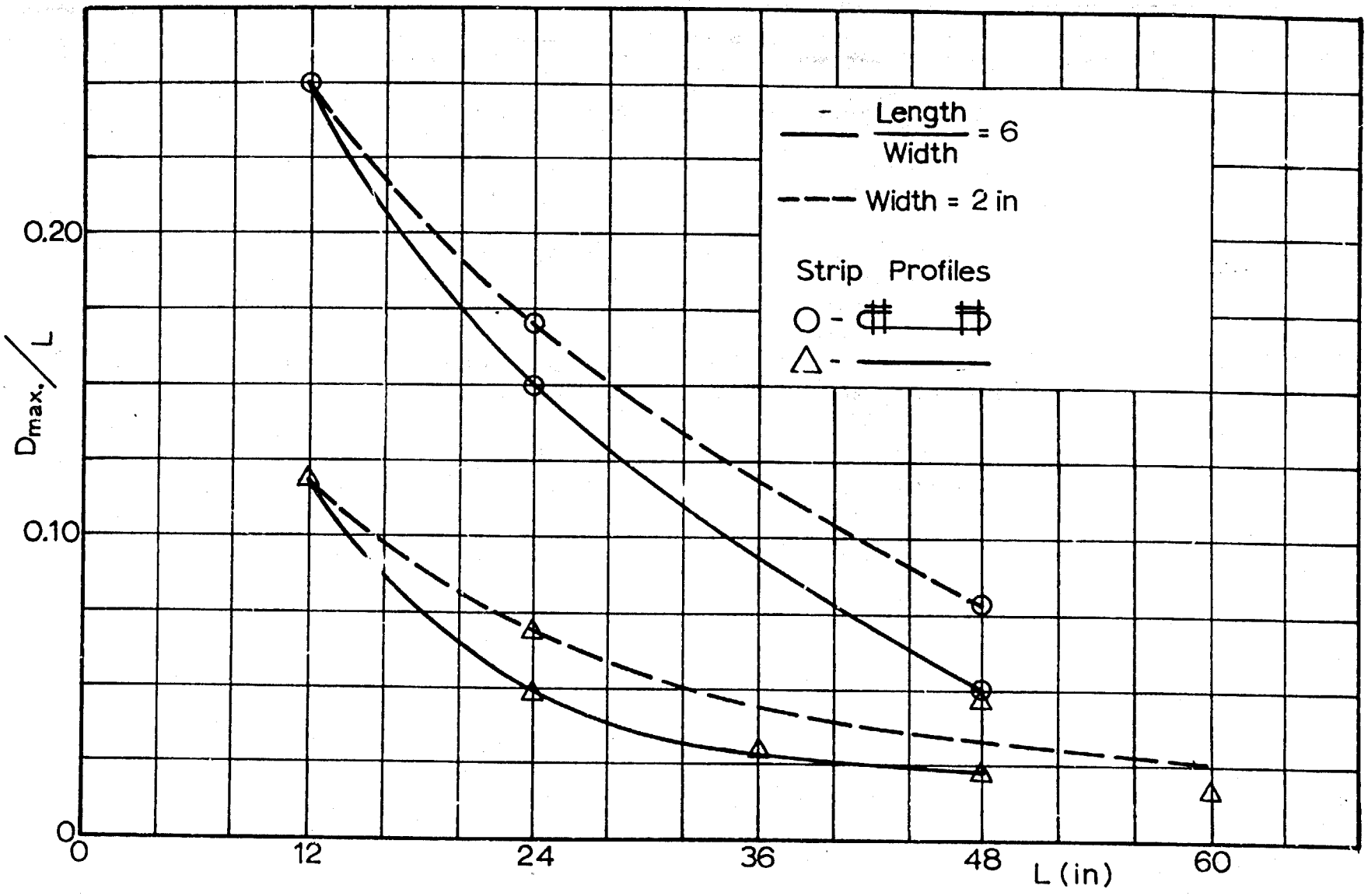

Fig 5 Stiffness Index as a Function of Length and Width of Strips Made of 1.1 oz Nylon Material

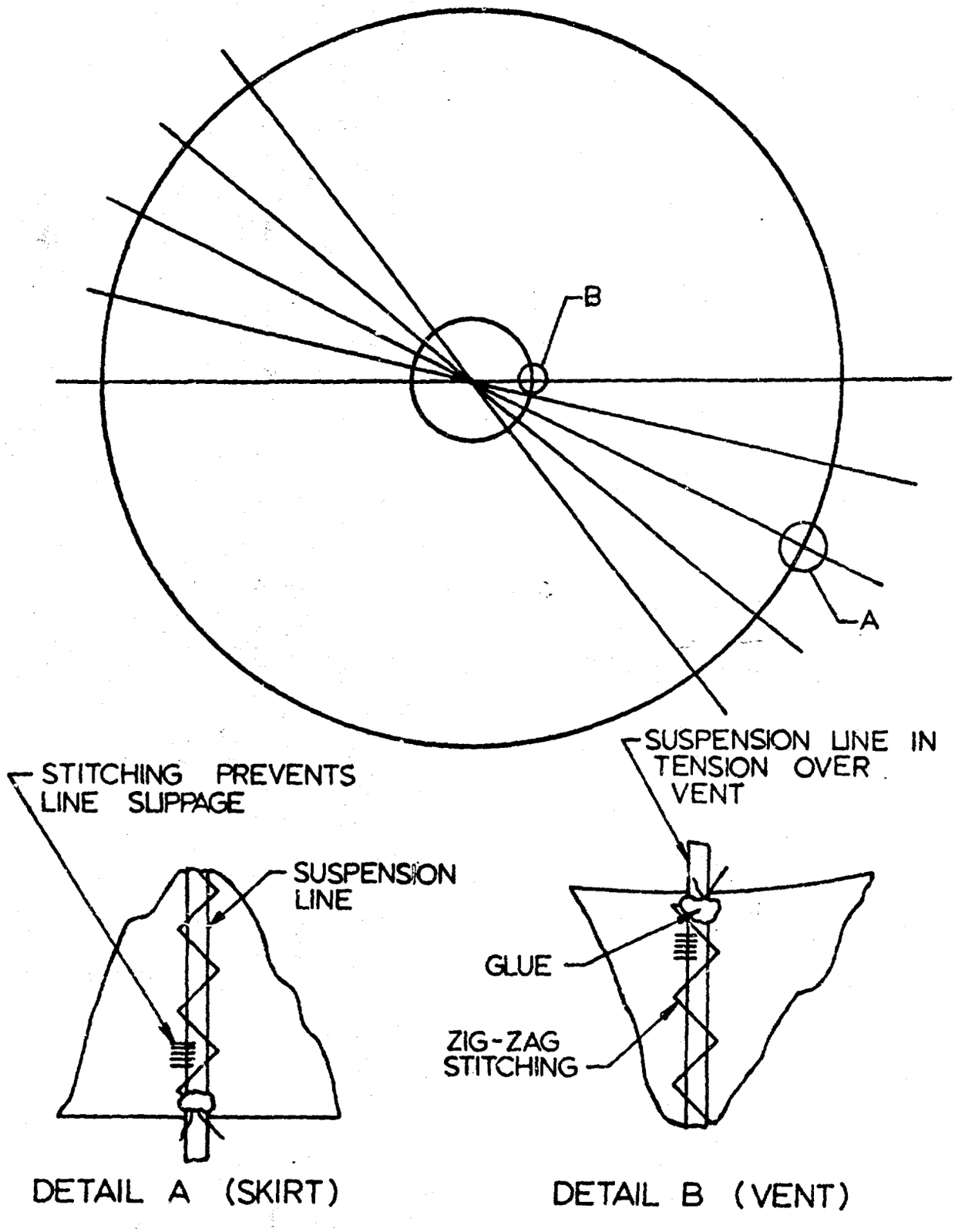

Fig 6 Flexible Solid Flat Parachute Construction Details

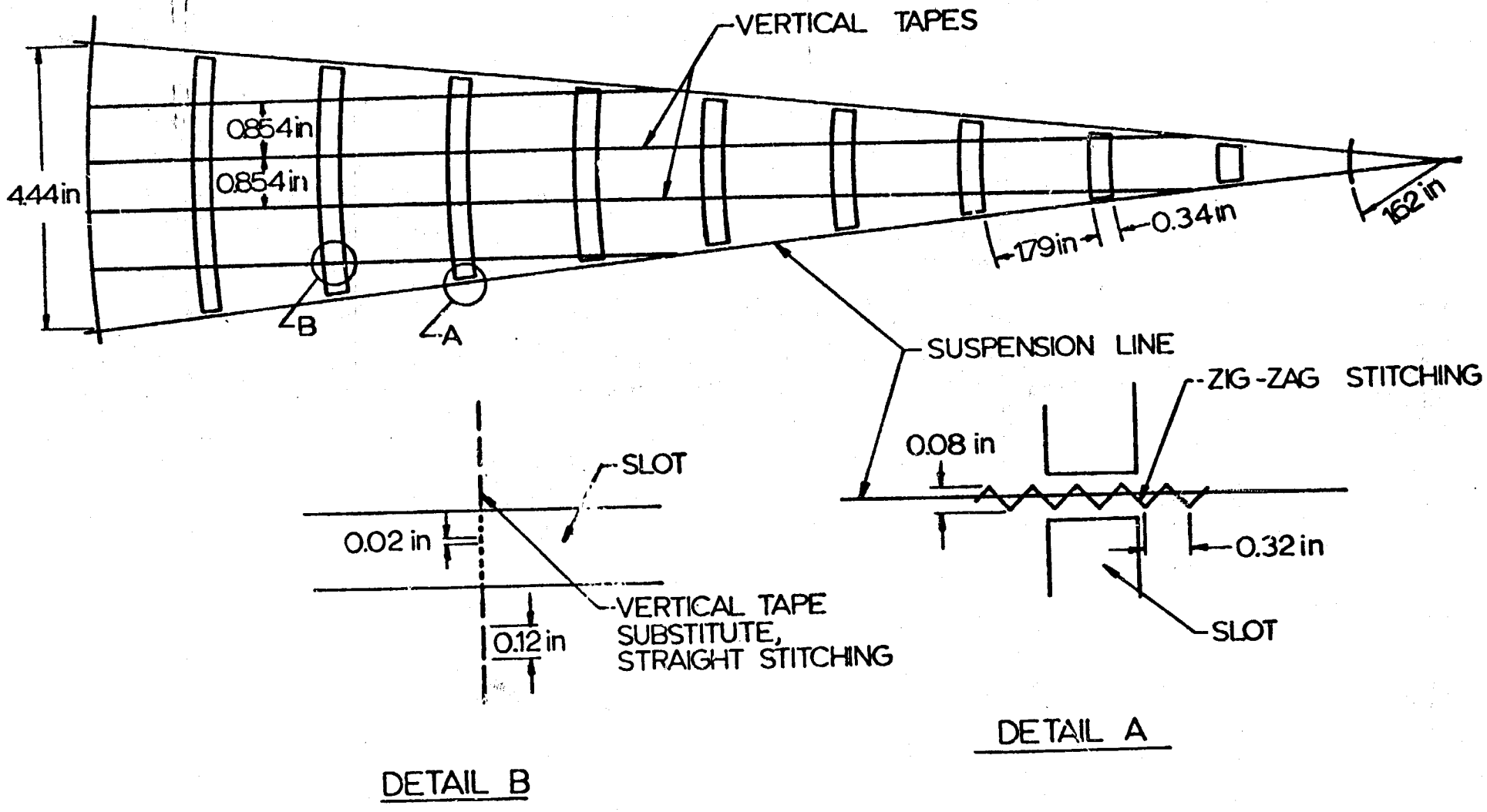

Fig 7 Details of a Ringsiot Parachute Gore Utilizing Hot Knife Cut Fabrication Method

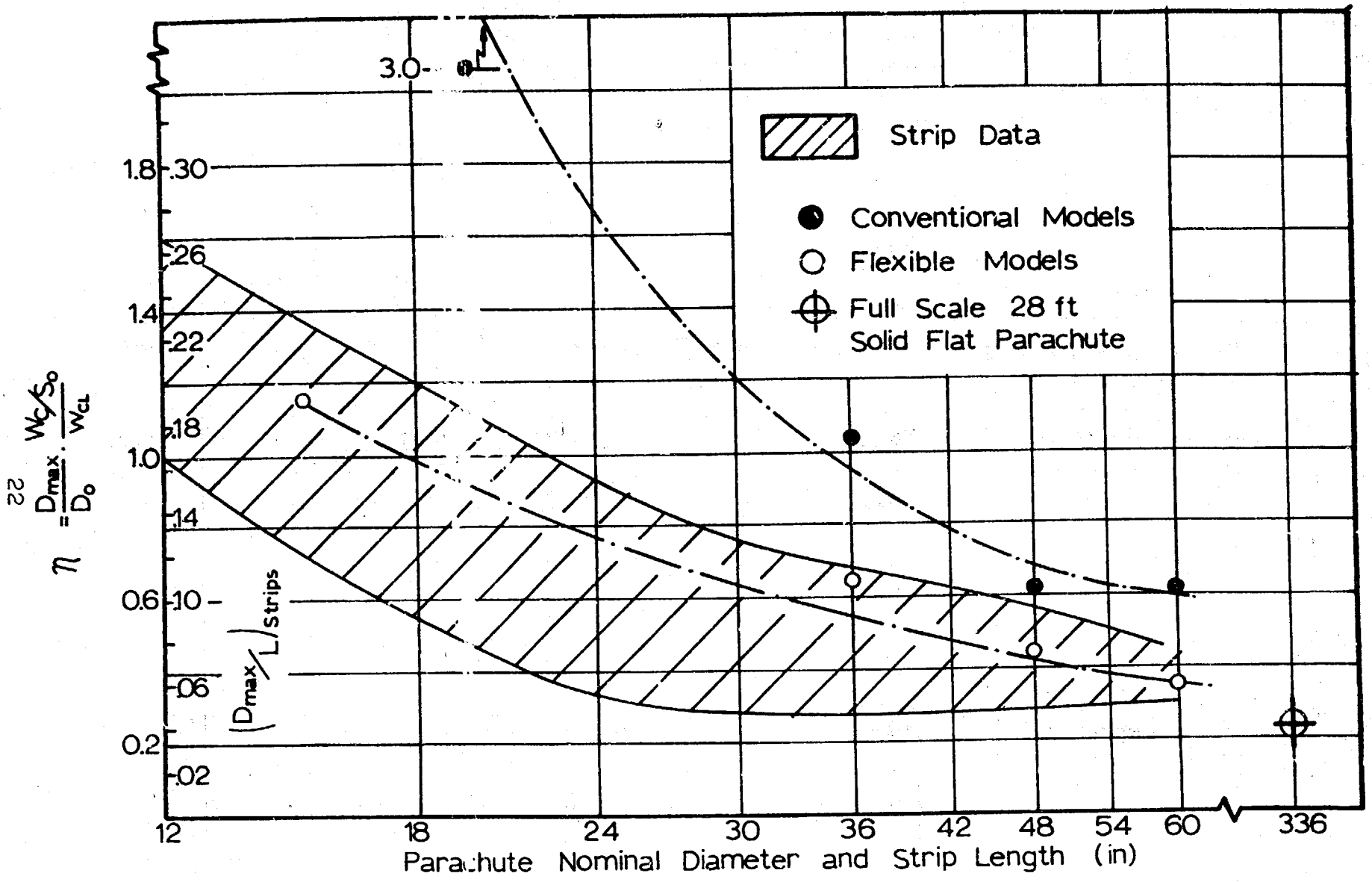

Fig 8 Stiffness Index Comparison of Suspended Model Solid Flat Parachutes and Strip Specimens

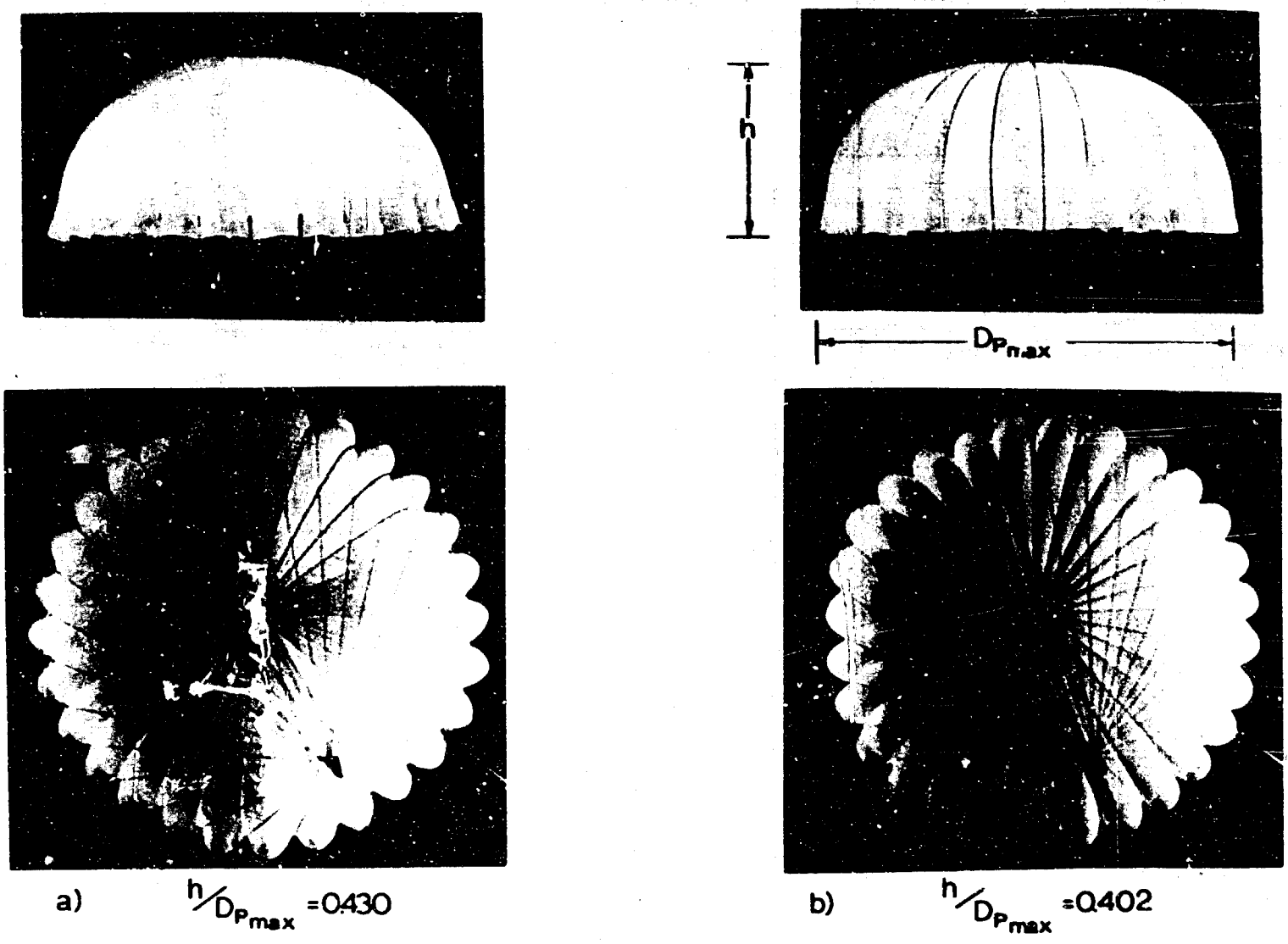

Fig. 9 Conventional, a, and Flexible, b, Models of a 28 Gore Solid Flat Parachute D_o=38 in. at 50 fps Air Velocity

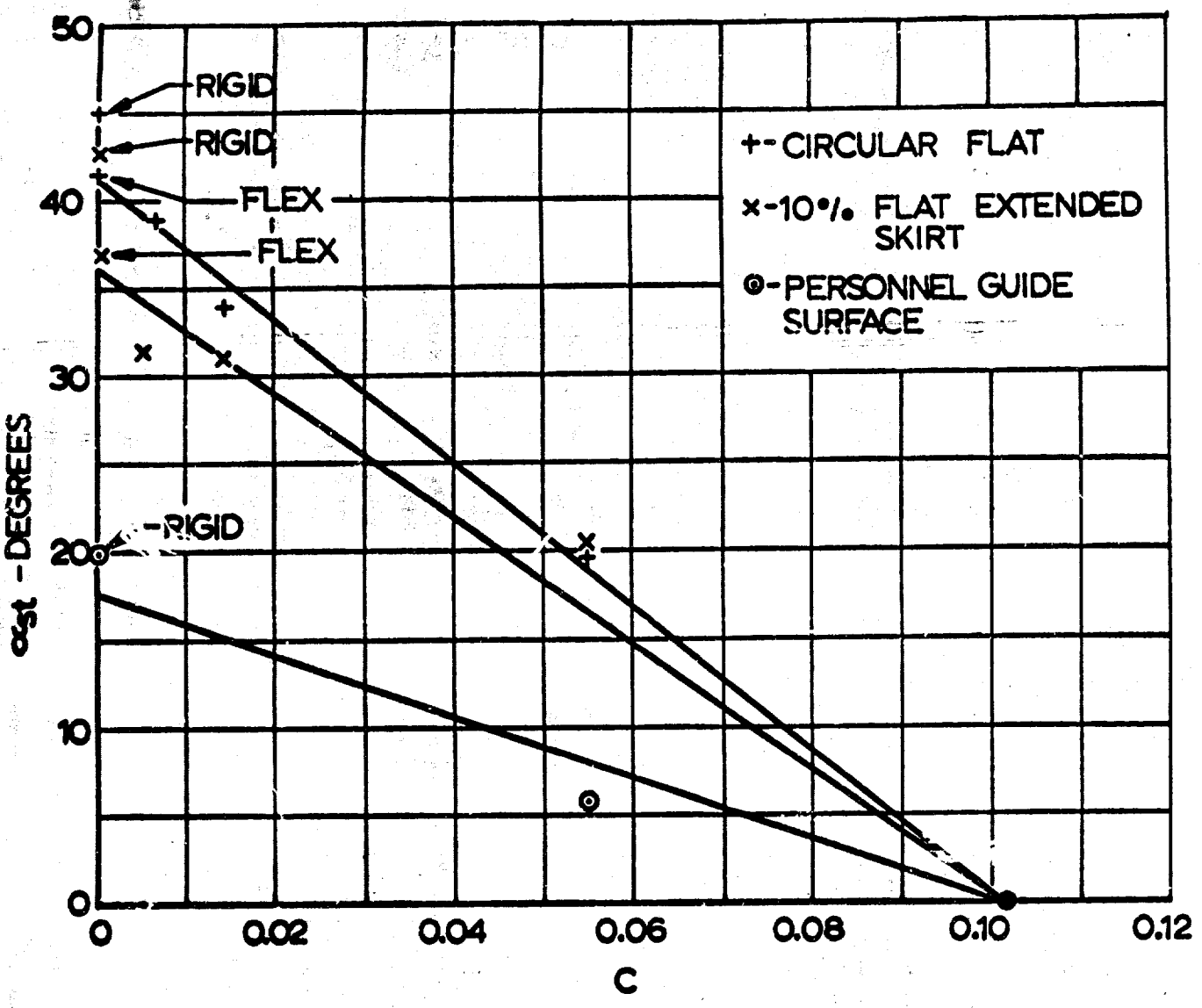

Fig 10 Trim Angle α_{st} of Three Subsonic Parachutes as a Function of Effective Porosity C

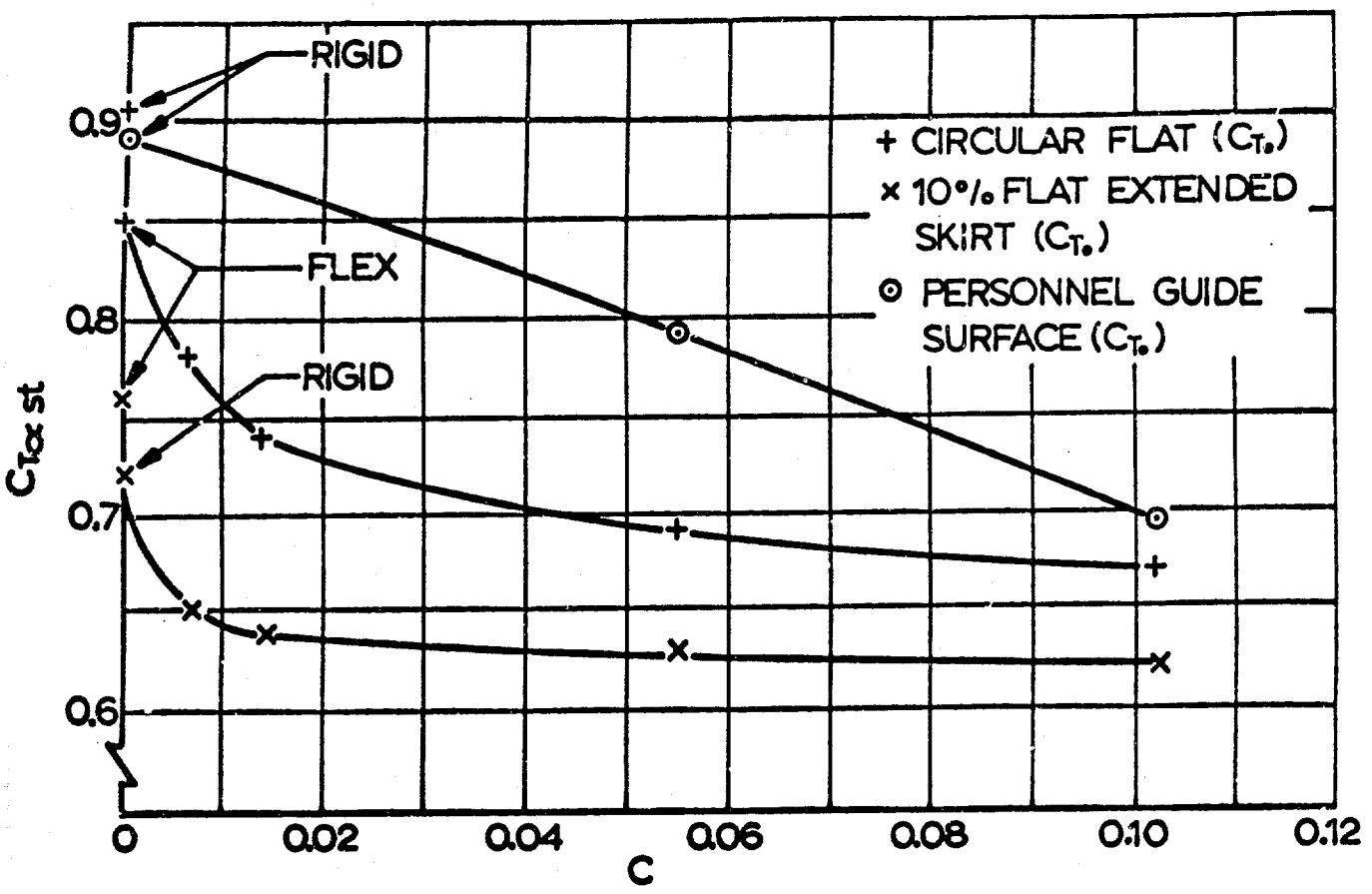

Fig 11 Force Coefficient C_T at Trim Angle α_{st} as Function of Effective Porosity C

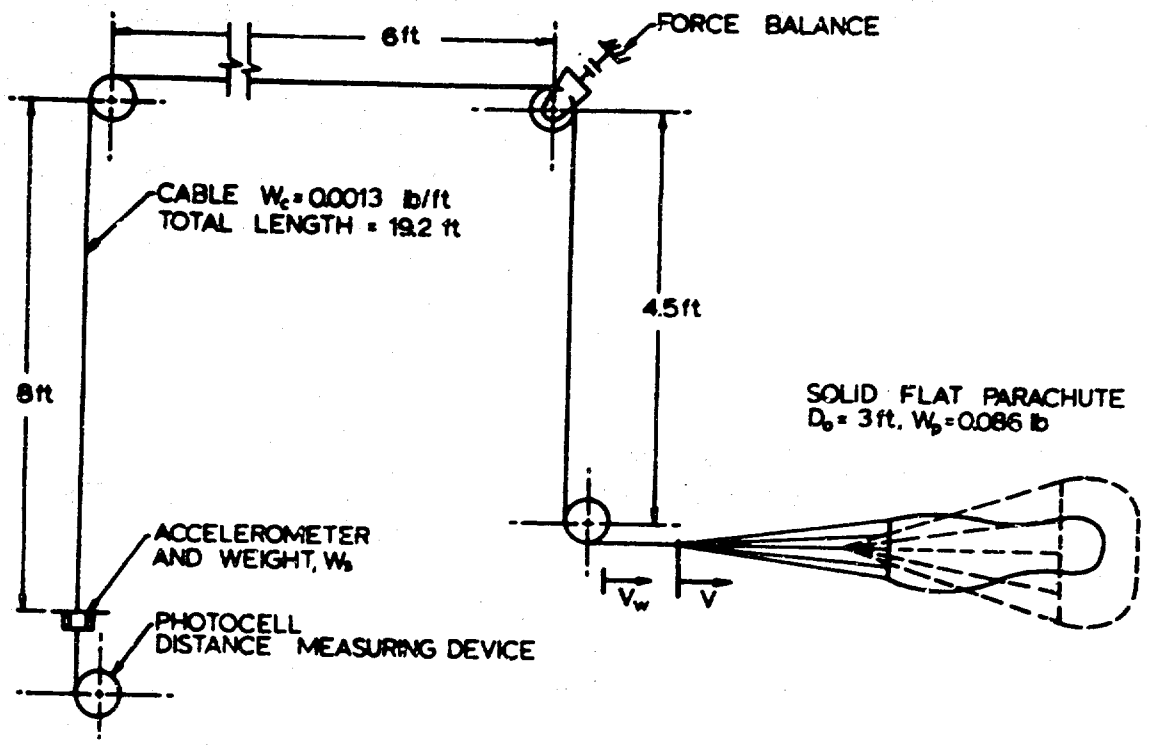

SIDE VIEW

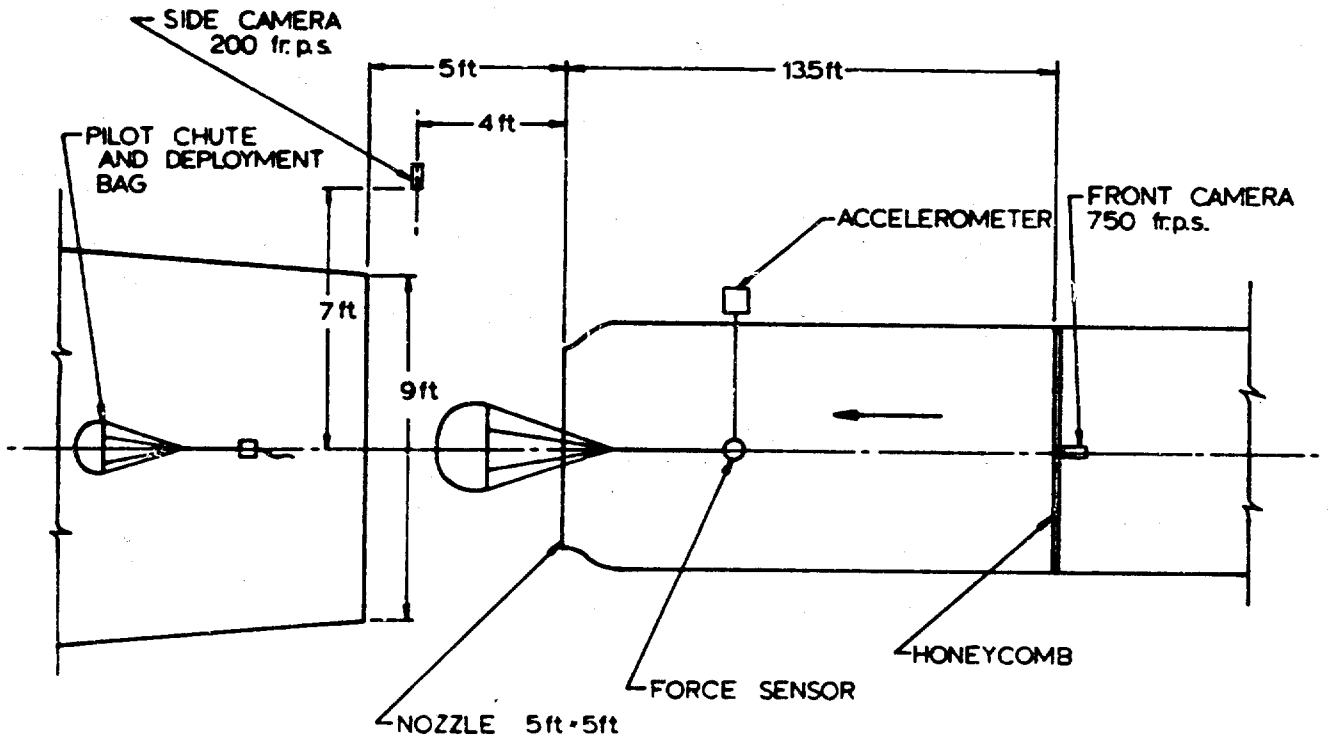

TOP VIEW

Fig12 Wind Tunnel Arrangement for Reproduction and Recording of Significant Characteristics of the Parachute Inflation Process

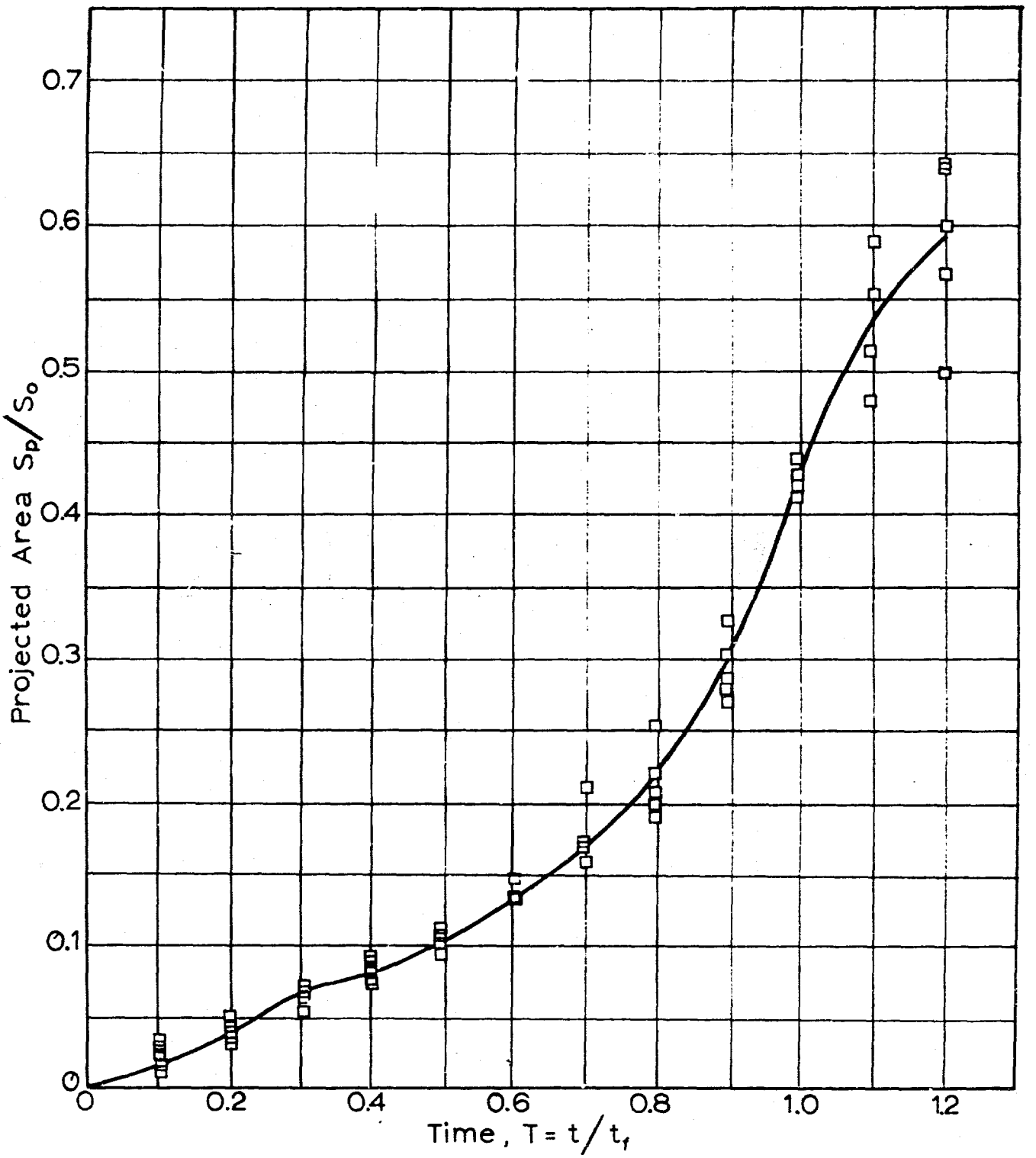

Fig 13 Projected Area, 3 ft Conventional Model, Snatch Velocity = 50 fps, Suspended Weight 0.5 lb

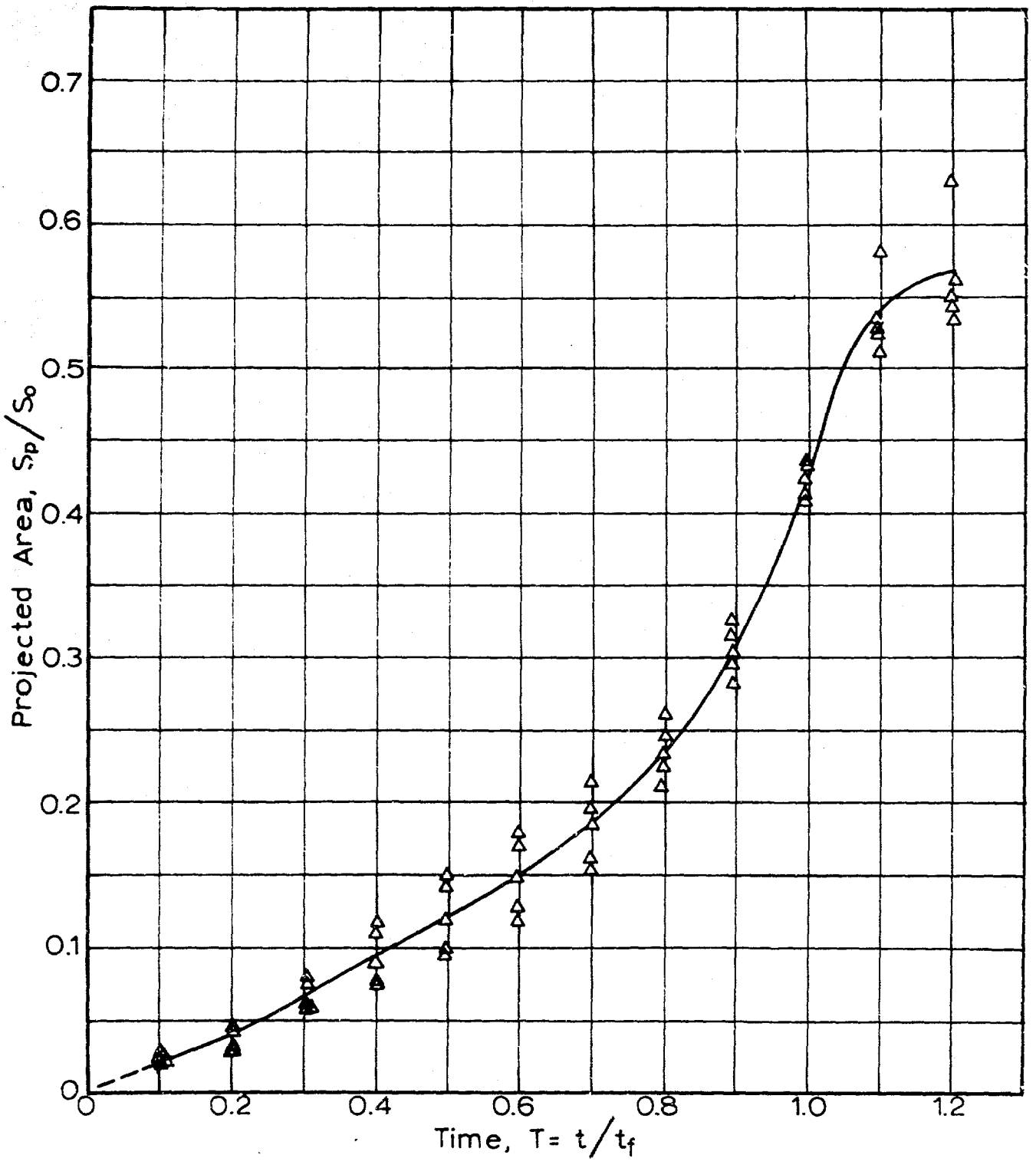

Fig 14 Projected Area, 3 ft Conventional Model, Snatch Velocity 70 fps, Suspended Weight 0.5 lb

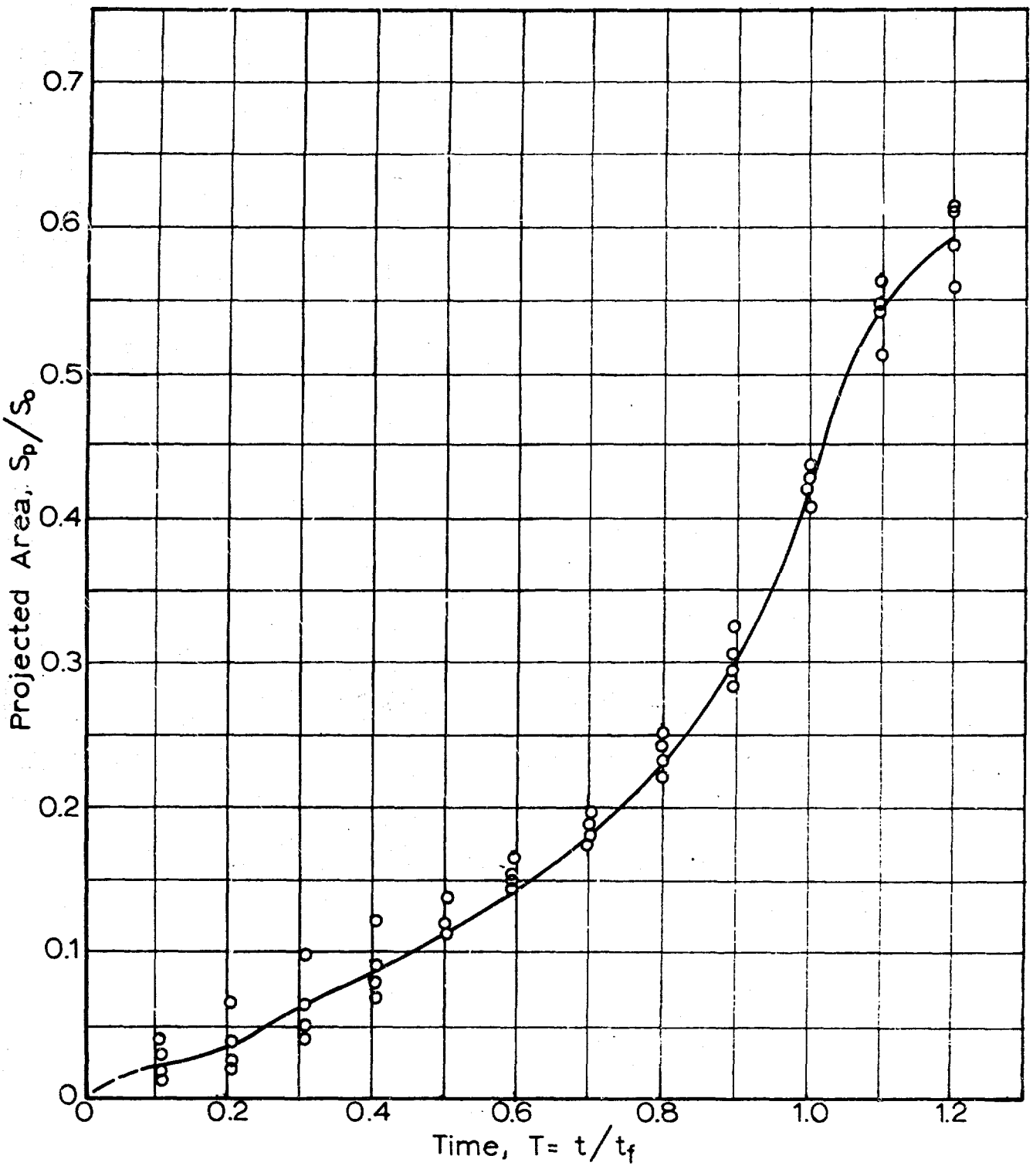

Fig15 Projected Area, 3 ft Conventional Model, Snatch Velocity 85 fps, Suspended Weight 0.5 lb

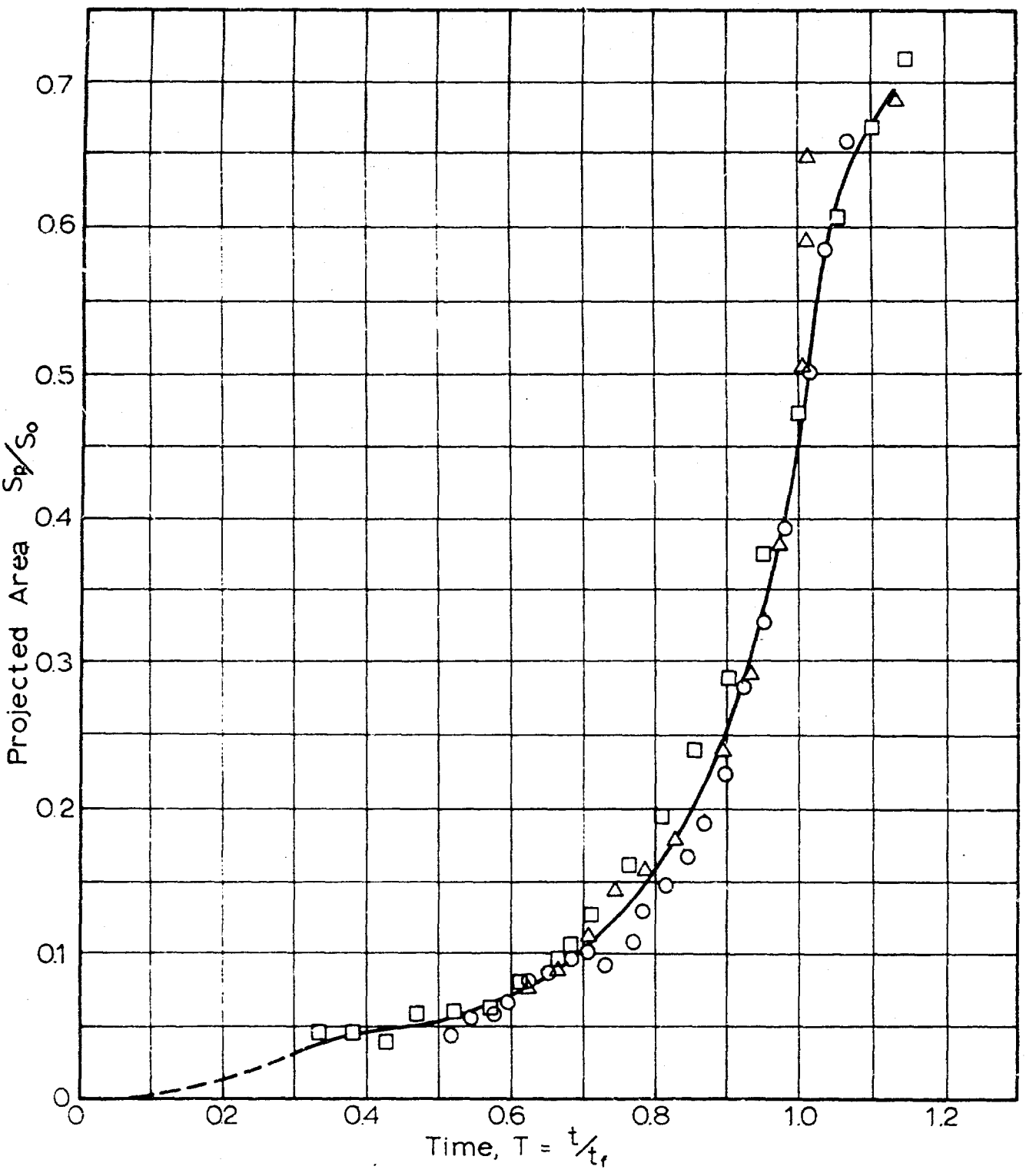

Fig 16 Projected Area 3 ft Flexible Model, Snatch Velocity 50 fps, Suspended Weight 0.5 lb.

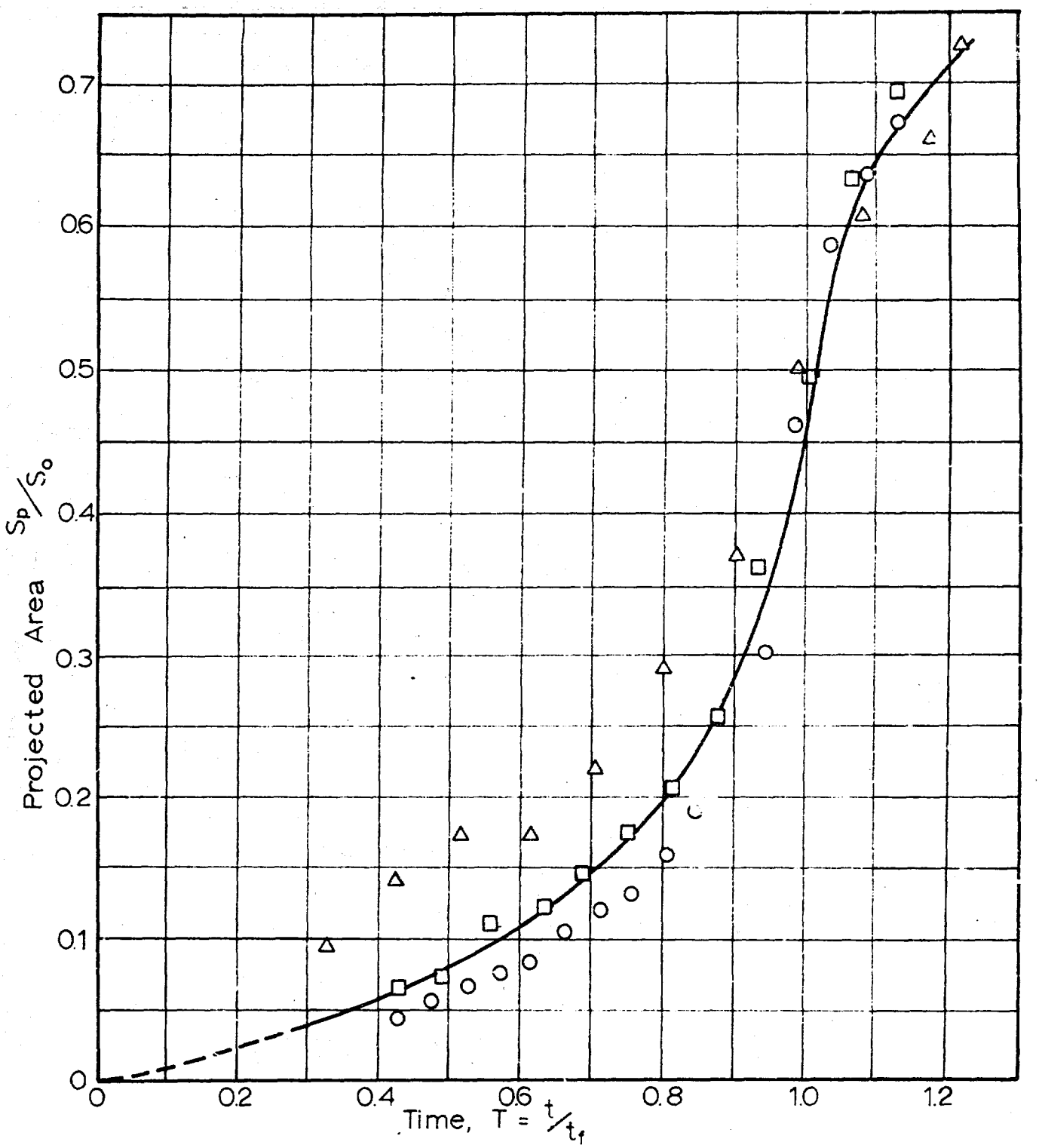

Fig 17 Projected Area, 3 ft Flexible Model, Snatch Velocity 70 fps, Suspended Weight 0.5 lb.

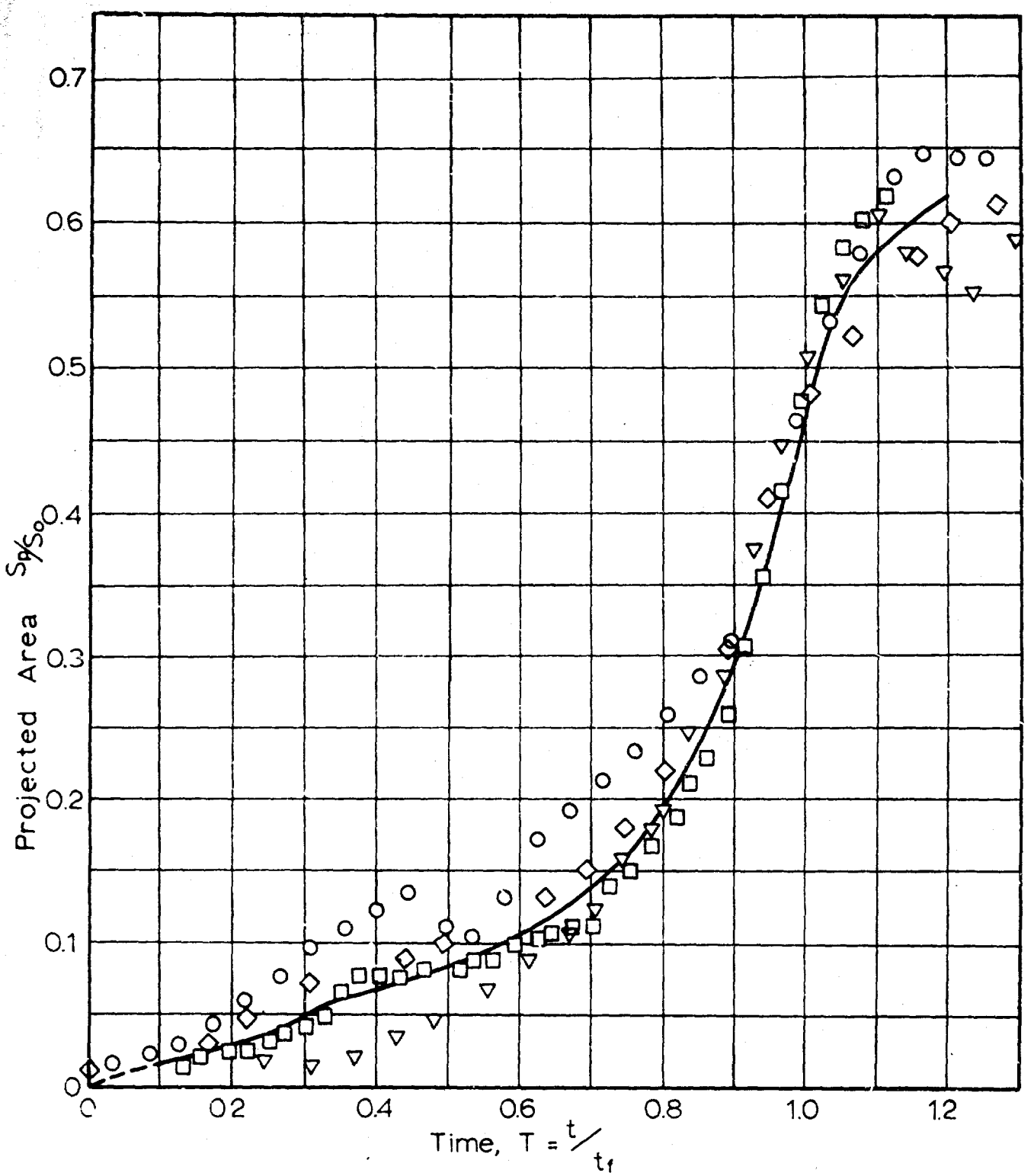

Fig 18 Projected Area, 3 ft Flexible Model, Snatch Velocity 85 fps, Suspended Weight 0.5 lb.

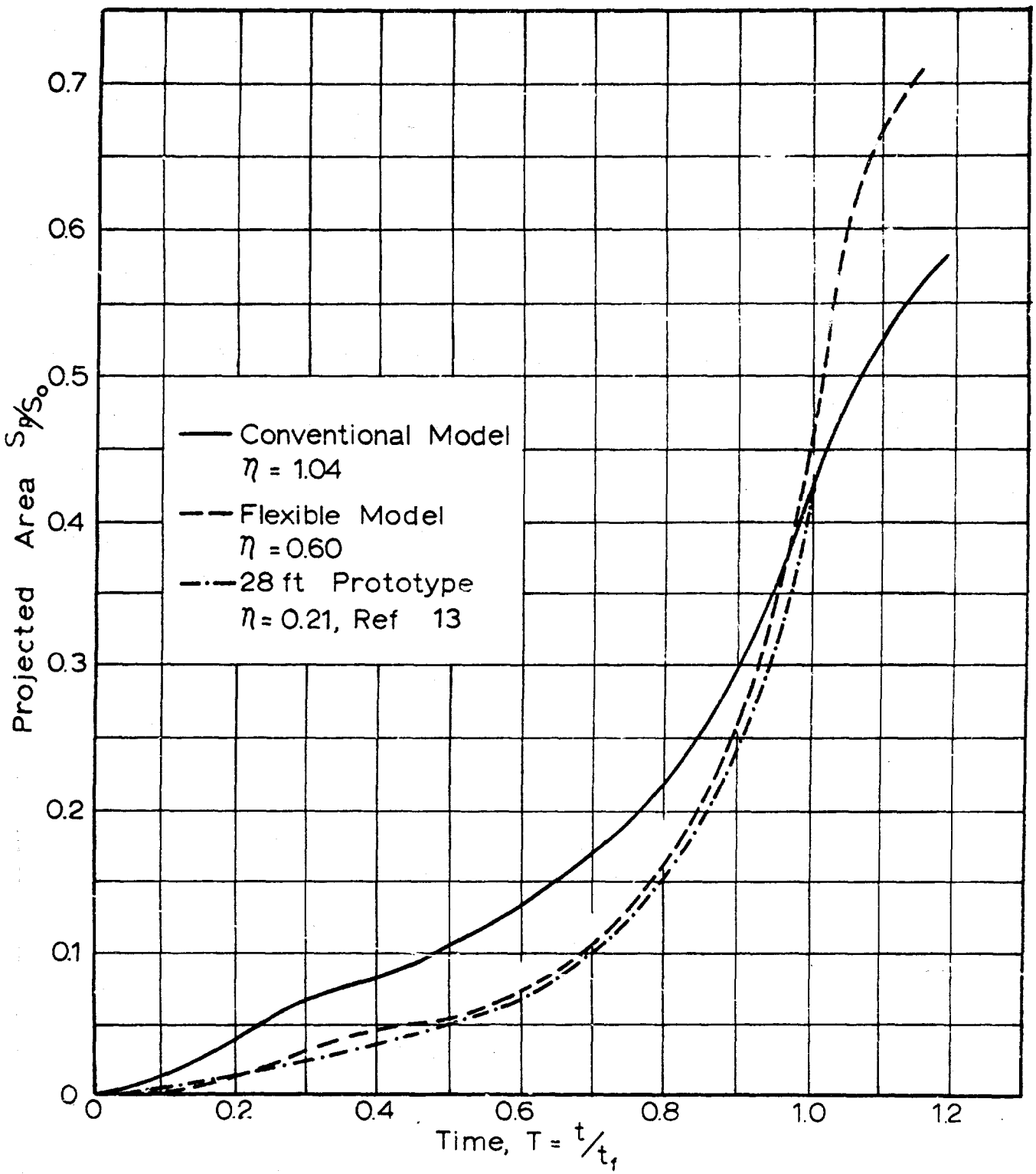

Fig 19 Area-Time History of a Conventional Model, η = 1.04, and a Flexible Model η=0.60, at 50 fps Snatch Velocity.

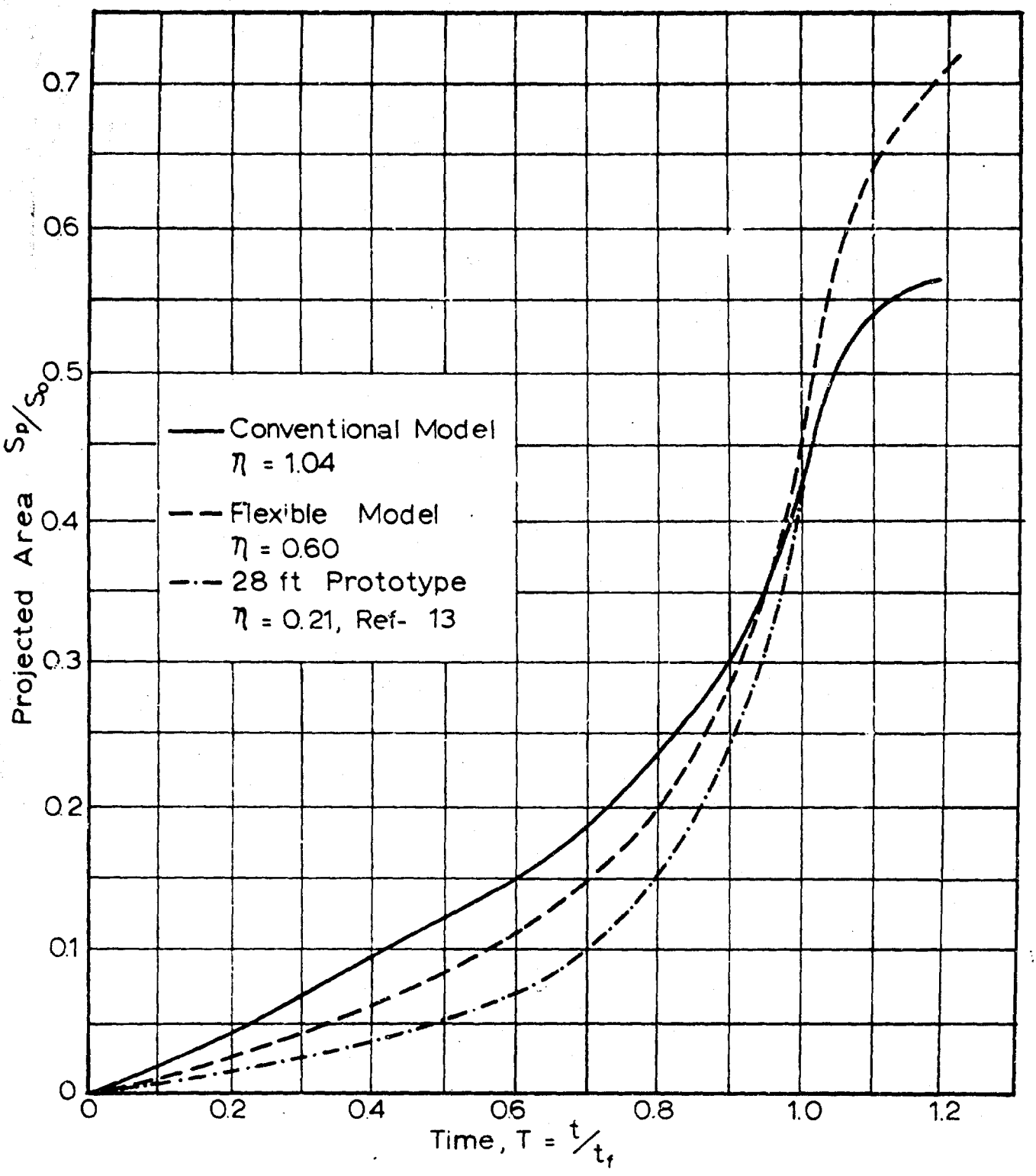

Fig 20 Area-Time History of a Conventional Model, η =1.04 and a Flexible Model η=0.60, at 70 fps Snatch Velocity

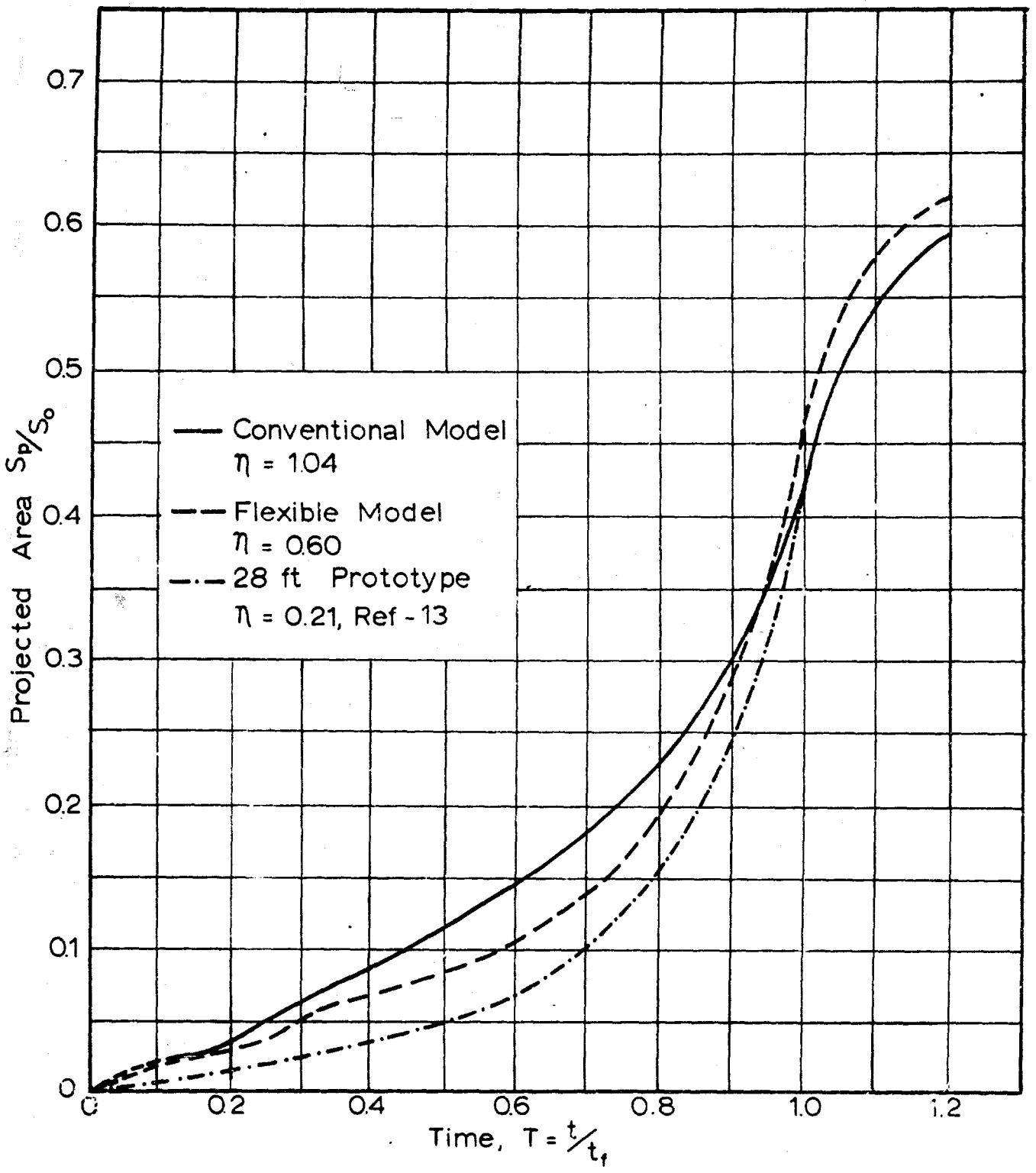

Fig 21 Area-Time History of a Conventional Model, η = 1.04, and a Flexible Model, η = 0.60 at 85 fps Snatch Velocity.

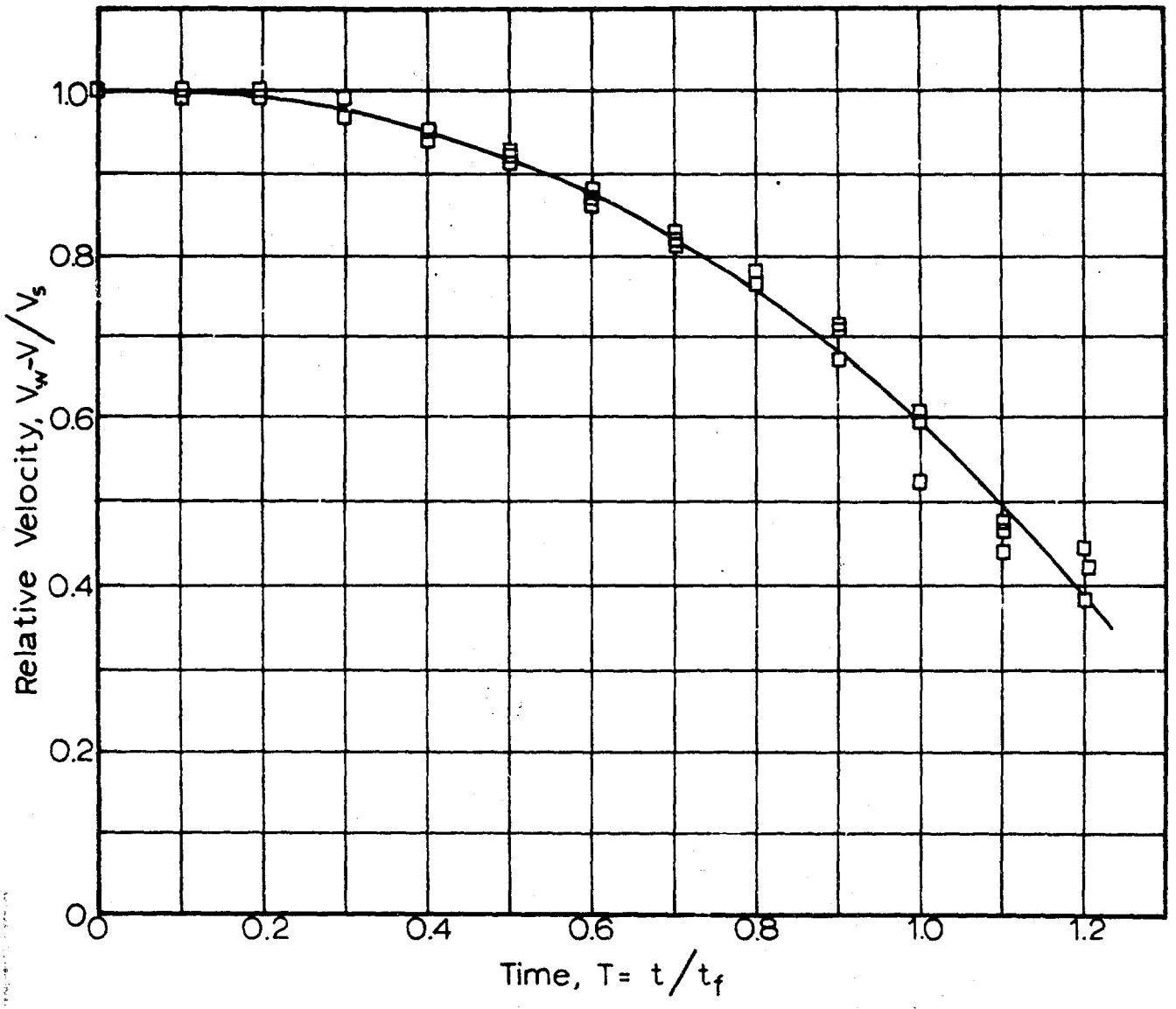

Fig 22 Relative Velocity, 3 ft Conventional Model, Snatch Velocity 50 fps, Suspended Weight 0.5 lb

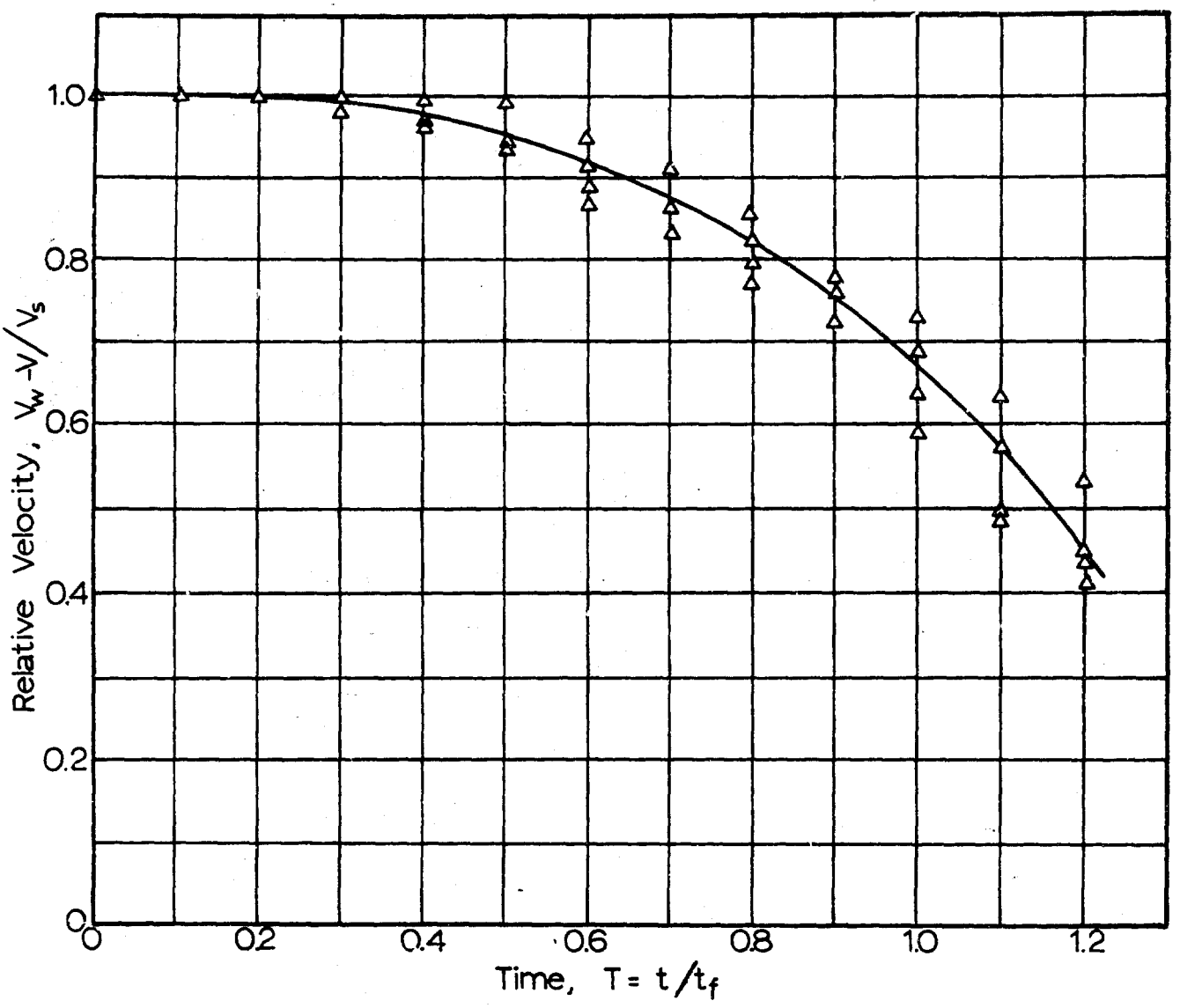

Fig 23 Relative Velocity, 3ft Conventional Model, Snatch Velocity 70 fps, Suspended Weight 0.5 lb

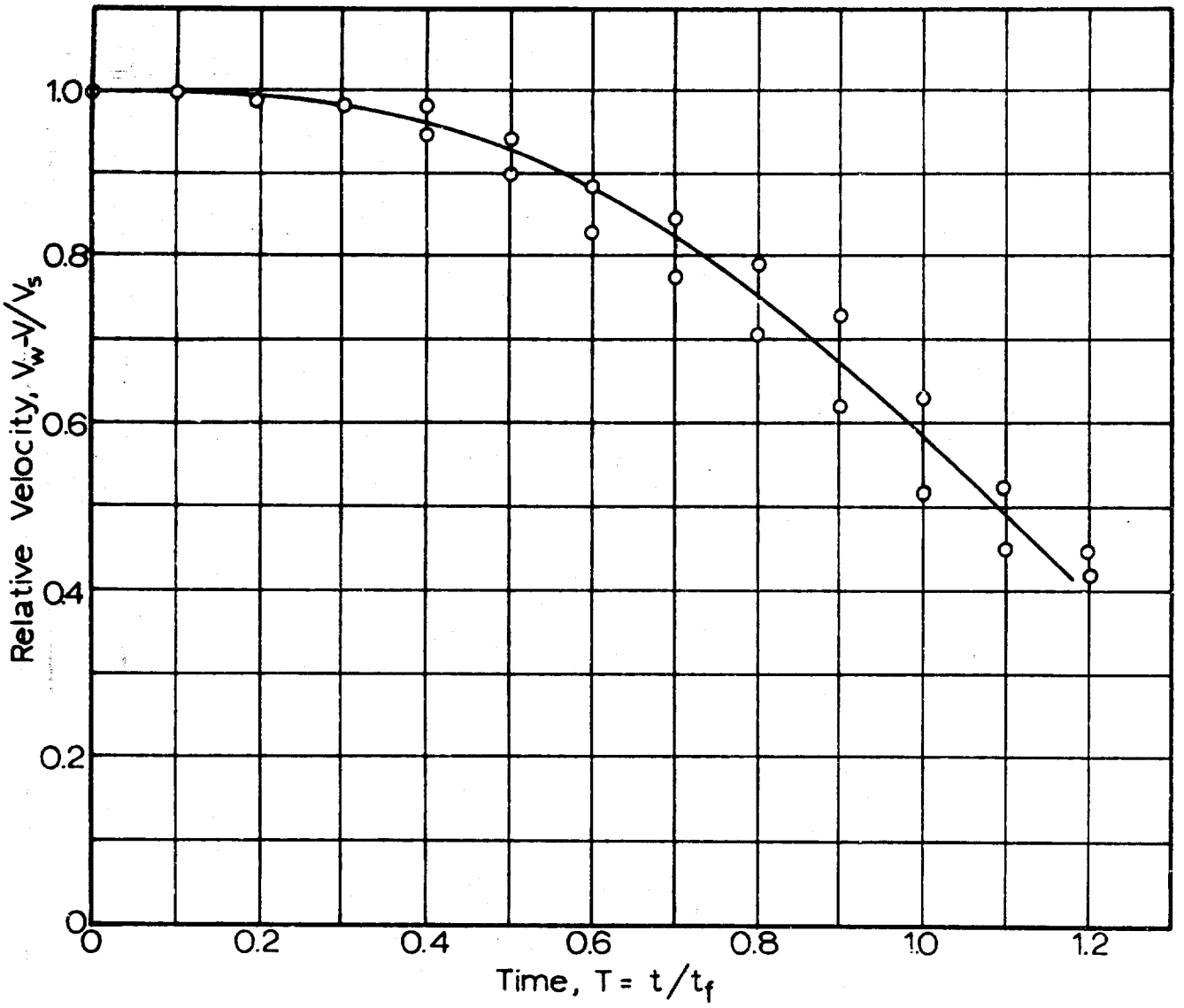

Fig 24 Relative Velocity, 3 ft Conventional Model, Snatch Velocity 85 fps, Suspended Weight 0.5 lb

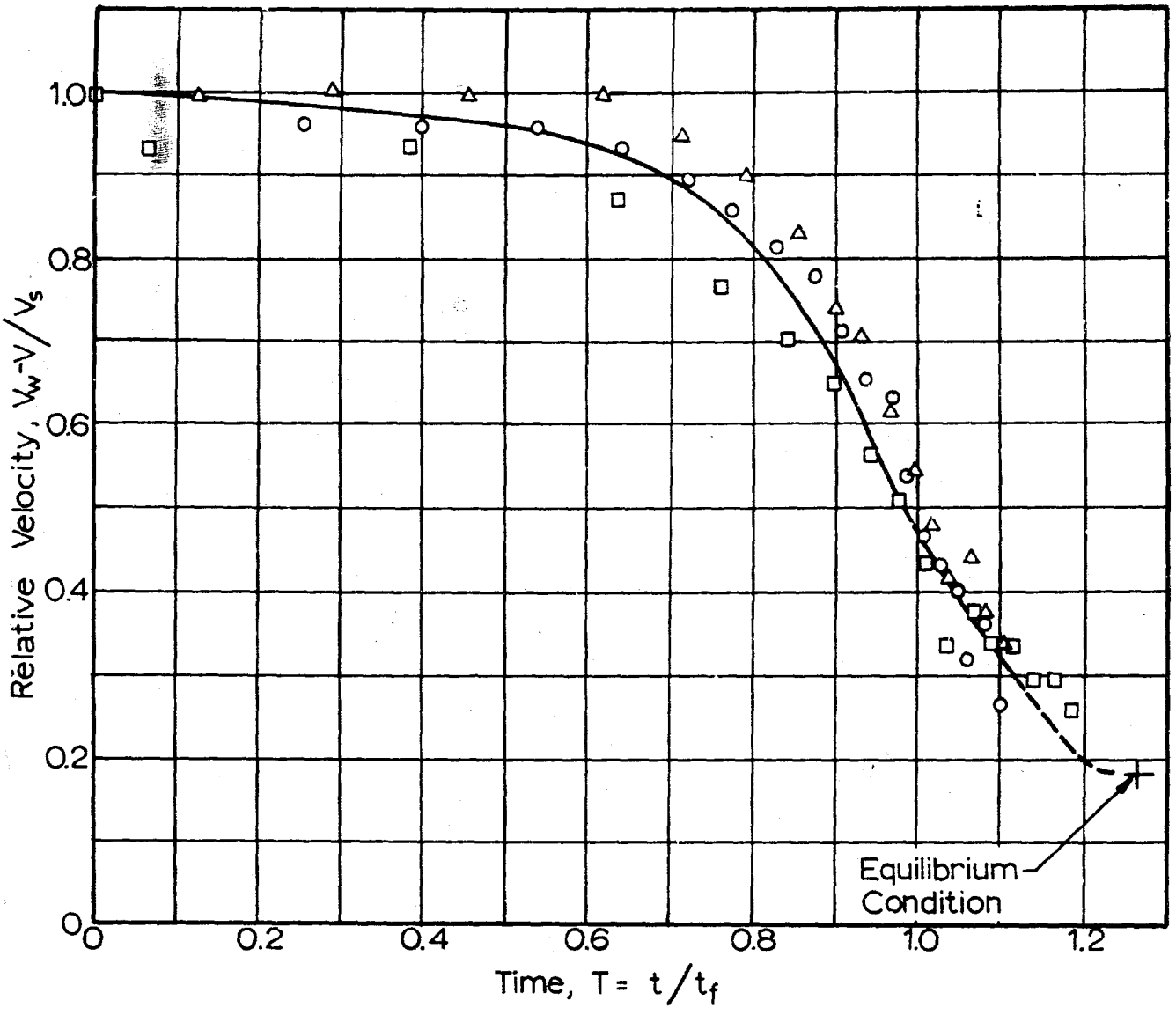

Fig 25 Relative Velocity, 3 ft Flexible Model, Snatch Velocity 50 fps, Suspended Weight 0.5 lb

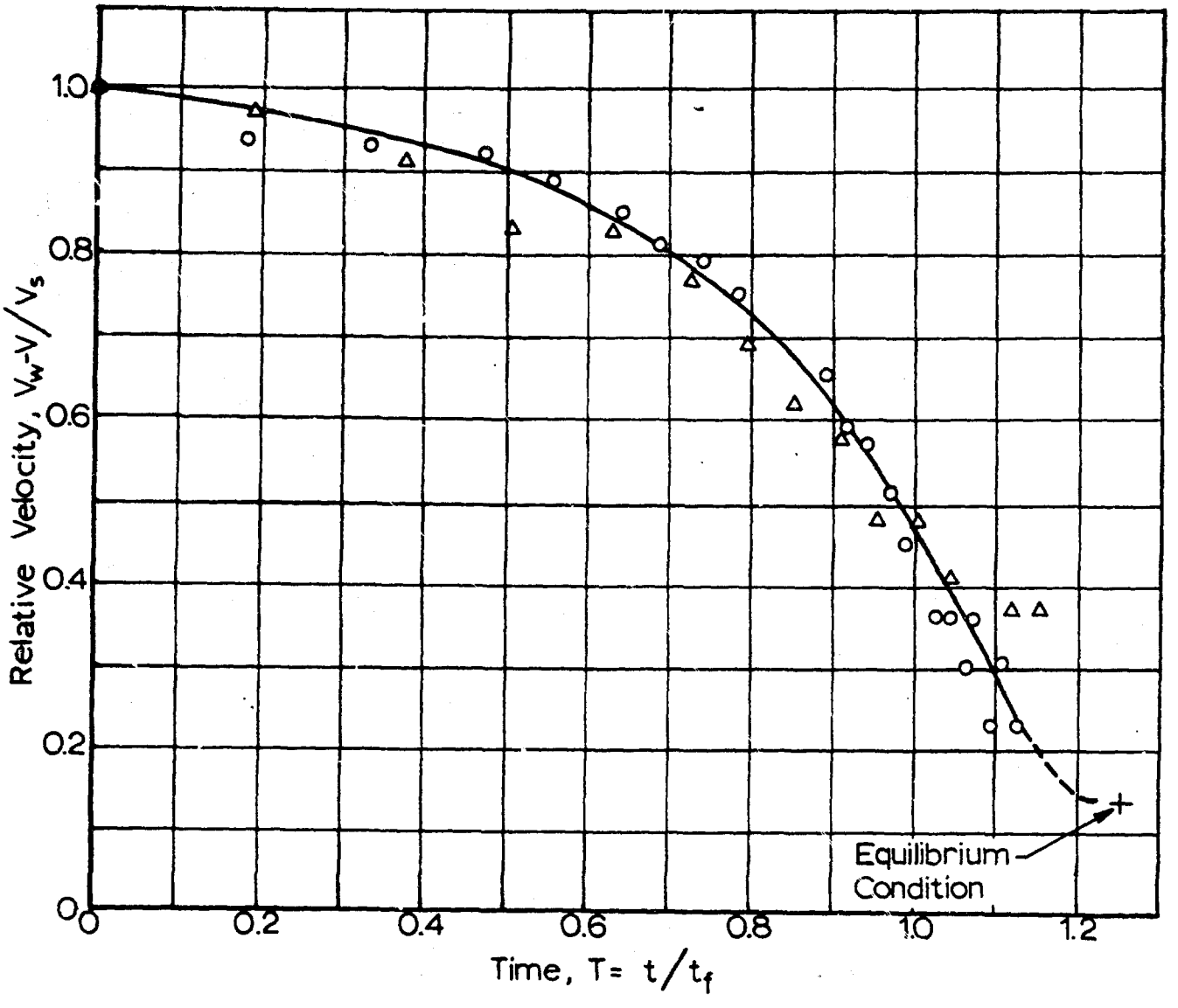

Fig 26 Relative Velocity, 3 ft Flexible Model, Snatch Velocity 70 fps, Suspended Weight 0.5 lb

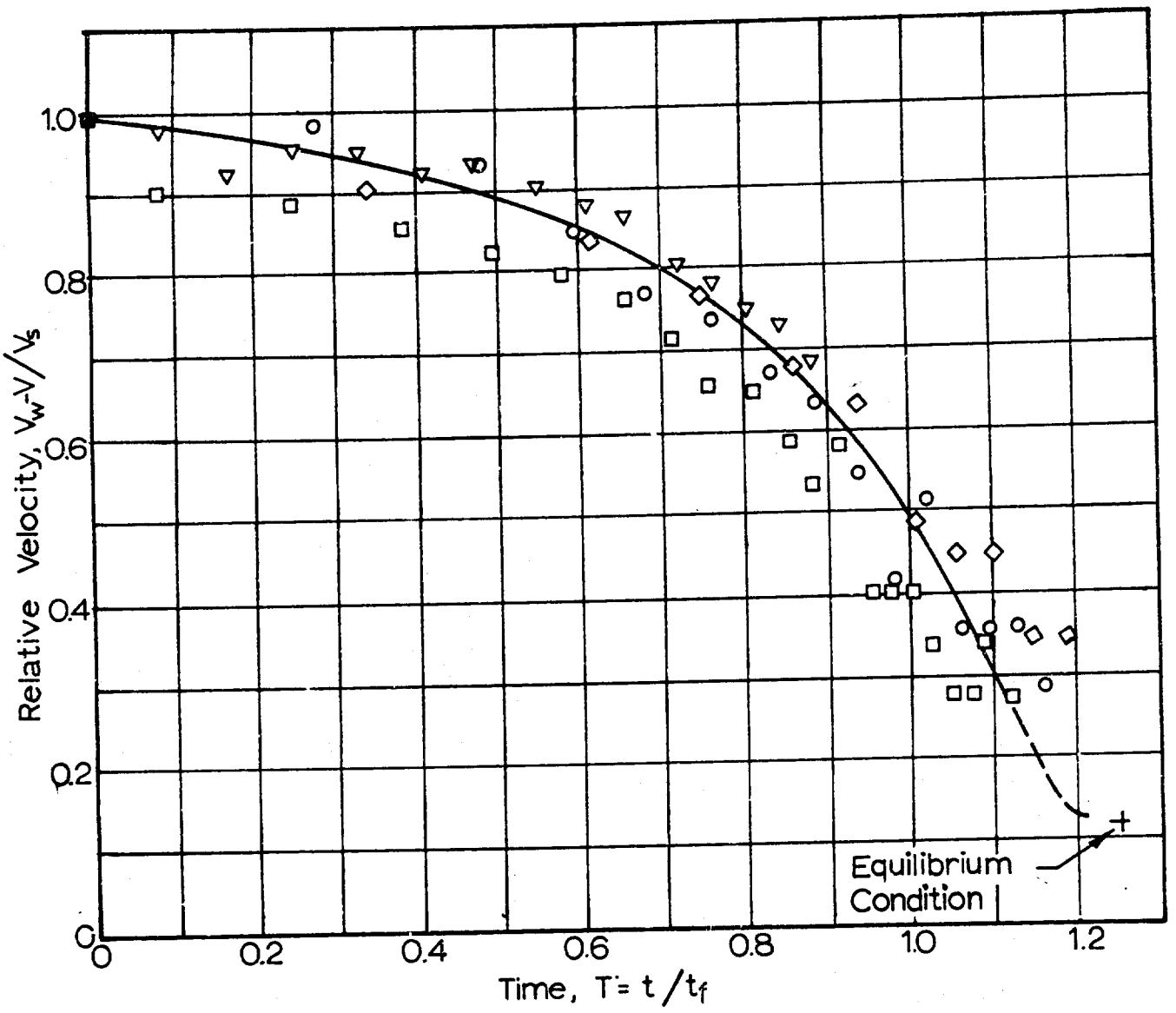

Fig 27 Relative Velocity, 3 ft Flexible Model, Snatch Velocity 85 fps, Suspended Weight 0.5 lb

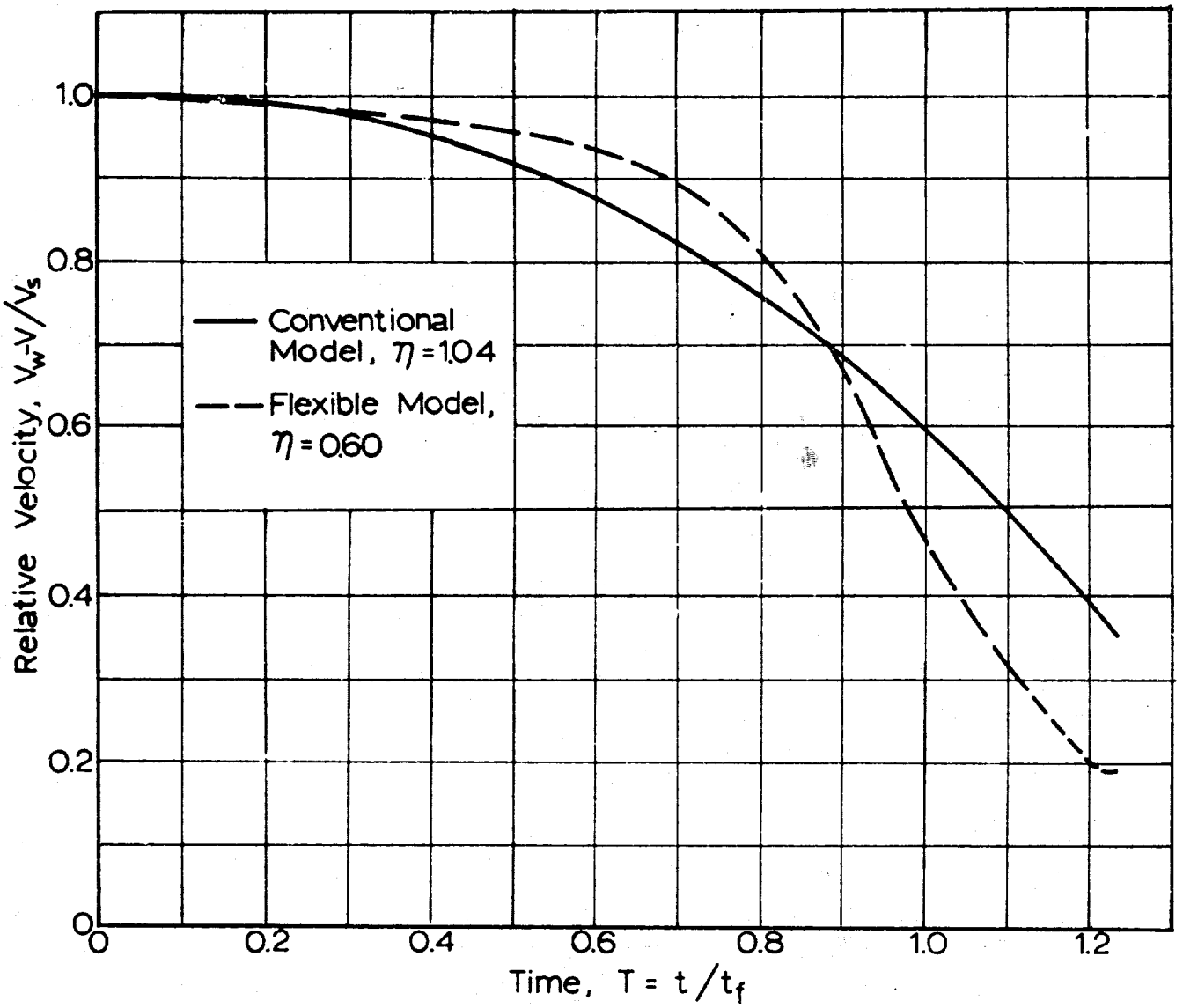

Fig 28 Velocity - Time Histories of a Conventional Model, η = 1.04, and a Flexible Model, η = 0.60, at 50 fps Snatch Velocity

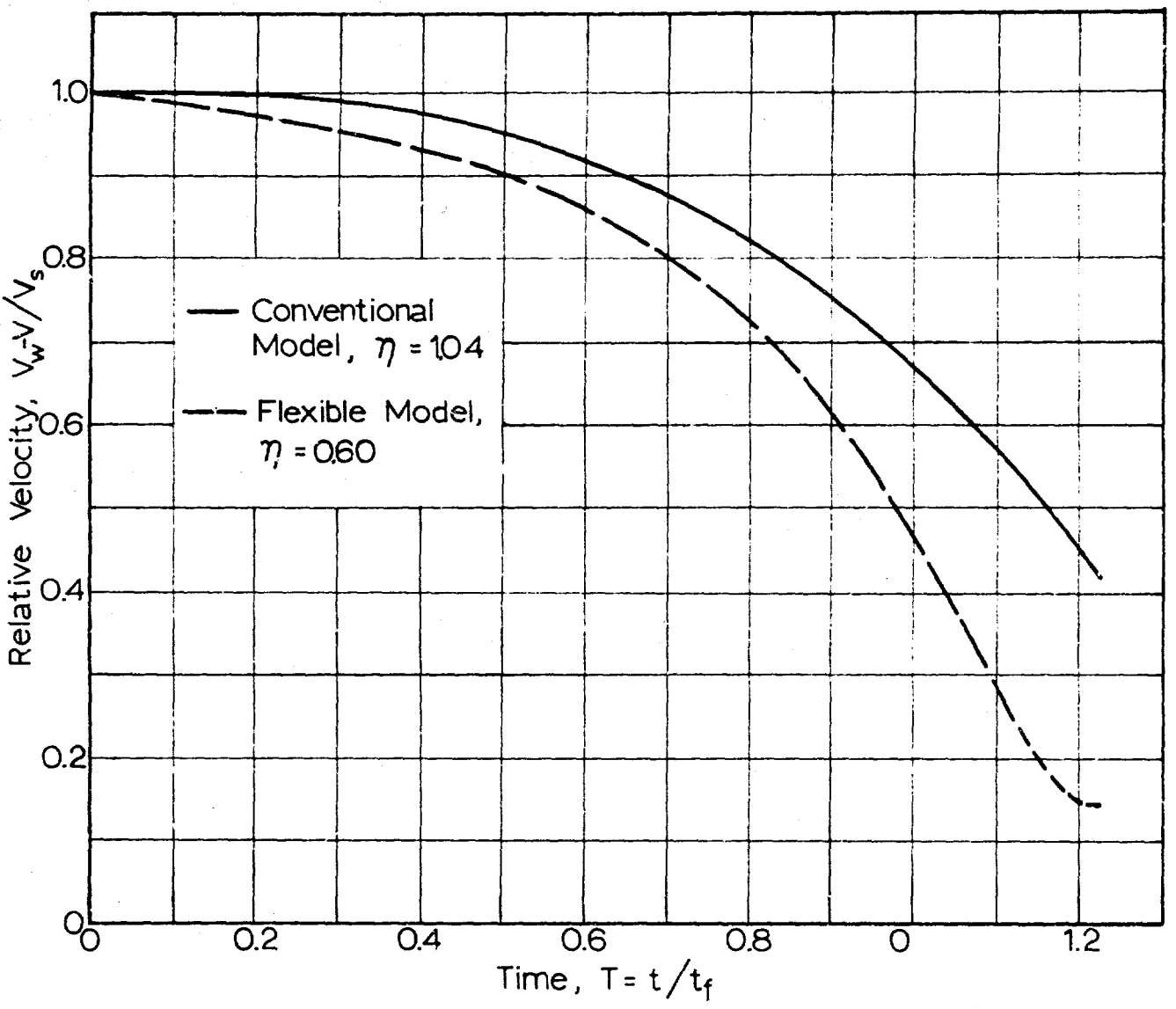

Fig 29 Velocity - Time Histories of a Conventional Model, $\eta = 1.04$, and a Flexible Model, $\eta = 060$, at 70 fps Snatch Velocity

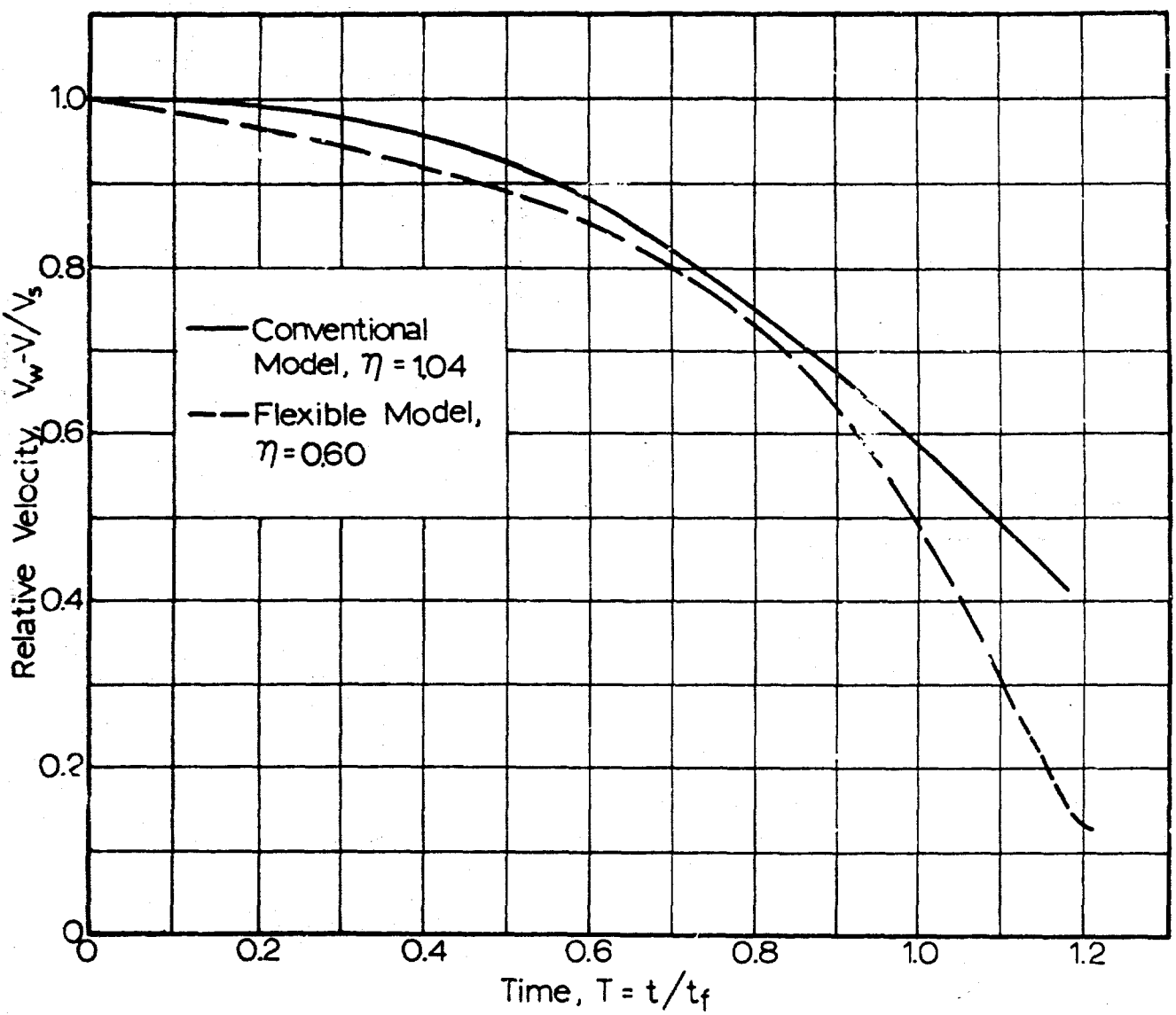

Fig 30 Velocity - Time Histories of a Conventional Model, $\eta = 1.04$, and a Flexible Model, $\eta = 0.60$, at 85 fps Snatch Velocity

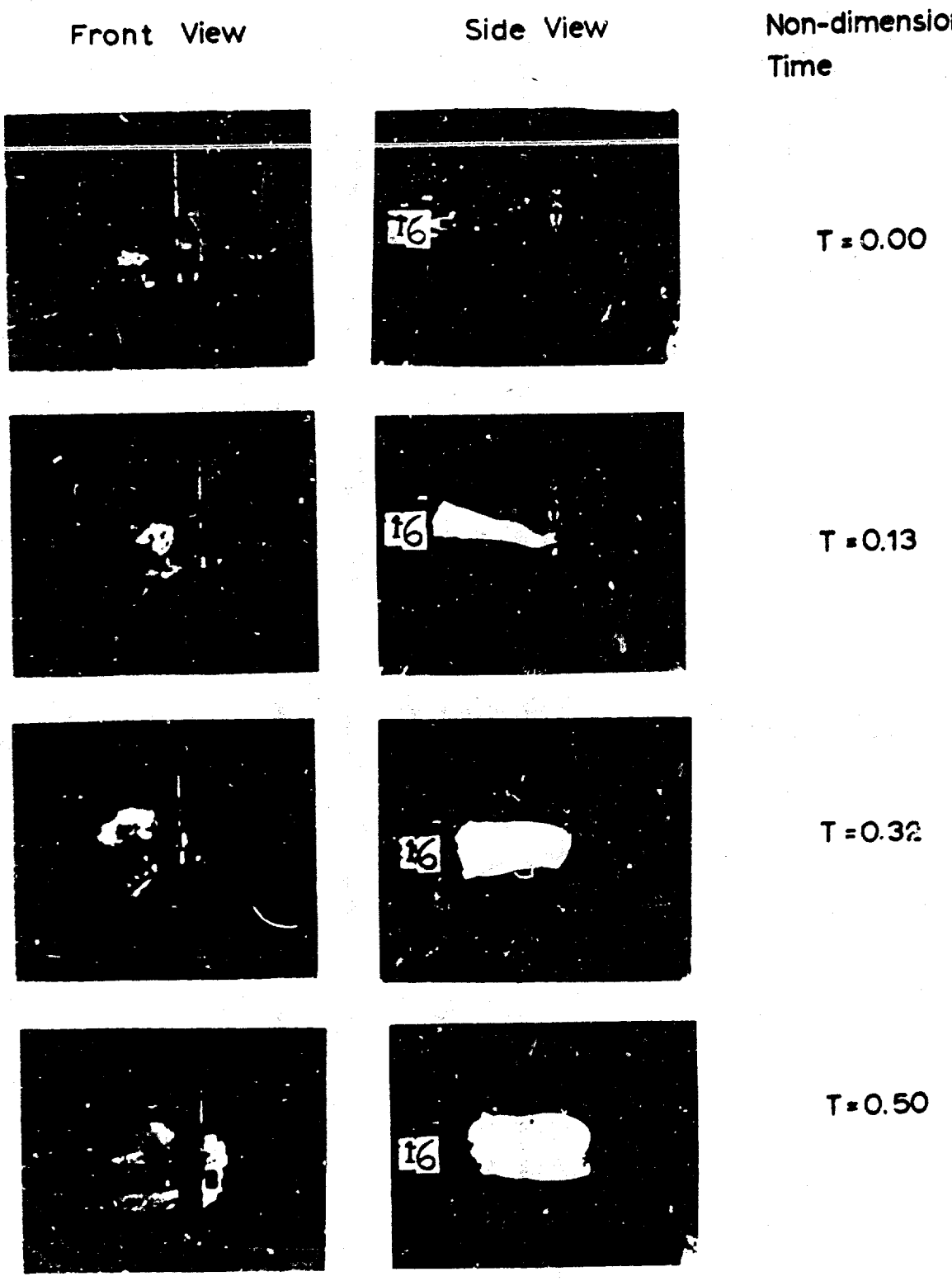

Fig. 31 Sequence Pictures of the Filling Process of a Conventional, 3 ft Parachute Model, η = 1.04, Snatch Velocity of 70 fps, Suspended Weight of 0.5 lb. (Continued)

Front View

Side View

Non-dimensional Time

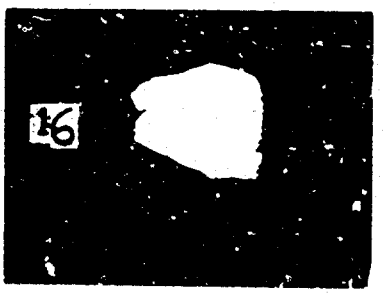

T = 0.63

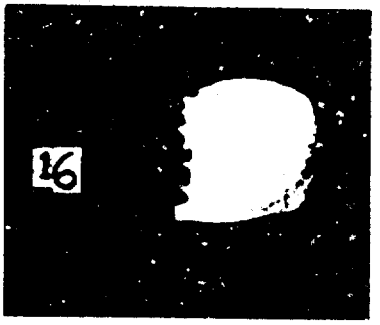

T = 0.81

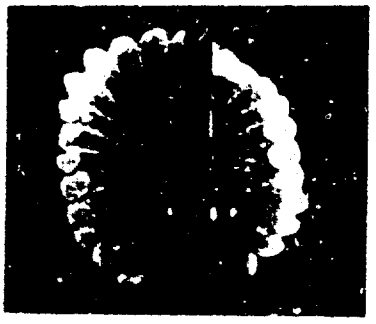

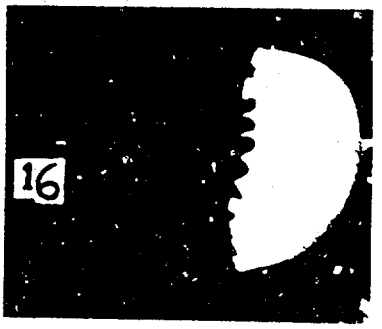

T = 1.00

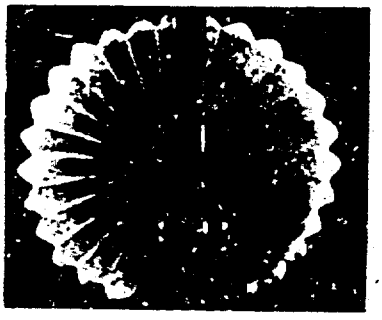

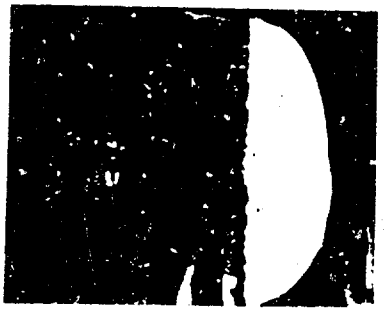

T = 1.15

Fig. 31 (Continued)

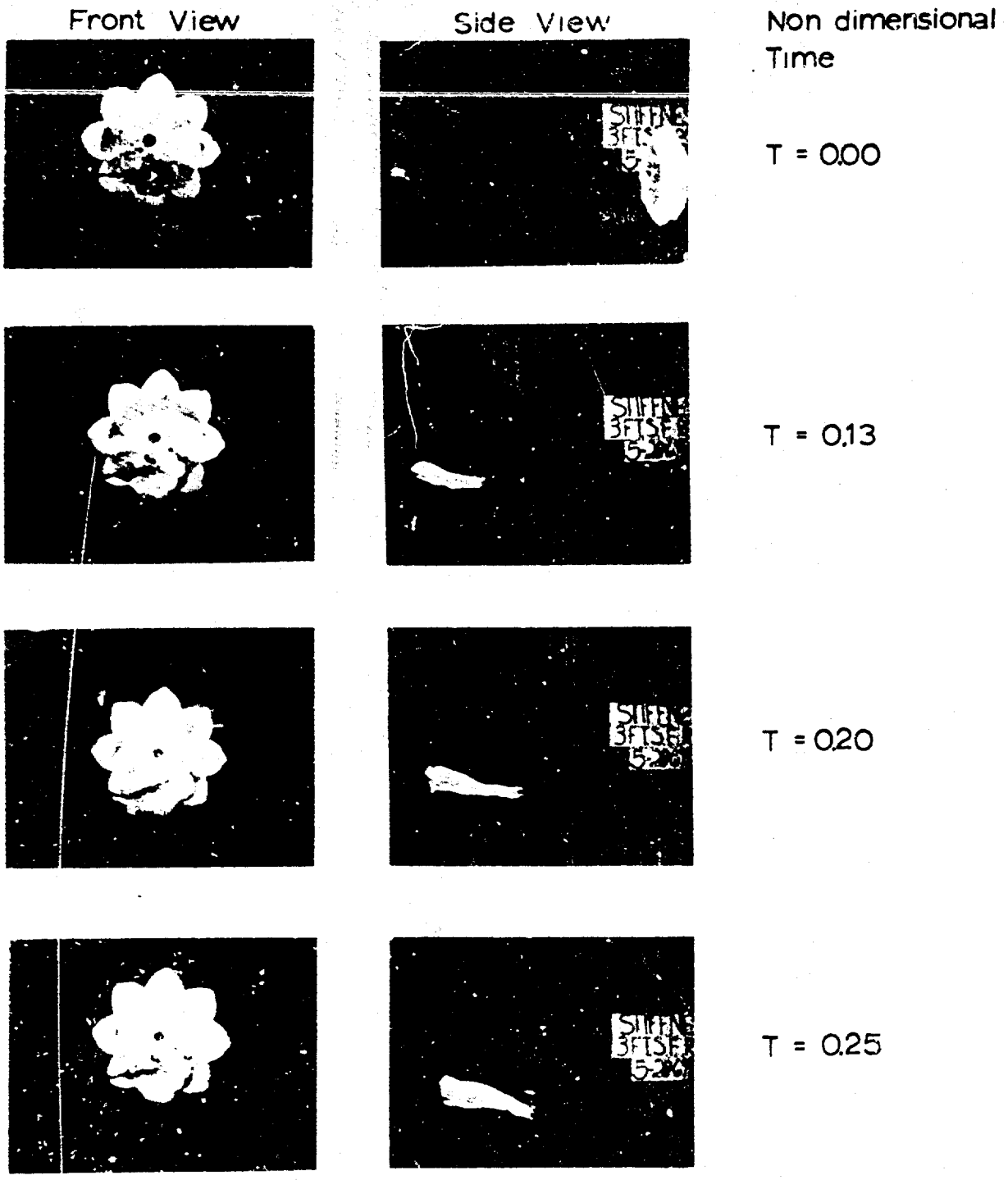

Fig. 32 Sequence Pictures of the Filling Process of a More Flexible, 3 ft Parachute Model, $\eta = 0.60$, Snatch Velocity of 70 fps, Suspended Weight of 0.50 lbs.

Front View

Side View

Non-dimenional Time

T = 0.32

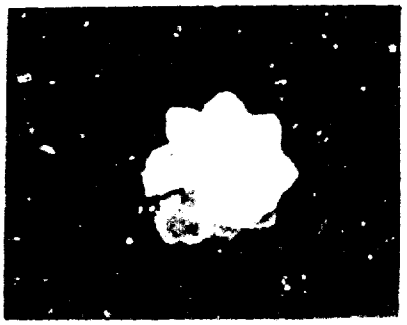

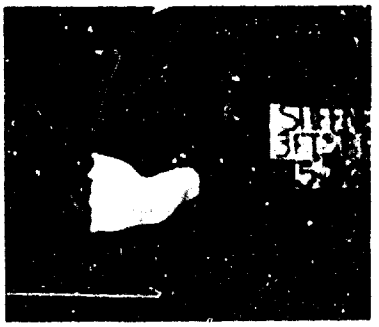

T = 0.40

T = 0.50

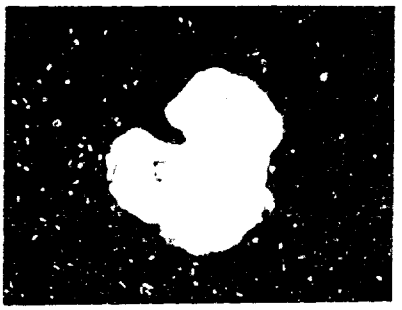

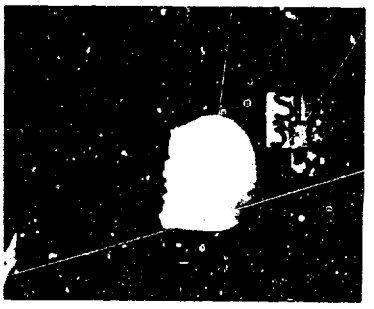

T = 0.63

Fig 32 (Continued)

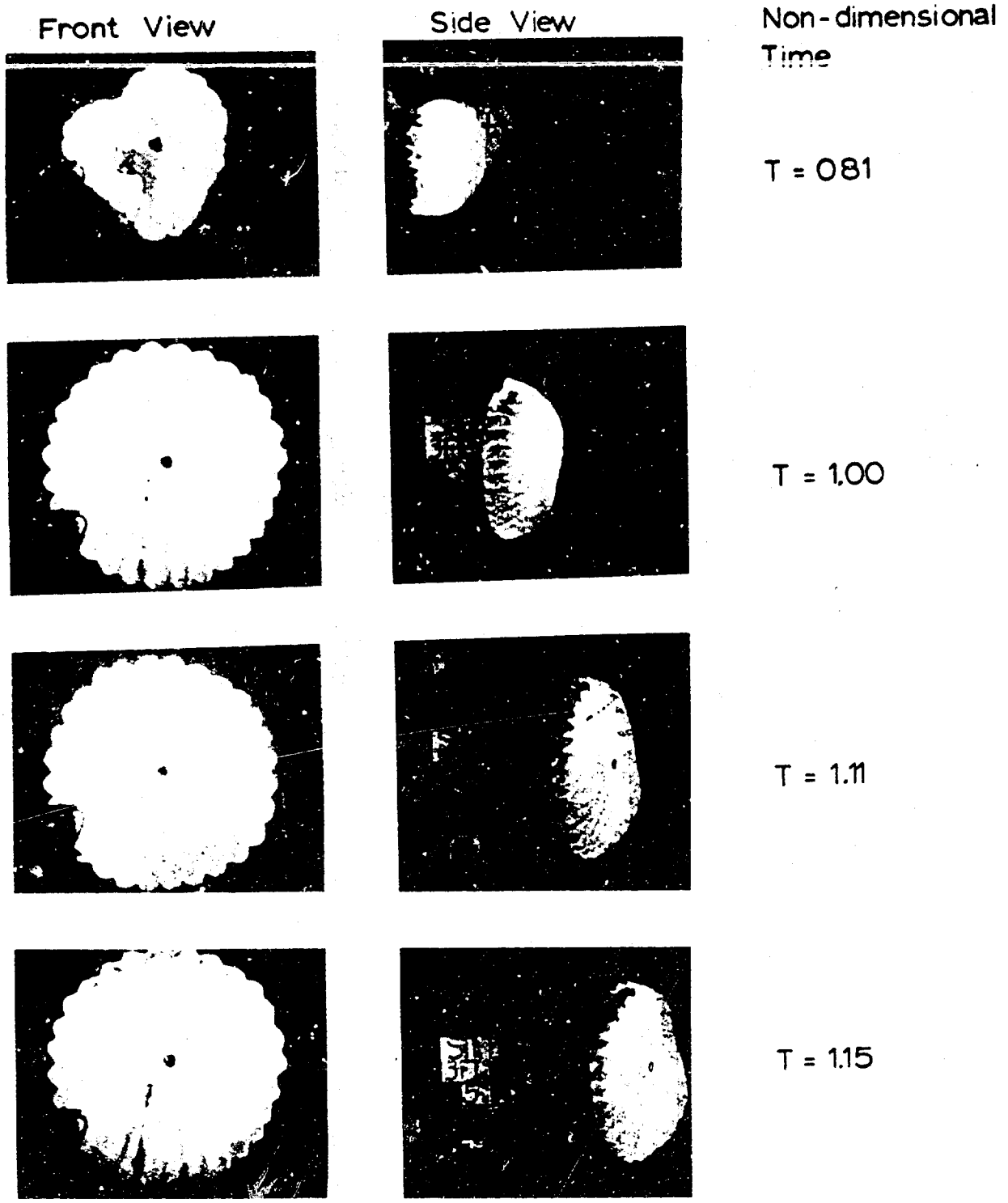

Fig 32 (Continued)

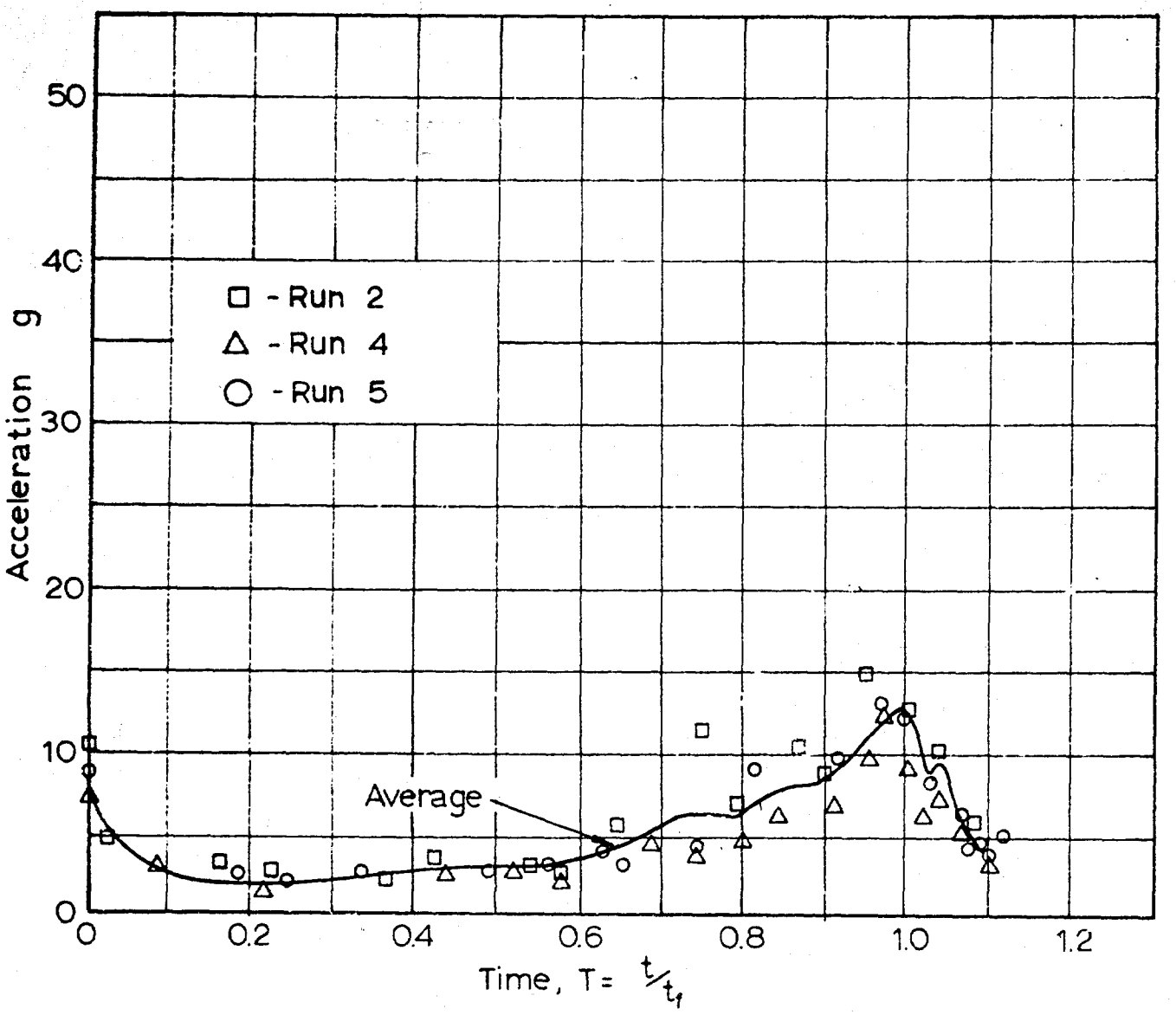

Fig 33 Wind Tunnel Experiments, Systems Acceleration, 3 ft Flexible Model Parachute, Snatch Velocity = 50 fps, Suspended Weight = 0.5 lb

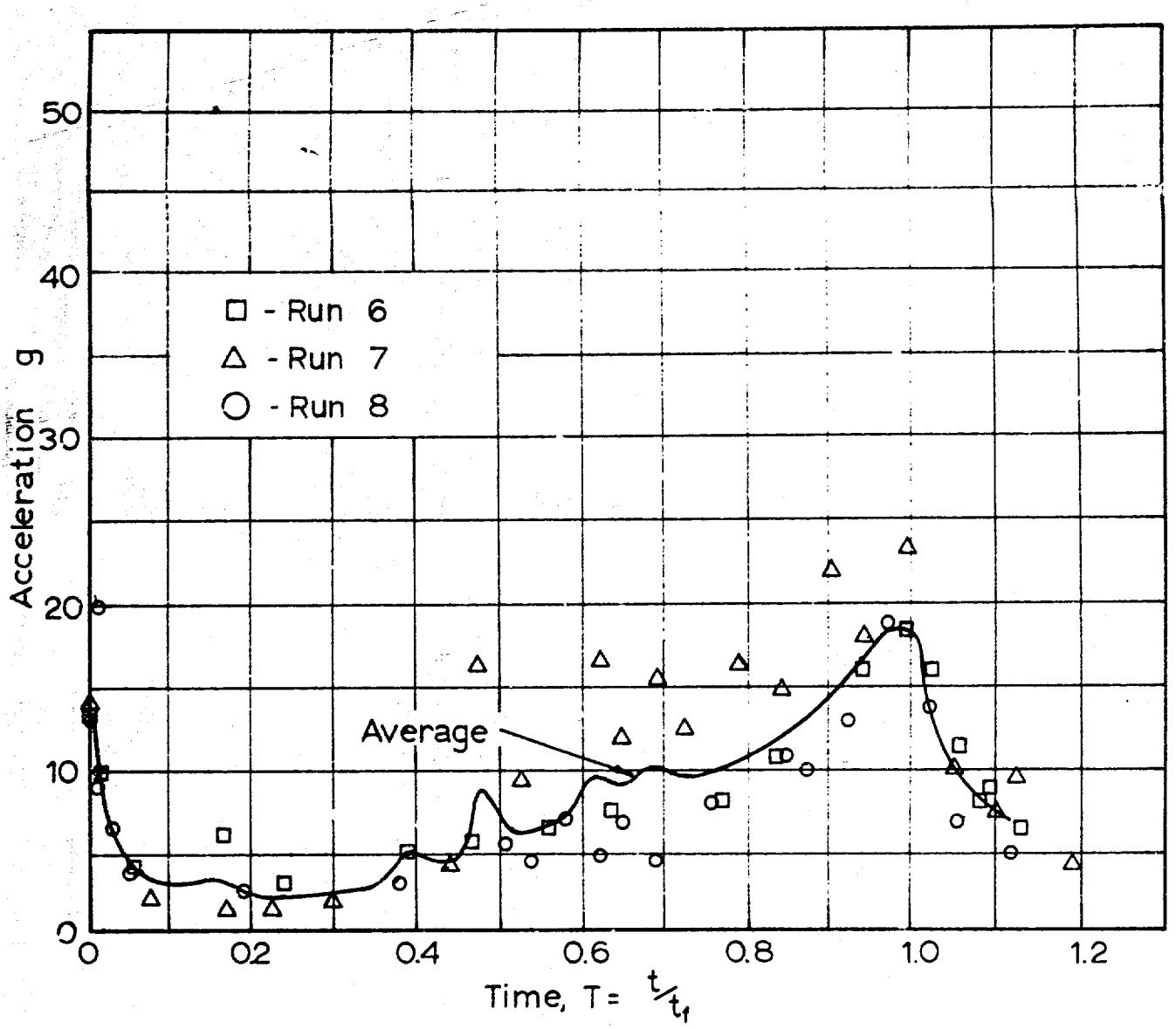

Fig34 Wind Tunnel Experiments, Systems Acceleration, 3 ft Flexible Model Parachute, Snatch Velocity = 70 fps, Suspended Weight = 0.5 lb

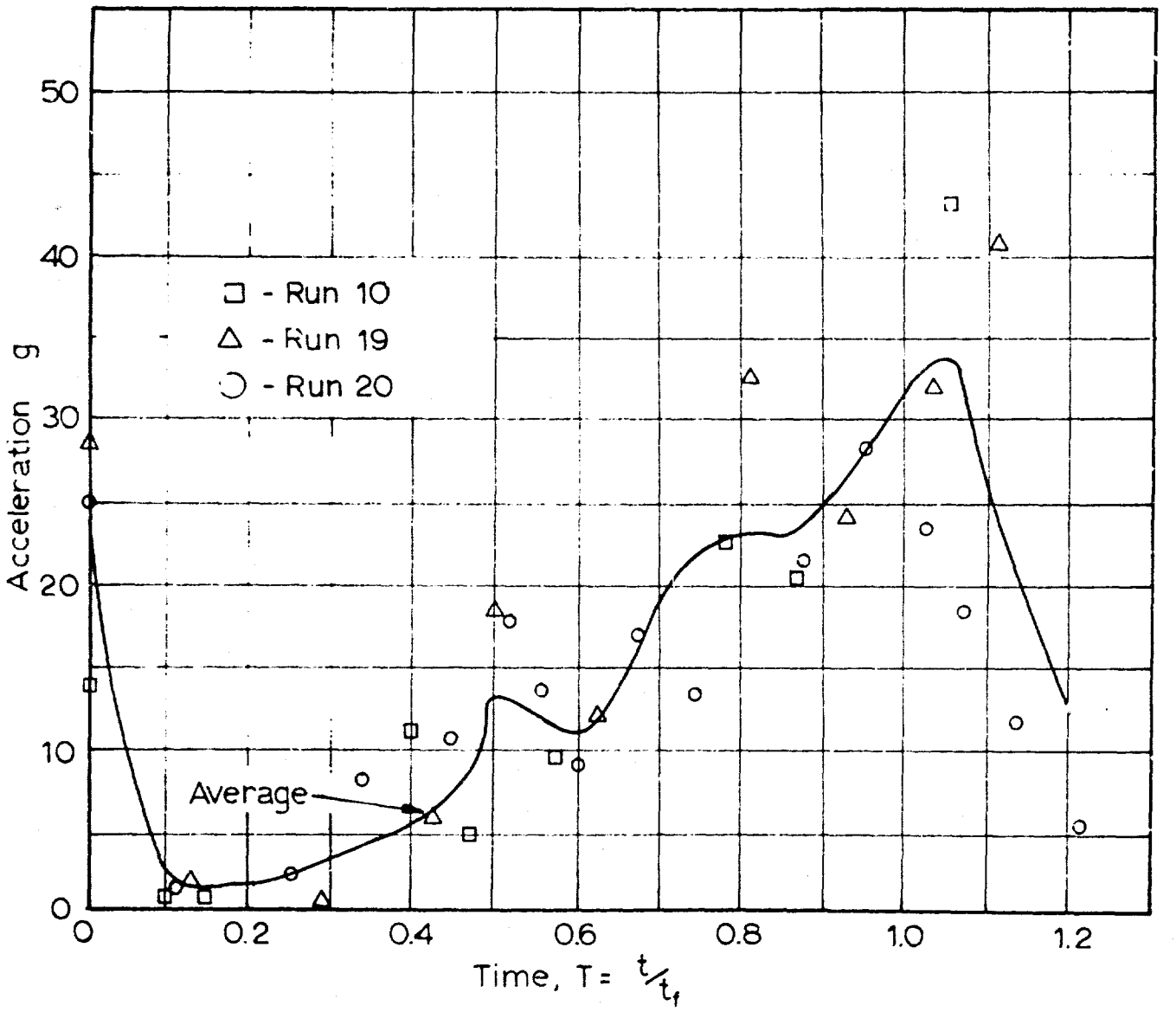

Fig35 Wind Tunnel Experiments, Systems Acceleration 3 ft Flexible Model Parachute, Snatch Velocity = 85 fps, Suspended Weight = 0.5 lb

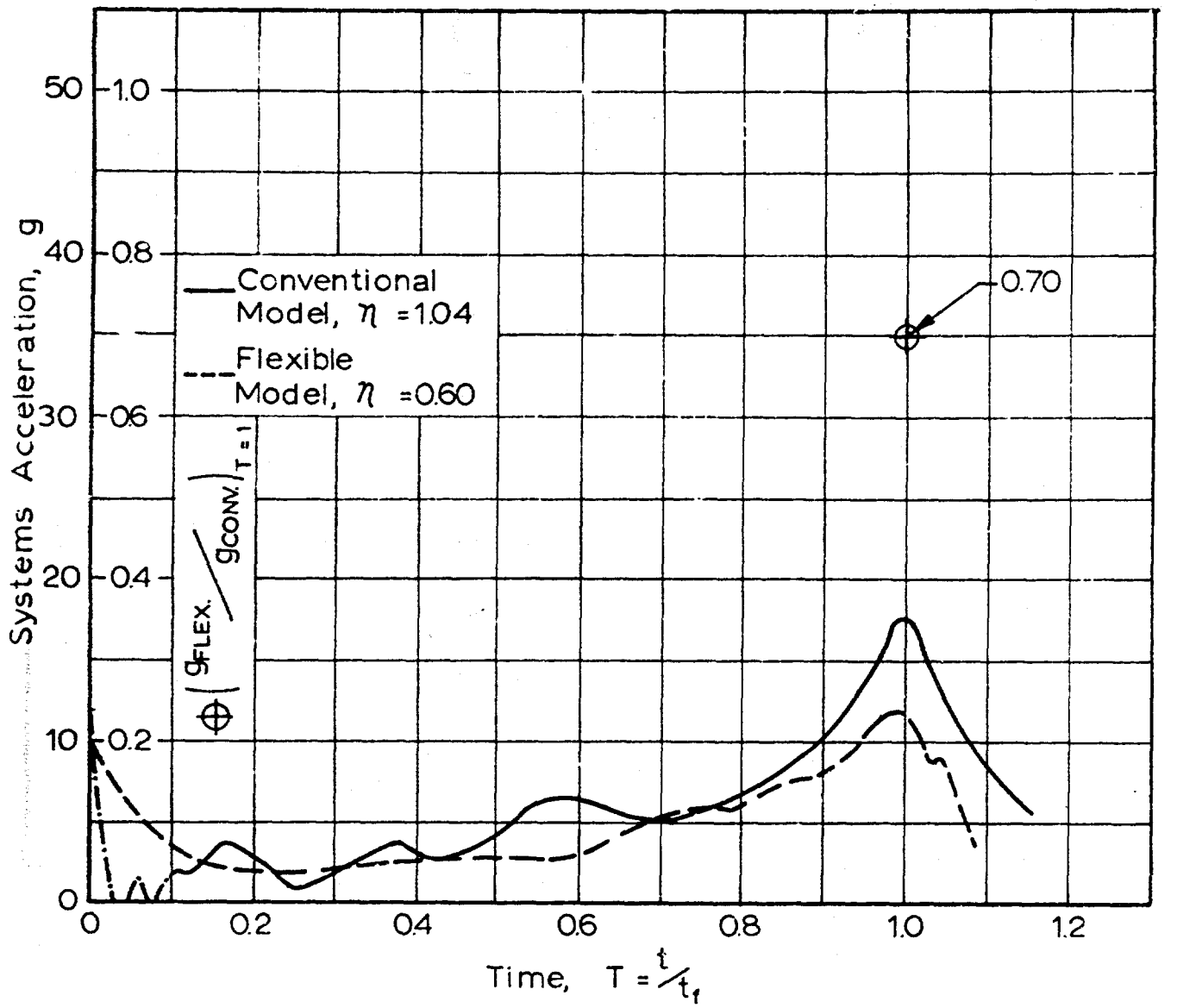

Fig 36 Comparison of Systems Acceleration Using Conventional and Flexible 3 ft Model Parachutes, Snatch Velocity V_S = 50 fps, Suspended Weight = 0.5 lb

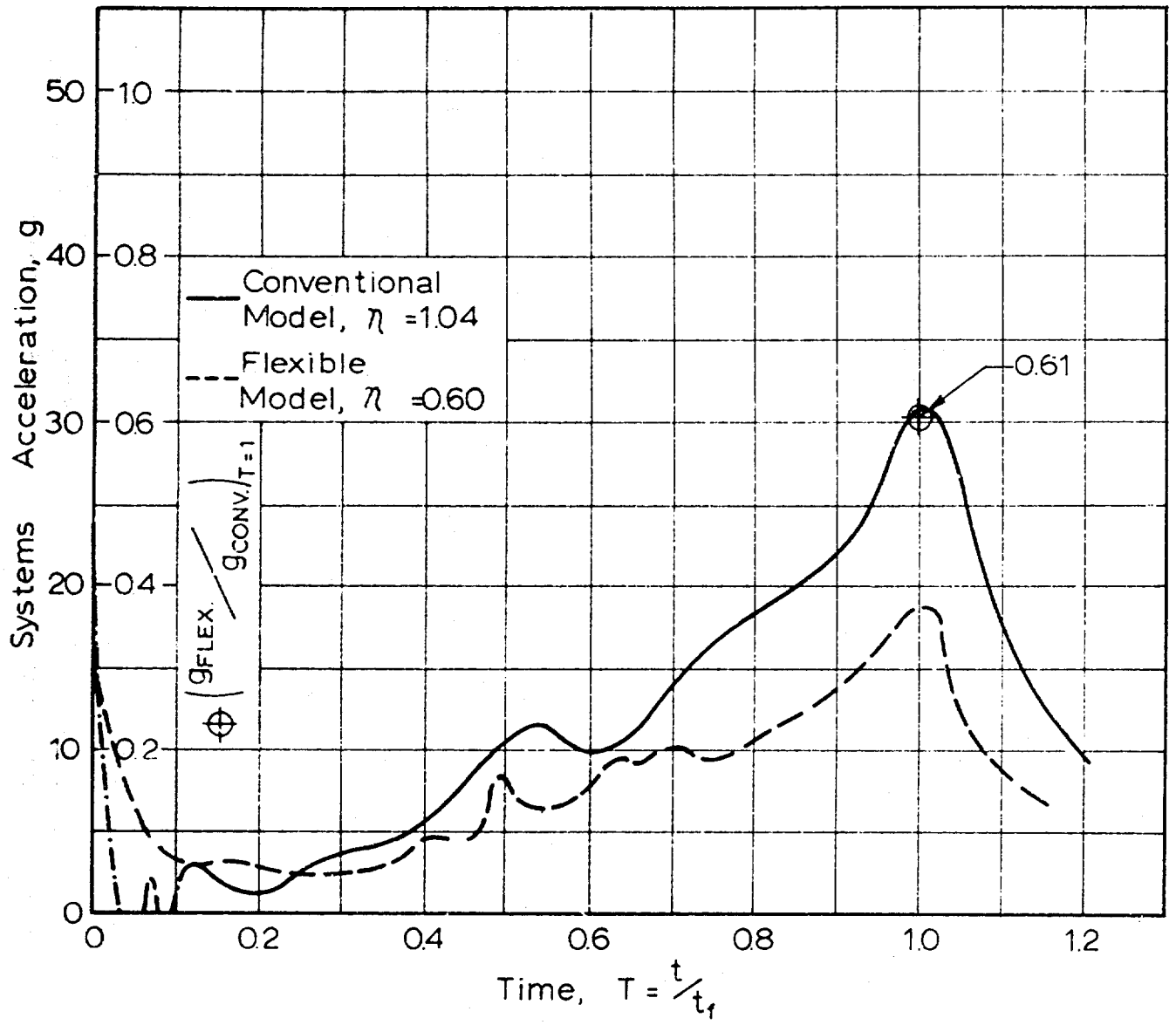

Fig 37 Comparison of Systems Acceleration Using Conventional and Flexible 3 ft Model Parachutes, Snatch Velocity V_S =70 fps, Suspended Weight =0.5 lb

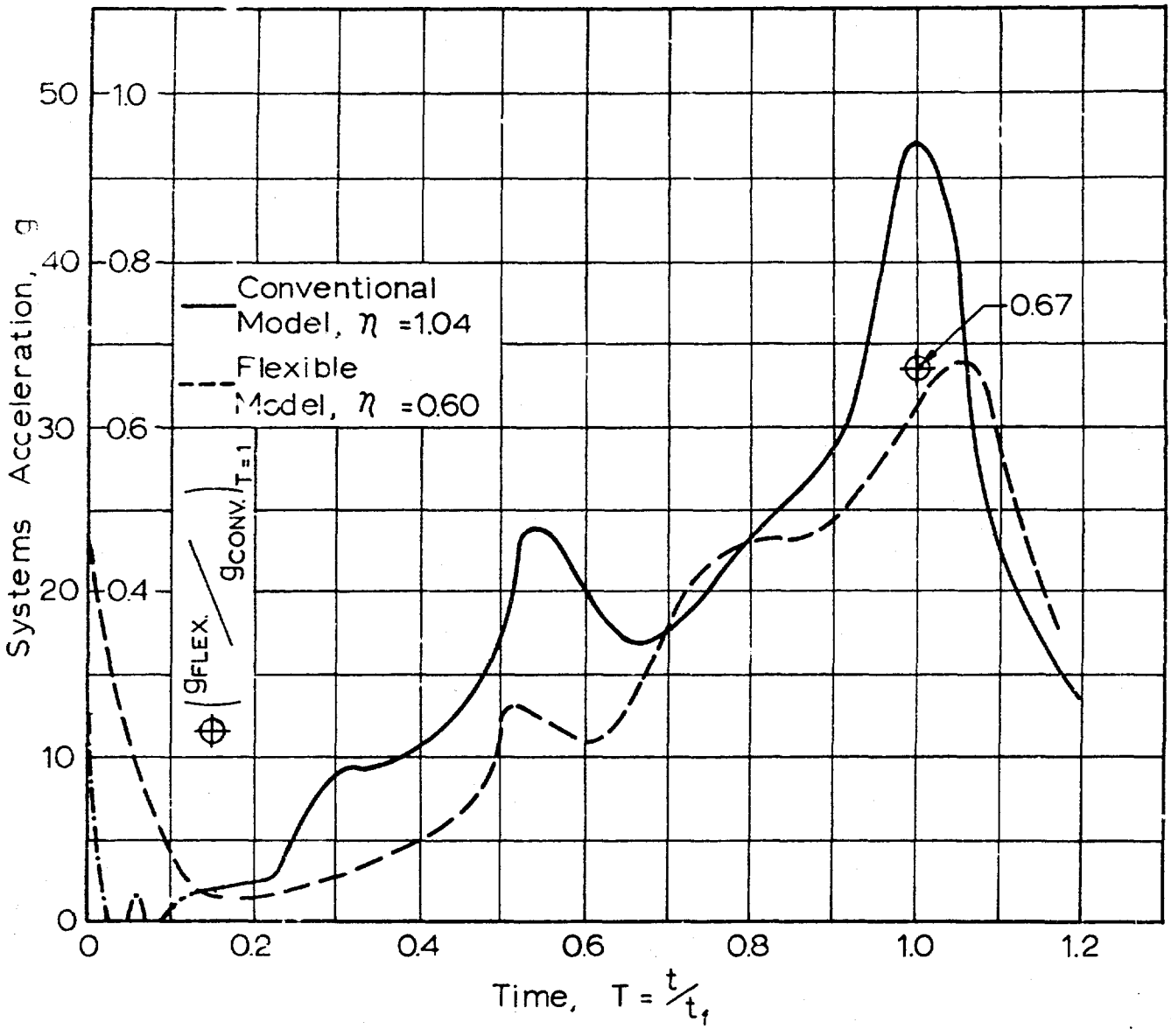

Fig 38 Comparison of Systems Acceleration Using Conventional and Flexible 3 ft Model Parachutes, Snatch Velocity V_S = 85 fps, Suspended Weight = 0.5 lb

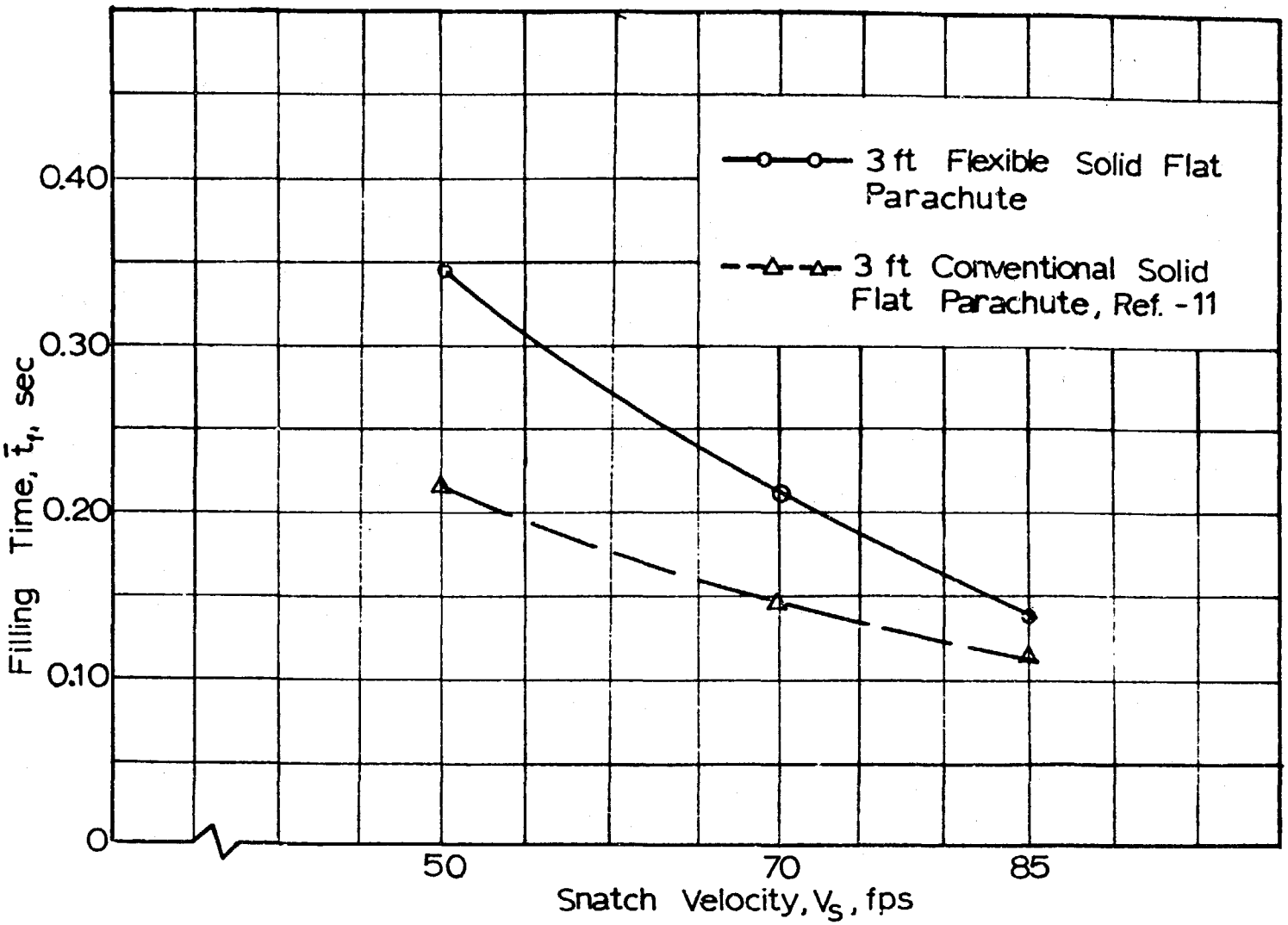

Fig 39 Average Filling Time, Wind Tunnel Experiments, 3 ft Conventional and Flexible Parachute Models, Snatch Velocities of 50, 70, and 85 fps

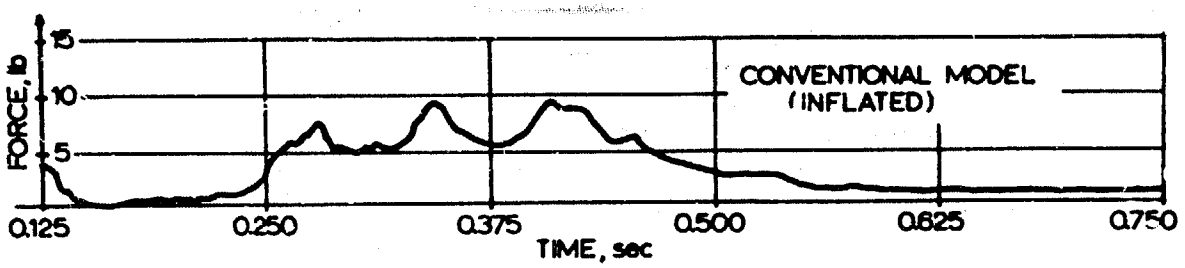

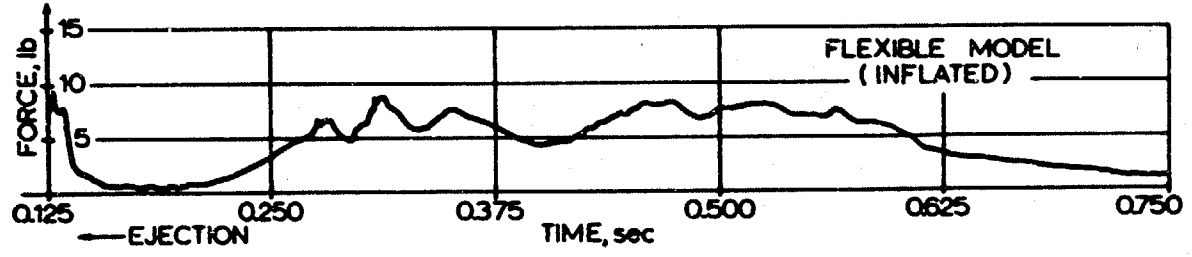

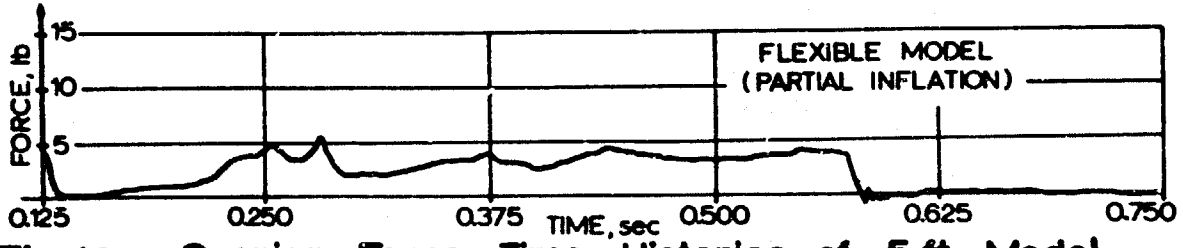

Fig 40 Opening Force - Time Histories of 5 ft Model Parachutes, Catapult Test, Suspended Weight = 1.14 lb, $m_1/m_s = 0.75$, Snatch Velocity = 50 fps

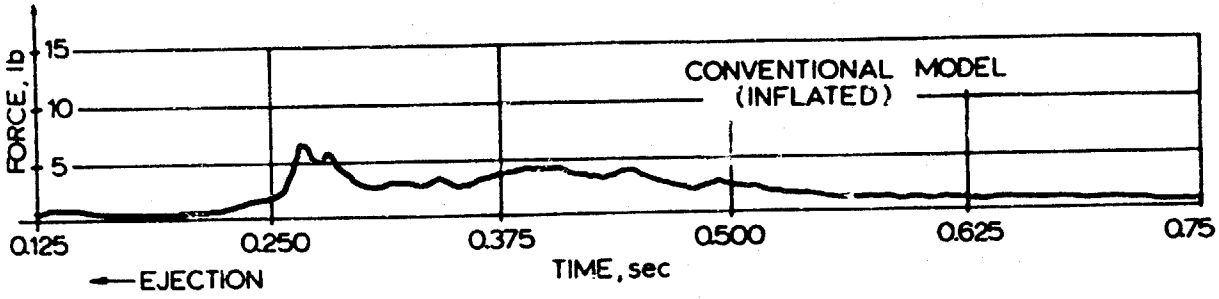

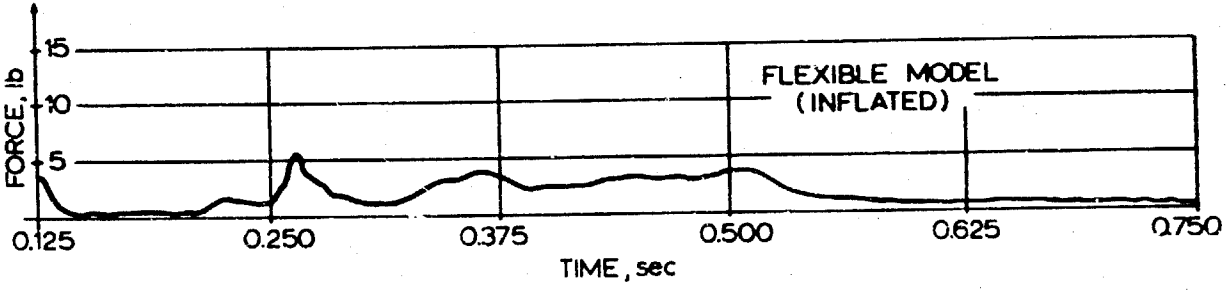

Fig 41 Opening Force - Time Histories of 4 ft Model Parachutes, Catapult Test, Suspended Weight = 0.6 lb, $m_i/m_s = 0.75$, Snatch Velocity = 50 fps

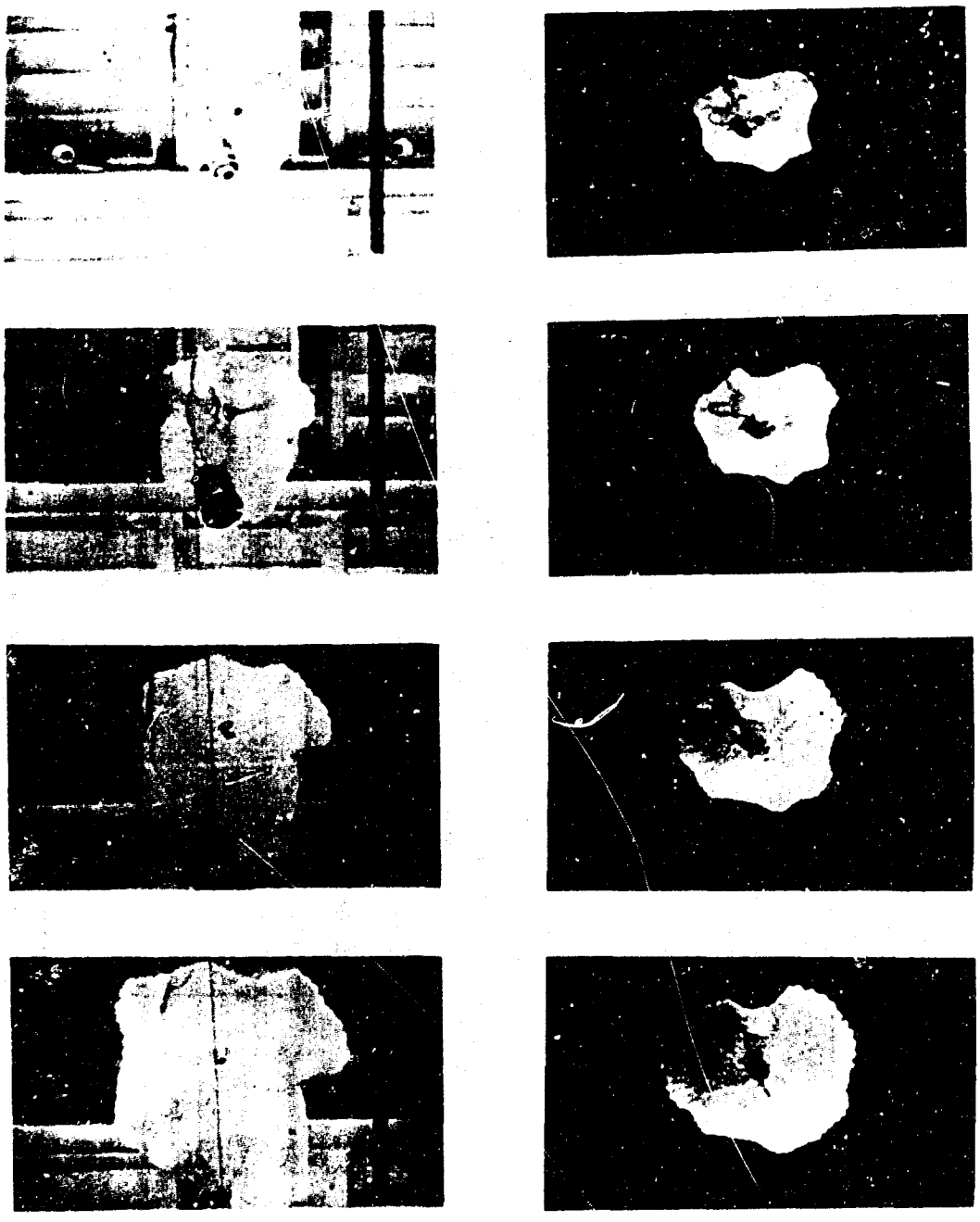

Flexible Model
Squidding

Conventional Model
Inflating

Fig.42 Sequence Pictures of Free Flying Parachutes; One Model Inflating, One Model Squidding, both under Similar Surface Loading and Mass Ratios, 0.025 sec Intervals.

TABLE I

Canopy Physical Characteristics and Stiffness Index

SOLID FLAT / Do	TYPE	D_{max}/D_o	W_c	W_c/S_o	w_{cl} *	η
in			gr	gr/ft^2	gr/ft^2	
(1)	(2)	(3)	(4)	(5)	(6)	(3)×(5)/(6)
12	Flex.	0.72	2	2.53	3.47	0.53
15	Flex.	0.71	7	5.74	3.47	1.17
19.5	Conv.	0.80	27	13.00	3.47	3.00
36	Flex.	0.48	31	4.38	3.47	0.60
36	Conv.	0.40	64	9.05	3.47	1.04
48	Flex.	0.36	54	4.30	3.47	0.45
48	Conv.	0.28	97	7.72	3.47	0.62
60	Flex.	0.23	103	5.25	3.47	0.35
60	Conv.	0.29	146	7.44	3.47	0.62
28 Ft-C9	Conv.	0.09	5000	8.13	3.47	0.21
RINGSLOT / Do						
45.2	Flex.	0.32	49	4.40	3.47	0.40
45.2	Conv.	0.32	160	14.36	**	1.00

* All canopies constructed of 1.1 oz/yd^2 Ripstop Nylon Cloth, MIL-C-7020, Type I, $w_{cl} = 3.47$ gr/ft^2.

** Nylon Tape, MIL-T-5608E.

APPENDIX

In the following section additional information is presented which was obtained in the course of the study. They contributed to the overall accomplishment but were not directly utilized in the construction of highly flexible models.

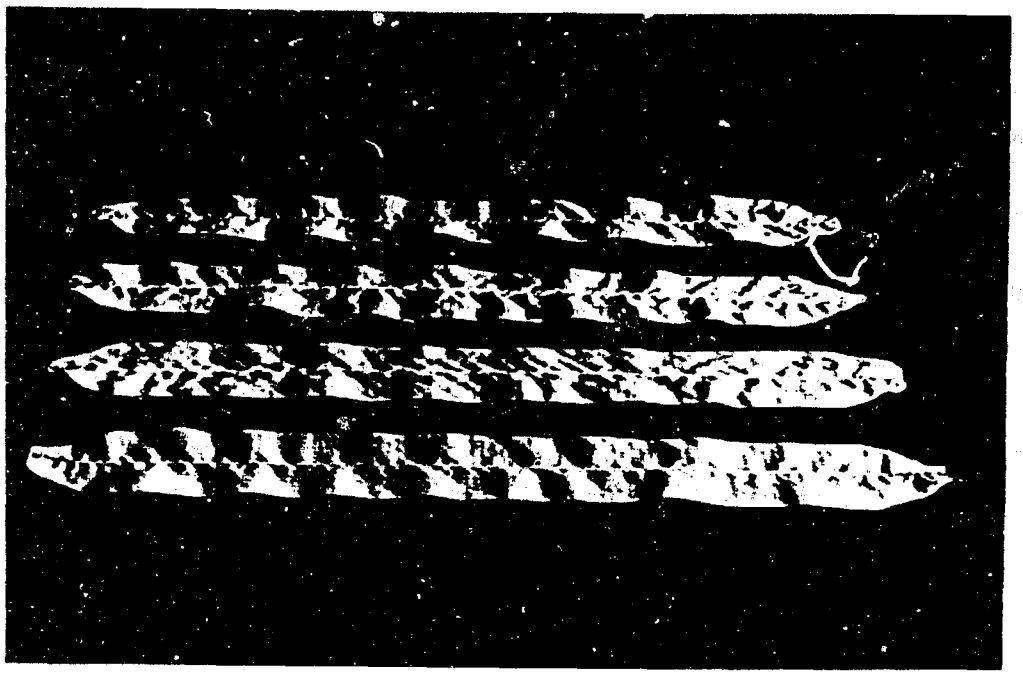

STITCH NO.	DESCRIPTION	ST in	Dmax L
4	STRAIGHT STITCH	12	014
2	.30 .12	3.3	017
3	.30 .06	3.3	012
1	.15 .06	6.7	015

Fig. 43 Strip Studies Involving Zig-Zag Stitching (12 in. Specimans)

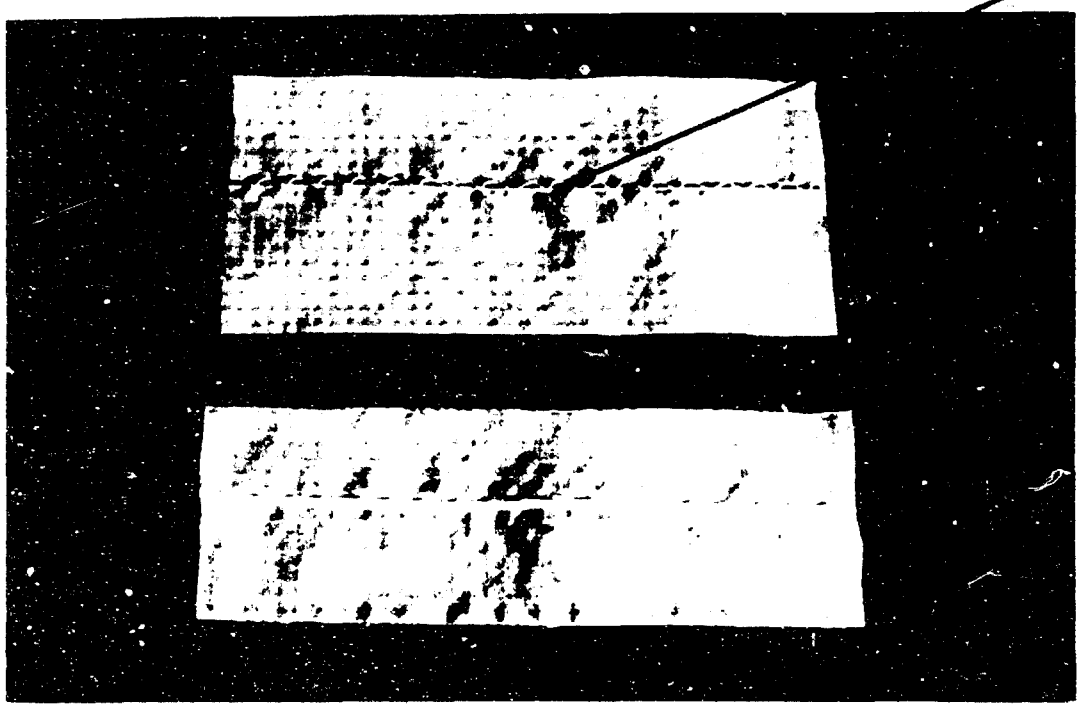

STITCH and SUSPENSION LINE CONFIGURATION used in CONSTRUCTION of 5ft SOLID FLAT CANOPY.

CLOTH - 1.1 oz yd NYLON
MIL-C-7020D, TYPE I

THREAD - SST-15 (NYLON 1/4 lb)

NEEDLE - NO. 9

STITCH - ZIG-ZAG

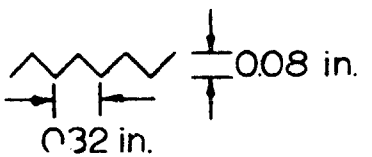

Fig 44 Strips Showing Details of Suspension Line Attachment used in Final Model Parachute Construction

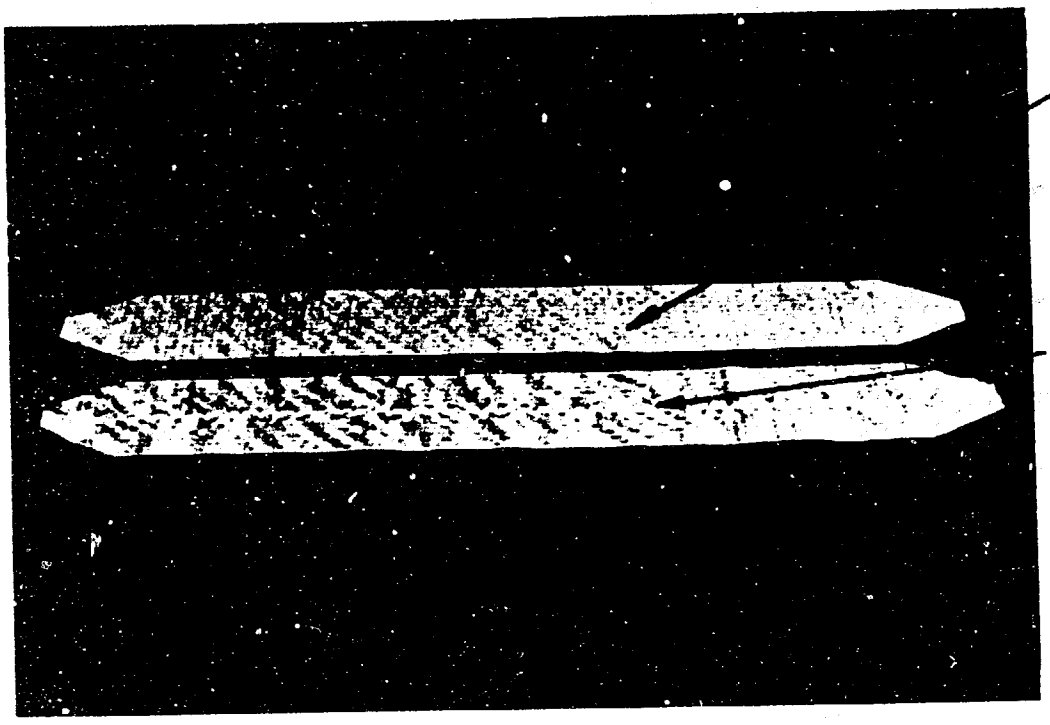

PLAIN HOT-KNIFE STRIP

$\frac{D_{max}}{L}$ = 0.12

STITCH NO.	DESCRIPTION	$\frac{ST}{in}$	$\frac{D_{max}}{L}$
5	0.32 / 0.08	3.2	0.13

Fig. 45 Comparison of Cloth Bulge and Take-up for Plain Strip and Strip with Stitch No. 5

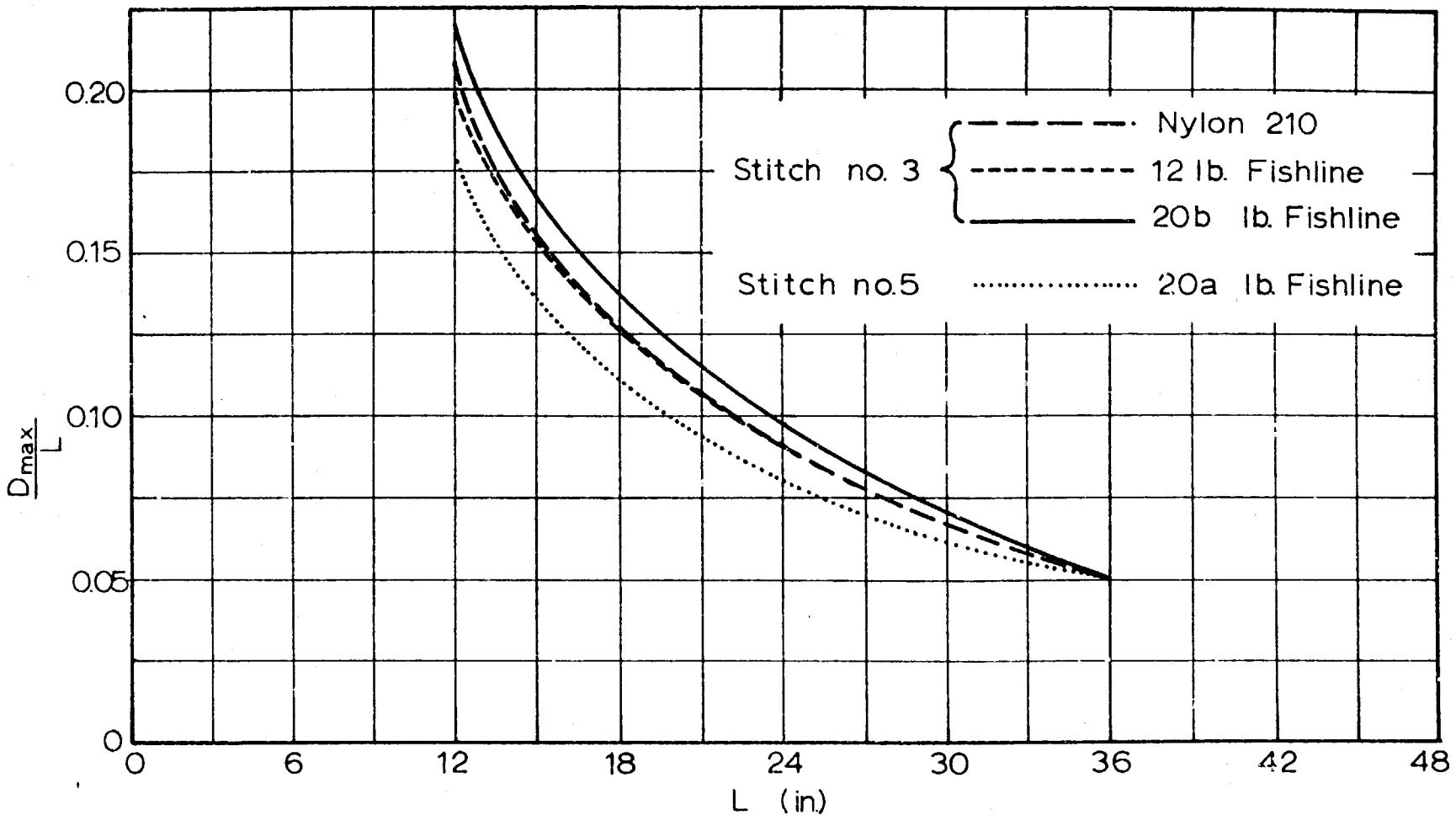

Fig 46 Stiffness Results of Seared Edge Strips with Suspension Lines Attached

Table II. Suspension Lines Tested for Stiffness (L = 36 in.)

Description	$\frac{D_{max}}{L}$	Wt. gm/ft	Comments
100 lb MIL-C-5040C Type 1A	0.07	0.433	Smooth
100 lb MIL-C-5040C Type 1A	0.10	0.433	Twisted and kinked
20a lb braided fishline (with core)	0.08	0.071	Round suspended profile 
20a lb braided fishline (without core)	0.07-0.08	0.064	"Necked" suspended profile 
12 lb braided fishline (with core)	0.09	0.033	----------
12 lb braided fishline (without core)	0.07	0.037	----------
Nylon 210 20 lb	0.11	0.123	----------
10 lb braided nylon fishline	0.08	-----	Not available
20b lb braided nylon fishline (with core)	0.08	0.071	----------
20b lb braided nylon fishline (without core)	0.07	0.064	Chosen for model canopy construction

Table III. Suspension Lines with Optimum Flexibility

Description	Cross-Sectional Dimension (inches)	$\frac{D_{max}}{L}$	
		L = 18 in.	L = 36 in.
Nylon 210 (20 lb)	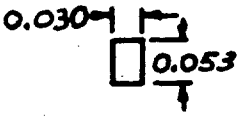	0.12	0.07
12 lb braided nylon fishline without core	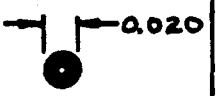	0.12	0.10
20a lb braided nylon fishline without core	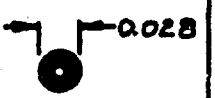	0.11	0.07
20b lb braided nylon fishline without core	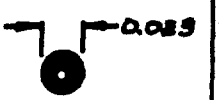	0.12	0.07

TABLE IV

Construction Details of
Conventionally Built Model Canopies

Solid Flat				
D_o (in)	No. Gores	Hem on Skirt	Strength of Susp. lns. (lbs)	Formation of Gores
12.5	64	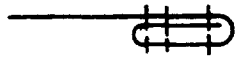	50	Solid Canopy
15	28	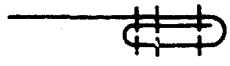	100	
16	28	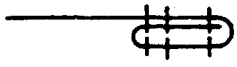	100	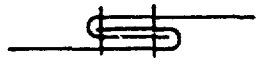
19	24	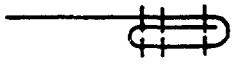	100	
36	28	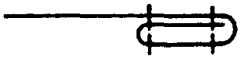	10	
48	28	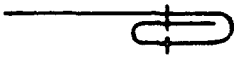	100	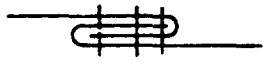
48	64	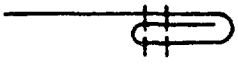	100	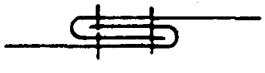
60	64	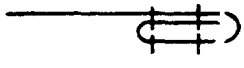	100	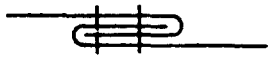

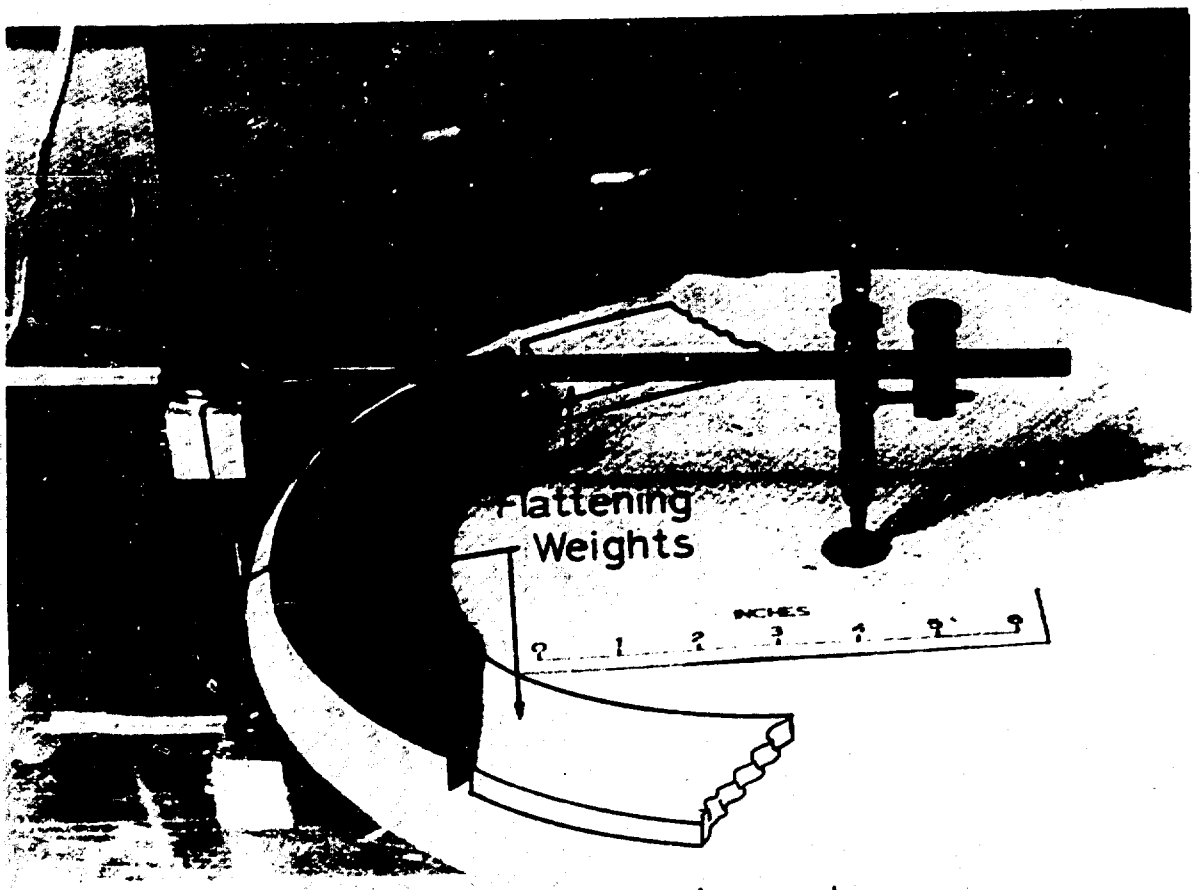

Cloth Cutting Apparatus

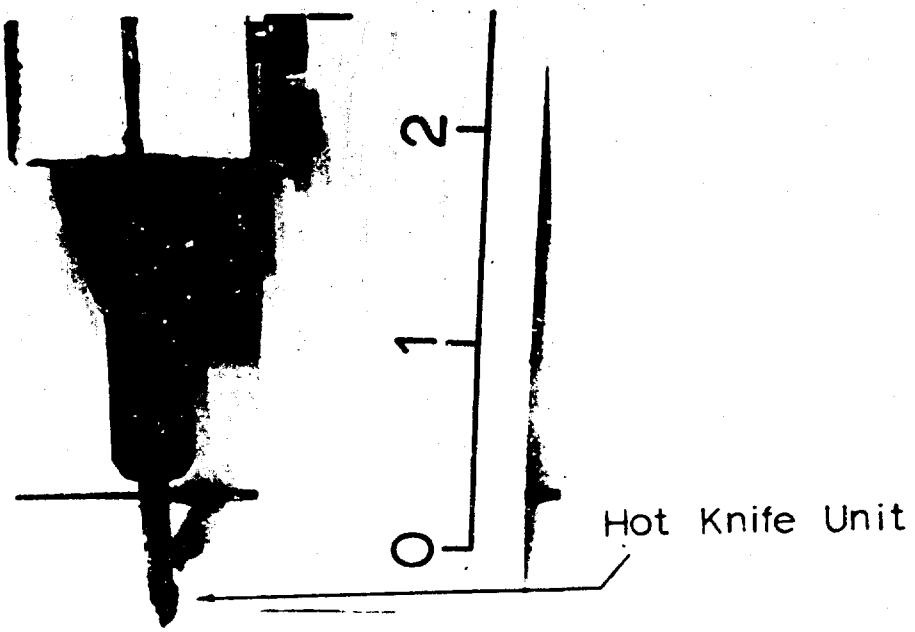

Fig47 Hot Knife Cloth Cutting Technique

REFERENCES

1. R. L. Bisplinghoff, H. Ashley, and R. L. Halfman: Aeroelasticity, Addison-Wesley Publishing Company, Cambridge, Mass., 1955.

2. Charles E. DeRose: Thin Altitude, Lift and Drag of the Apollo Command Module with Offset Center-of-Gravity Positions, Ames Research Center, Moffet Field, California, NASA TND-5276, 1969.

3. C. D. Perkins and R. E. Hage: Airplane Performance Stability and Control, John Wiley and Sons Inc., New York, 1949.

4. H. G. Heinrich: Drag and Stability of Parachutes, Aeronautical Engineering Review, AIAS, June 1956.

5. F. N. Scheubel: Der Entfaltungsvorgang des Fallschirmes (The Opening Process of Parachutes), Deutsche Akademie der Luftfahrtsforschung, AIT 23025, 1941.

6. H. G. Heinrich and E. L. Haak: Stability and Drag of Parachutes with Varying Effective Porosity, ASD-TDR-62-100, December 1961.

7. H. G. Heinrich: The Effective Porosity of Parachute Cloth, Sonderdruck aus "Zeitschrift fuer Flugwissenschaften" 11 (1963), Heft 10, Verlag Friedr. Vieweg & Sohn, Braunschweig.

8. F. M. White and D. F. Wolf: A Theory of Three-Dimensional Parachute Dynamic Stability, Paper presented at AIAA Aerodynamic Deceleration Systems Conference, Houston, Texas, September 1966.

9. Stanley J. Shute, Jr.*: The Design and Test of a Parachute to be used in Cluster to Airdrop 50,000 Lbs, Lecture, Summer Course "Aerodynamic Deceleration '69", University of Minnesota, July 1969.

10. E. Pounder: Parachute Inflation Process Wind Tunnel Study, WADC Technical Report 56-391, September 1956.

*Airdrop Engineering Laboatory, U.S. Army Natick Laboratories, Natick, Massachusetts.

11. H. G. Heinrich and R. A. Noreen: Analysis of Parachute Opening Dynamics with Supporting Wind Tunnel Experiments, AIAA Paper No. 68-924, AIAA 2nd Aerodynamic Deceleration Systems Conference, El Centro, California, September 23-25, 1968.

12. R. J. Berndt: Experimental Determination of Parameters for the Calculation of Parachute Filling Times, Jahrbuch des Wissenschaftlichen Gesellschaft fuer Luft- und Raumfahrt E.V. (WGLR), 1964, pp. 299-316.

13. R. J. Berndt and J. H. DeWeese: Filling Time Prediction Approach for Solid Cloth Type Parachute Canopies, Paper presented at AIAA Aerodynamic Deceleration Systems Conference, Houston, Texas, September 1966.

Unclassified

Security Classification

DOCUMENT CONTROL DATA - R & D

(Security classification of title, body of abstract and indexing annotation must be entered when the overall report is classified)

1. ORIGINATING ACTIVITY *(Corporate author)*
University of Minnesota
Minneapolis, Minnesota 55455

2a. REPORT SECURITY CLASSIFICATION
Unclassified

2b. GROUP
N/A

3. REPORT TITLE
Flexibility as Parameter of Model Parachute Performance Characteristics

4. DESCRIPTIVE NOTES *(Type of report and inclusive dates)*
Final Report December 1967 - October 1969

5. AUTHOR(S) *(First name, middle initial, last name)*
Helmut G. Heinrich
Thomas R. Hektner

6. REPORT DATE	7a. TOTAL NO. OF PAGES	7b. NO. OF REFS
August 1970	71	13

8a. CONTRACT OR GRANT NO.	9a. ORIGINATOR'S REPORT NUMBER(S)
F33615-68-C-1227	
b. PROJECT NO. 6065	
c. Task No. 606503	9b. OTHER REPORT NO(S) *(Any other numbers that may be assigned this report)* AFFDL-TR-70-53
d.	

10. DISTRIBUTION STATEMENT
This document is subject to special export controls and each transmittal to foreign governments or foreign nations may be made only with prior approval of the Vehicle Equipment Division (FDF), Air Force Flight Dynamics Laboratory, Wright-Patterson AFB, Ohio.

11. SUPPLEMENTARY NOTES	12. SPONSORING MILITARY ACTIVITY
	Air Force Flight Dynamics Laboratory Wright-Patterson AFB, Ohio 45433

13. ABSTRACT

Parachute model tests offer the possibilities of efficiently conducting parametric performance studies. Meaningful model experiments must, however, consider besides the effects of Reynolds and Mach Numbers, those of porosity as well as structural characteristics if non-steady processes shall be investigated. In the following the model stiffness index is defined and its effect upon static and dynamic performance characteristics investigated. Quantitative data and stiffness indexes of cloth samples and parachute models are determined. A new technique of construction is described which provides parachute models with a lower stiffness index than previously available. Results of wind tunnel and catapult experiments with parachute models of different stiffness indexes are shown and, when possible, compared with results of full size tests.

DD FORM 1 NOV 65 1473

Unclassified

Security Classification

14. KEY WORDS	LINK A		LINK B		LINK C	
	ROLE	WT	ROLE	WT	ROLE	WT
Parachute Model Canopies						
Model Stiffness						
Opening Characteristics						
Wind Tunnel Tests						
Model Construction						